ÉCOLE DE TECHNOLOGIE SUPÉRIEURE
UNIVERSITÉ DU QUÉBEC

A THESIS PRESENTED TO THE
ÉCOLE DE TECHNOLOGIE SUPÉRIEURE

IN PARTIAL FULFILIMENT OF THE THESIS
REQUIREMENT FOR THE DEGREE OF
PHILOSOPHIAE DOCTOR IN ENGINEERING
PH.D.

BY
NABIL NASSIF

OPTIMIZATION OF HVAC CONTROL SYSTEM STRATEGY USING TWO-OBJECTIVE GENETIC ALGORITHM

MONTRÉAL, MAY 4 2005

CETTE THÈSE A ÉTÉ ÉVALUÉ

PAR UN JURY COMPOSÉ DE :

M. Stanislaw Kajl, directeur de thèse
Département de génie mécanique à l'École de technologie supérieure

M. Robert Sabourin, codirecteur
Département de génie de la production automatisée à l'École de technologie supérieure

M. Christian Masson, président du jury
Département de génie mécanique à l'École de technologie supérieure

M. Stéphane Hallé, jury
Département de génie mécanique à l'École de technologie supérieure

M. Radu Grigore Zmeureanu, jury
Department of Building Engineering in Concordia University

IL A FAIT L'OBJET D'UNE SOUTENANCE DEVANT JURY ET PUBLIC

LE 30 MARS 2005

À L'ÉCOLE DE TECHNOLOGIE SUPÉRIEURE

OPTIMISATION MULTICRITÈRE DE LA STRATÉGIE DE CONTRÔLE DES SYSTÈMES CVCA UTILISANT LES ALGORITHMES GÉNÉTIQUES

Nabil Nassif

RÉSUMÉ

Une méthode d'optimisation multicritère de l'opération des systèmes CVCA, appelée «procédure d'optimisation » est développée. La procédure d'optimisation fonctionnant en parallèle avec le système de contrôle permettent l'opération optimale des systèmes CVCA. Cette procédure pourra être utilisée par la majorité de systèmes de gestion d'énergie dans les bâtiments existants en optimisant les points de consigne de l'opération des systèmes. Les critères de l'optimisation sont le confort ainsi que la consommation totale d'énergie du système. Les points de consigne optimisés sont : la température d'alimentation, la pression statique dans la gaine d'alimentation, la température d'eau glacée, le débit d'air frais, les températures dans les zones, et la chauffage d'appoint dans les zones (ou températures d'alimentation dans les zones).

Les algorithmes génétiques MOGA (Multi-objective genetic algorithm) validés en utilisant un exemple théorique et le modèle simplifié d'un système CVCA seront utilisés pour obtenir les points de consigne optimaux des systèmes CVCA. Les modèles détaillés des composants du système CVCA sont développés et validés avec les données provenant directement ou indirectement du monitoring réalisé dans le bâtiment existant. Pour que la procédure d'optimisation puisse être facilement adaptable à un autre système, les modèles des composants du système CVCA en utilisant les réseaux des neurones sont aussi développés.

Une nouvelle stratégie de contrôle de ventilation basée sur la mesure de la concentration de CO_2 dans l'air soufflé est développée et utilisée par la procédure d'optimisation. Cette nouvelle stratégie puisse le contrôle de débit d'air frais en temps réel en répandent aux besoin actuels de chaque zone.

Les résultats d'optimisation sur le système CVCA du bâtiment de l'École de technologie supérieure (ÉTS) montrent que l'application de la procédure d'optimisation proposée permet de diminuer la consommation d'énergie du bâtiment tout en maintenant la qualité de l'air et le confort des occupants. Les résultats montrent aussi que l'application d'une méthode d'optimisation multicritère de l'opération des systèmes CVCA permet une plus grande diminution de la consommation d'énergie que la méthode d'optimisation une mono-critère.

OPTIMIZATION OF HVAC CONTROL SYSTEM USING TWO-OBJECTIVE GENETIC ALGORITHM

Nabil Nassif

ABSTRACT

Intelligent building technology for building operation, called the optimization process, is developed in this thesis. The optimization process, when installed in parallel with a building's central control system, will permit the optimal operation of HVAC systems. Using this proposed optimization process, the supervisory control strategy set points, such as supply air temperature, supply duct static pressure, chilled water supply temperature, supply CO_2 concentration (or minimum outdoor ventilation), reheat (or zone supply air temperature), and zone air temperature are optimized with respect to energy use and thermal comfort.

The multi-objective genetic algorithm that is developed and validated using mathematic and simplified HVAC system problems is used to solve the optimization problem. Detailed VAV components are developed and validated against the monitored data of the investigated existing HVAC system. Adaptive VAV component models using artificial neural networks are also developed for working with most existing building energy management control systems.

A ventilation control strategy using supply CO_2 concentration set points is developed and integrated into the optimization process. The strategy allows the on-line control of the outdoor air in response to actual building occupancy while ensuring the ventilation requirements of each individual zone.

The optimization of the existing HVAC system is done for the three different weather weeks taken from July 2002, February 2003, and May 2003. The simulation results show that by comparing actual and optimal energy use, the on-line implementation of the optimization process could save energy by 19.5%, 50%, and 40%, respectively, while satisfying minimum zone airflow rates and zone thermal comfort. It also shows that the application of a two-objective optimization problem could help control daily energy use or daily building thermal comfort while providing further energy use savings as compared to the one-objective optimization problem.

OPTIMISATION MULTICRITÈRE DE LA STRATÉGIE DE CONTRÔLE DES SYSTÈMES CVCA UTILISANT LES ALGORITHMES GÉNÉTIQUES

Nabil Nassif

SOMMAIRE

Une méthode d'optimisation multicritère de l'opération des systèmes CVCA, appelée «procédure d'optimisation» est développée. La procédure d'optimisation fonctionnant en parallèle avec le système de contrôle permettent l'opération optimale des systèmes CVCA. Cette procédure pourra être utilisée par la majorité de systèmes de gestion d'énergie dans les bâtiments existants en optimisant les points de consigne de l'opération des systèmes. Les critères de l'optimisation sont le confort ainsi que la consommation totale d'énergie du système. Les points de consigne optimisés sont : la température d'alimentation, la pression statique dans la gaine d'alimentation, la température d'eau glacée, le débit d'air frais, les températures dans les zones, et la chauffage d'appoint dans les zones (ou températures d'alimentation dans les zones).

Les algorithmes génétiques MOGA (Multi-objective genetic algorithm) validés en utilisant un exemple théorique et le modèle simplifié d'un système CVCA seront utilisés pour obtenir les points de consigne optimaux des systèmes CVCA. Les modèles détaillés des composants du système CVCA sont développés et validés avec les données provenant directement ou indirectement du monitoring réalisé dans le bâtiment existant. Pour que la procédure d'optimisation puisse être facilement adaptable à un autre système, les modèles des composants du système CVCA en utilisant les réseaux des neurones sont aussi développés.

Une nouvelle stratégie de contrôle de ventilation basée sur la mesure de la concentration de CO_2 dans l'air soufflé est développée et utilisée par la procédure d'optimisation. Cette nouvelle stratégie puisse le contrôle de débit d'air frais en temps réel en répandent aux besoin actuels de chaque zone.

Les résultats d'optimisation sur le système CVCA du bâtiment de l'École de technologie supérieure (ÉTS) montrent que l'application de la procédure d'optimisation proposée permet de diminuer la consommation d'énergie du bâtiment tout en maintenant la qualité de l'air et le confort des occupants. Les résultats montrent aussi que l'application d'une méthode d'optimisation multicritère de l'opération des systèmes CVCA permet une plus grande diminution de la consommation d'énergie que la méthode d'optimisation une mono-critère.

OPTIMISATION MULTICRITÈRE DE LA STRATÉGIE DE CONTRÔLE DES SYSTÈMES CVCA UTILISANT LES ALGORITHMES GÉNÉTIQUES

Nabil Nassif

RÉSUMÉ

L'opération des systèmes mécaniques des bâtiments est une activité critique pour optimiser la consommation énergétique du bâtiment et ainsi diminuer les coûts, assurer le confort des occupants et préserver la qualité de l'air. Pour la plupart des 430 000 bâtiments commerciaux et institutionnels au Canada, l'opération des systèmes mécaniques n'est pas optimale, ce qui entraîne des pertes énergétiques d'environ 15 à 30 % et, par conséquent, une augmentation des émissions de gaz à effet de serre (GES). Par exemple, une lacune dans l'opération des systèmes mécaniques peut être le fonctionnement simultané des systèmes de climatisation et de chauffage. L'optimisation de la stratégie de contrôle de ces systèmes CVCA (chauffage, ventilation et conditionnement d'air) permet une diminution de la consommation d'énergie du bâtiment tout en maintenant la qualité de l'air et le confort des occupants.

L'opération actuelle des systèmes CVCA est pilotée par plusieurs boucles de contrôle indépendantes avec les paramètres de contrôle comme par exemple : la température d'alimentation, la pression statique dans la gaine d'alimentation, etc. Les points de consigne des paramètres de contrôle sont déterminés selon les règles spécifiques à chaque paramètre. Par conséquent, il se peut que les points de consigne ainsi déterminés ne fassent pas un ensemble optimal du point de vue de la consommation d'énergie. Cependant, la tendance actuelle de construire des bâtiments intelligents permet l'émergence des nouvelles méthodes visant à améliorer l'efficacité énergétique des bâtiments. Il s'agit de méthodes ayant pour but d'optimiser l'opération des systèmes CVCA en temps réel.

L'objectif de notre recherche est donc de développer une méthode d'optimisation multicritère de l'opération des systèmes CVCA, appelée «procédure d'optimisation ». Les critères de l'optimisation sont : le confort ainsi que la consommation totale d'énergie du système incluant par exemple les énergies consommées par le ventilateur et les serpentins de chauffage et de refroidissement. Les points de consigne optimisées sont : la température d'alimentation, la pression statique dans la gaine d' alimentation, la température d'eau glacée, le débit d'air frais, les températures dans les zones, et le chauffage d'appoint dans les zones (ou températures d'alimentation dans les zones). Les systèmes CVCA du bâtiments de l'École de technologie supérieure (ÉTS) sont étudiés.

La qualité de l'air à l'intérieur des bâtiments et de l'utilisation associée de l'énergie a été d'accroître de manière significative le souci au cours des 20 dernières années. Beaucoup de publications ont discuté des différentes stratégies de contrôle de ventilation. La

stratégie de contrôle de ventilation basée sur la mesure de la concentration de CO_2 dans l'air soufflé est développée et intégrée dans le processus d'optimisation.

La procédure d'optimisation proposée comprend : (*i*) un système d'acquisition de données, (*ii*) un module de prédiction des charges de locaux desservis par le système CVCA, (*iii*) programme d'optimisation et (*iv*) un module de sélection de la solution optimale. Pour amorcer la procédure d'optimisation, les modèles des composants du système CVCA sont développés et validés avec les données provenant directement ou indirectement du monitoring réalisé dans le bâtiment existant. Pour que la procédure d'optimisation puisse être facilement adaptable à un autre système, les modèles des composants du système CVCA en utilisant les réseaux des neurones sont aussi développés. Les algorithmes génétiques MOGA (Multi-objective genetic algorithm) seront utilisés pour obtenir les points de consigne optimaux des systèmes CVCA. La méthode C-NSGA-II (controlled elitist non-dominated sorting genetic algorithm) a été sélectionnée et validée en utilisant un exemple théorique et le modèle simplifié d'un système CVCA. Les paramètres de C-NSGA-II sont aussi ajustés pour donner la meilleure performance.

Pour atteindre notre objective, la méthodologie suivante est utilisées : (*i*) monitoring et acquisition de données sur les systèmes CVCA du bâtiments de l'ÉTS, (*ii*) développement et validation d'une stratégie de contrôle de ventilation qui est intégrée dans le processus d'optimisation, (*iii*) développement et validation des modèles de composants d'un système CVCA qui seront validés en utilisant les données enregistrées, (*iv*) développement et validation des algorithmes génétiques pour optimiser l'opération d'un système CVCA , et (*v*) validation de la procédure d'optimisation en utilisant les données obtenue de l'opération actuelle du système CVCA.

Les résultats d'optimisation sur le système CVCA existant montrent que l'application de la procédure d'optimisation proposée permet de diminuer la consommation d'énergie du bâtiment tout en maintenant la qualité de l'air et le confort des occupants. Les contributions originales de ce travail sont résumées comme suit :

- Définition d'une méthodologie robuste pour l'optimisation en temps réel de l'opération des systèmes CVCA
- Application de la procédure d'optimisation proposée permet de diminuer la consommation d'énergie du bâtiment tout en maintenant la qualité de l'air et le confort des occupants
- Développement d'une nouvelle stratégie de contrôle de ventilation basée sur la mesure de la concentration de CO_2 dans l'air soufflé. La nouvelle stratégie pour le contrôle de débit d'air frais en temps réel en répondent aux besoin actuels de chaque zone.
- Applications de l'intelligence artificielle telles que les réseaux de neurones et les algorithmes génétiques au développement de la procédure d'optimisation. Cette

procédure pourra être utilisée par la majorité de systèmes de gestion d'énergie dans les bâtiments existants.

- Evaluation des performances des MOGA (multi-objective genetic algorithm) en utilisant le modèle simplifié d'un système CVCA. Les paramètres de MOGA sont sélectionnés et ajustés pour améliorer sa performance sur le système CVCA.
- Développement des modèles de composants d'un système CVCA qui seront validés en utilisant les données enregistrées. Les modèles de composants peuvent utiliser à un autre système CVCA. Les validations mettent en évidence les contraintes rencontrées tels que le manque et la précision de données mesurées provenant du monitoring.

ACKNOWLEDGEMENTS

CONTENTS

Page

LIST OF TABLES

Page

LIST OF FIGURES

Page

LIST OF ACRONYMS AND SYMBOLS

A	valve authority
a_{cr}	Adaptive value determined from the on-line data
ACHM	Adaptive chiller model
a_i	Fan model coefficients
AFM	Adaptive fan model
AHU-4	Existing air handling unit
AHU-6	Existing air handling unit
b_i	Fan model coefficients
$B_{\Delta CO_2}$	CO_2 concentration difference between the return and supply air, ppm
C	Pressure drop coefficient in the duct where the outdoor damper is installed
C	Flow coefficient of VAV damper
C_{comp}	Flow coefficient in components
C_p	Specific heat of air
CAP_FT	Chiller capacity factor
CCDET	Detailed cooling coil model
CCSIM	Simple cooling coil model
C_{damper}	Damper model coefficient
COP	Coefficient of chiller performance
d	Fan diameter, m
DCHM	Detailed Chiller model
DFM	Detailed fan model
DM	Damper model
ΔP_{comp}	Static pressure drops in the cooling and heating coils, in the filter, and in the humidifier, Pa
ΔP_{damper}	Damper pressure drop, Pa

	the humidifier, Pa
ΔP_{damper}	Damper pressure drop, Pa
ΔP_{duct}	Pressure drop between the static pressure sensor and VAV box inlet, Pa
ΔP_{system}	System pressure drop valve authority, Pa
ΔP_{valve}	Full flow valve pressure drop, Pa
ΔTs	Sampling time step
ER_PLR	Adjustment to rated efficiency due to change in load calculated by Equation 4.19
ER_FT	Adjustment to rated efficiency due to environmental variables calculated by Equation 4.20
η_f	Shaft power dimensionless coefficient
η_m	Motor efficiency
η_c	Distribution index
GA	Genetic algorithm
Ho	Enthalpy of outdoor air
Hs	Enthalpy of air leaving the cooling coil
HVAC	Heating, ventilating, and air conditioning
INVCCDET	Inverse form of the detailed cooling coil model
K	Inherent flow rate factor
L	Thermal load on the body
MCCSIM	Modified simple cooling coil model
N	Fan speed
N_b	Actual occupancy in the building
NNCCM	Adaptive cooling coil model based on the artificial neural network
NSGA	Non-dominated sorting genetic algorithm
NSGAII	Elitist non-dominated sorting genetic algorithm
$N_{z,i}$	Number of occupants in each zone i,
σ_{share}	Sharing value

$O_{D,min}$	Minimum damper position, %
O_{Sco2}	Outdoor air CO_2 concentration, ppm
$O_{D,pr}$	Principal damper position, %
$O_{V,cd}$	Cooling coil valve position, %
$O_{V,h}$	Heating coil valve position, %
p_c	Crossover probability
PLR	Chiller part load ratio based on available capacity
PLR_r	Chiller part load ratio based on rated capacity
p_m	Mutation probability
PMV	Predicted mean vote
$P_{operation}$	Chiller power draw at specified operating conditions, kW
PPD	Predicted percentage of dissatisfied, %
$P_{S,fan}$	Fan static pressure, Pa
$P_{S,fan,dsg}$	Design fan static pressure, Pa
$P_{S,mix}$	Mixing plenum static pressure, Pa
$P_{S,out}$	Outlet fan static pressure, Pa
$P_{S,sd}$	Supply duct static pressure, Pa
P_{rated}	Rated chiller power draw at ARI conditions, kW
p_z	Population size
φ_o	Outdoor air relative humidity
φ	Return air relative humidity
$\varphi_{in,c}$	Inlet air cooling coil relative humidity
$\varphi_{ou,c}$	Outlet air cooling coil relative humidity
Φ_t	Flow dimensionless coefficient
Ψ	Pressure head dimensionless coefficient
$\dot{Q}_b$	Building or fan airflow rate, l/s
$\dot{Q}c$	Cooling coil load, kW

$\dot{Q}_l$	Liquid flow rate through the heating or cooling coils, l/s
$q_{l,b}$	Building latent, kW
$\dot{Q}_{l,rate}$	Liquid flow rate at rating, l/s
$\dot{Q}_{l,inh}$	Inherent liquid flow rate at rating, l/s
$\dot{Q}_{fan}$	Fan airflow rate, l/s
$\dot{Q}_{fan,dsg}$	Design fan airflow rate, l/s
$\dot{Q}_o$	Outdoor airflow rate, l/s
$\dot{Q}_{o,b}$	Amount of outdoor air to be introduced into whole building, l/s
$\dot{Q}_{o,b,dsg}$	Design amount of outdoor air to be introduced into whole building, l/s
$\dot{Q}_{o,z}$	Amount of outdoor air to be introduced into each zone i, l/s
$\dot{Q}_{o,z,dsg,i}$	Design amount of outdoor air to be introduced into each zone i, l/s
$q_{s,i}$	Indoor sensible loads at each zone i
q_t	Total load of the building
$\dot{Q}_z$	Zone airflow rate, l/s
$\dot{Q}_{z,i}$	Airflow rate at zone i, l/s
$\dot{Q}_{z\max}$	Maximum airflow rate, l/s
$\dot{Q}_{z,\max,dsg}$	Maximum airflow rate based on design static pressure, l/s
R	Valve rangeability
$R_{a,b}$	The airflow part-load ratio of the building
$R_{a,z,i}$	The airflow part-load ratio of the zone i
R_{CO_2}	CO_2 concentration at return air duct, ppm
$R_{v,b}$	The ventilation part-load ratio of the building

$R_{v,z\ i}$	The ventilation part-load ratio of the zone i
ρ	Air density
S_1	Fixed minimum outdoor air percentage ventilation control strategy
S_2	Fixed minimum outdoor air rate ventilation control strategy
S_3	CO_2- based demand-controlled ventilation
S_4	Multiple space equation ventilation control strategy
S_5	Supply CO_2- based demand-controlled ventilation
SBX	Simulated binary crossover operator
S_{CO_2}	CO_2 concentration of supply air, ppm
$S_{CO_2,set}$	CO_2 concentration set point of supply air, ppm
TBM	Temperature balance method
T_{cws}	Entering condenser water temperature, ^oC
T_o	Outdoor air temperature, ^oC
T_r	Return air temperatures, ^oC
T_{sa}	Supply air and water temperatures, ^oC
T_{sw}	Chilled water supply temperature, ^oC
$T_{z,i}$	Temperature of zone i, ^oC
UA_{ext}	External (air) heat transfer coefficient
$UA_{ext,\ rating}$	External (air) heat transfer coefficient at rating
U_{int}	Internal (water) heat transfer coefficient
$U_{int,\ rating}$	Internal (water) heat transfer coefficient at rating
VAV	Variable air volume
VL	Ventilation load
V_{out}	Output values
V_{ref}	Reference values
V_z	Air velocity in zone, m/s
$\dot{W}_c$	Chiller energy use, kW
$\dot{W}_f$	Fan energy use, kW

$\dot{W}_s$	Shaft fan power, kW
$\dot{W}_t$	Total energy use, kW
X	Uncorrected fraction of outdoor ventilation air in the supply system
x	Damper model coefficient
Y_b	The fraction of outdoor air in supply system introduced into building
$Y_{b,dsg}$	The fraction of outdoor air in supply system introduced into building at design condition
$Y_{z,dsg,i}$	The fraction of outdoor air introduced into zone i at design condition
Z	Ratio of the required outdoor air to the primary air in the critical zone
$Z_{CO2,th\ t}$	Required threshold, ppm
Z_{CO_2}	Indoor CO_2 concentration, ppm
$Z_{\Delta CO_2,i}$	CO_2 concentration difference between supply and return air in zone i

INTRODUCTION

Since the energy crisis of the 1970s, great efforts have been invested in minimizing the energy costs associated with the operation of the HVAC system. Computer-aided energy management techniques as well as rigorous applications of the variable air volume (VAV) concept were accepted as means of achieving an energy-efficient and comfortable building environment. Not all VAV systems are successful and efficient. Multiple factors contribute to this unfortunate situation, including the system control strategy. This lack of efficiency is due to the fact that they are not wide-interaction optimized.

Most existing HVAC system processes are optimized at the local loop level; for example, in the existing HVAC system investigated in this thesis, which is installed at the Montréal campus of the *École de technologie supérieure* (ÉTS), one of the most advanced "intelligent buildings" in North America today, each local control of an individual subsystem is individually determined, thus leading to the poor performance.

The air supply temperature set point for this HVAC system is determined as a function of the outdoor air temperature and fan airflow rate, without taking into consideration other subsystems, such as supply duct static pressure and chilled water supply temperature set points. Decreasing the supply air temperature set point may result in a lower supply duct static pressure and fan energy. Zone reheats for the investigated HVAC system that are used on winter days – only when the zone temperatures and airflow rates fall to their minimum limits – are not optimized, given their interaction with other set points. Applying some reheat in the low-load zone (ventilation critical zone) could significantly reduce the system's outdoor air ventilation. The zone air temperature set points of the investigated system are kept constant in the comfort zone during occupied periods. However, a strategy using the optimization of the individual

zone air temperature set points combined with other controller set points during occupied periods could further reduce system energy use.

The quality of the air inside buildings and the associated energy use has been of growing significantly concern over the last 20 years. Many publications have discussed different ventilation control strategies. The CO_2-based demand-controlled ventilation (CO_2-DCV) is one of the strategies that could reduce energy use by reducing the unnecessary over-ventilation of buildings. The energy consumption reduction benefits derived through the use of this strategy have been demonstrated for many different applications. When this strategy is applied for multiple spaces by detecting the CO_2 concentration in return air, poor air quality may result inside certain zones. To overcome this problem, ASHRAE Standard 62-2001 (ASHRAE 2001) proposes the multiple space equation (*MSE*), which corrects the fraction of outdoor ventilation air in a supply system in order to minimize energy use while maintaining a proper indoor air quality (IAQ) in all zones, including the critical one. Since the amount of outdoor air is based on the design number of occupants, this amount could be more than required by the actual number (off-design), and result in waste in energy use. The "supply CO_2-based demand-controlled ventilation" (S-CO_2-DCV) technique proposed in this research paper is a compromise between the *MSE* and the CO_2-DCV, taking into account: (*i*) the actual occupancy of the building and (*ii*) the critical zone ventilation requirement. This proposed strategy allows the on-line control of the outdoor air in response to actual building occupancy (as in CO_2-DCV) while ensuring the ventilation requirements of each individual zone, including the critical zone (as in *MSE*).

Existing studies on the optimization of the controller set point have demonstrated that the performance of HVAC systems can be improved through optimized supervisory control strategies. Set points can be adjusted by the optimized supervisor to improve the operating efficiency. These studies did not address the interaction between all controller

set points, including zone temperatures and supply CO_2 concentration set points, using the two-objective optimization problem.

This thesis presents a system approach that takes into account wide system interactions involving reheat (or zone supply air temperature); zone air temperature, including supply air temperature; supply duct static pressure; chilled water supply temperature, and supply CO_2 concentration (or minimum outdoor ventilation) using two-objective optimization problem.

Problem Statement

The operation of heating, ventilating and air conditioning (HVAC) systems is a critical activity in terms of optimizing a building's energy consumption (and, hence, reducing costs), ensuring occupants' comfort, and preserving air quality. The operation of these systems in most of the 430,000 commercial and institutional buildings in Canada is suboptimal, resulting in energy losses of 15 to 30% and, consequently, greenhouse gas emissions (GHGs). One example of the deficient operation of HVAC systems is the simultaneous use of air conditioning and heating systems. The performance of HVAC systems can be improved through better supervisory control. Set points and operating modes for an HVAC system can be adjusted by the supervisor to maximize overall operating efficiency. The optimization process developed in this proposed research makes it possible to reduce a building's energy consumption, while maintaining air quality and ensuring occupant comfort.

Goals of the Research

The main objective of this research project is to develop an optimization process allowing the on-line optimization of the HVAC supervisory control strategy. This supervisor sends the optimal controller set points to local control loops. The set points, such as supply air temperature, zone temperatures, zone supply air temperature (zone reheat), duct static pressure, chilled water supply temperature, and supply CO_2

concentration (minimum airflow rate) are then the problem variables, while the thermal comfort and the energy use are the objective functions. The optimization process could use the developed and validated detailed component model which is based on detailed manufacturer data or the adaptive component models based on artificial neural networks. These two detailed and adaptive VAV models are developed and discussed. To that end, the following methodology is employed:

(i)   Monitoring of the investigated existing HVAC system;

(ii)   Development of the new ventilation control strategy;

(iii)   Modeling and validation of HVAC components;

(iv)   Development of optimization algorithm;

(v)   Development of proposed optimization process;

(vi)   Validation of the developed optimization process on multi-zone HVAC systems.

Proposed Optimization Process

HVAC systems are typically controlled using a two-level control structure. The lower-level local-loop control of single set points is handled using an actuator. The upper control level, the supervisory control, specifies the set points and the modes of operation. For the investigated existing HVAC system at the ÉTS campus, the supervisor specifies the set points that are locally determined. For example, the air supply temperature set point for this system is determined as a function of outdoor temperature and airflow rate without taking into consideration the other subsystems, such as supply duct static pressure and chilled water supply temperature set points. Zone reheats are used on winter days only when the winter zone temperatures and airflow rates fall to their minimum limits. The air temperature set point of each zone is maintained at a constant value within the comfort range during occupied periods. Although the supply duct static pressure set point changes gradually from zero to a maximum value (250 Pa) when the system is started up, this maximum value is always

maintained at normal operation. The minimum outdoor damper position is maintained at a constant value in order to provide the required outdoor air ventilation. The chilled water supply temperature of the existing system is also constant at 7.2°C. Since these set points are determined at the local loop level rather than through global system optimization, the system does not perform at its full potential.
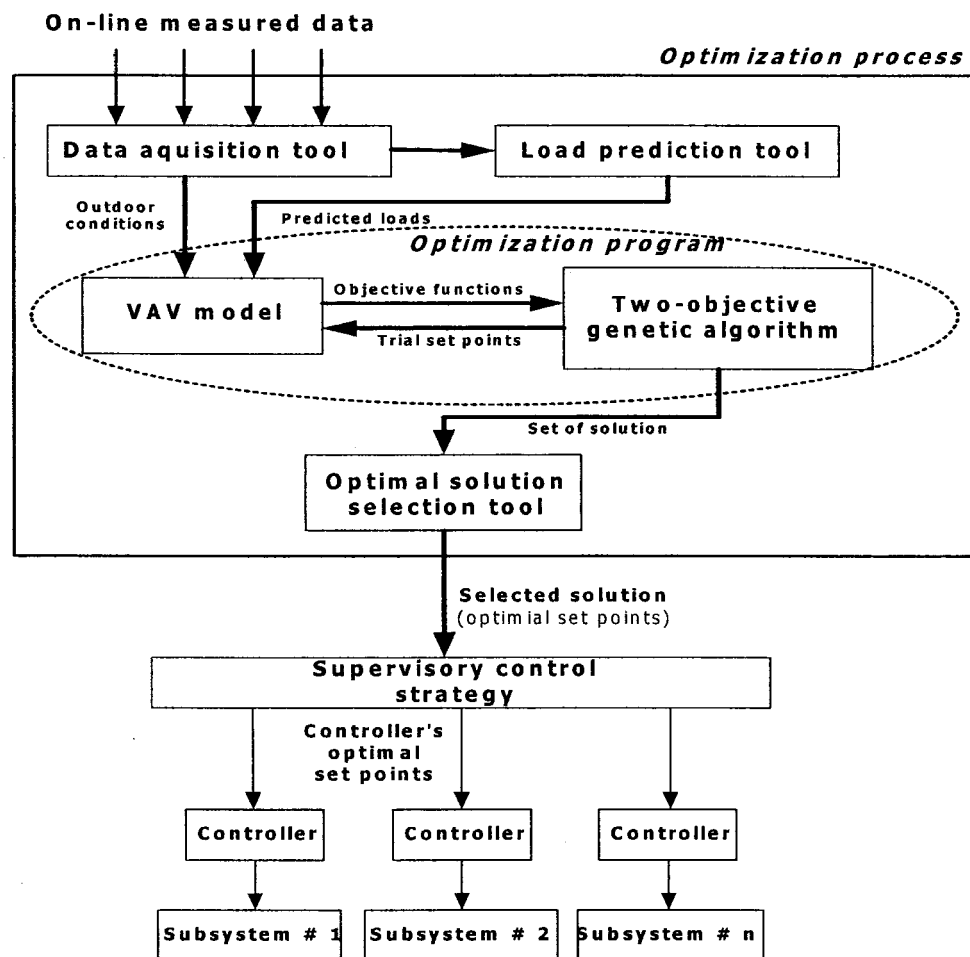
Figure 1   Schematic of optimization process of on-line optimization of supervisory control strategy

The performance of this HVAC system can be improved through the optimization of the supervisor control strategy. The *"optimized supervisor"* specifies the set points using the

optimization process as shown in Figure 1, which includes (*i*) the adaptive or detailed VAV model, (*ii*) the two-objective genetic algorithm optimization program, and (*iii*) three main tools, namely, data acquisition, load prediction, and optimal solution selection tools. The data acquisition tool receives and processes the on-line measured data.

The load prediction tool predicts sensible indoor zone loads, the latent building load, and the ventilation load for the optimization period, using the on-line measured data of the previous one. Since a set of optimal solutions is obtained by using the two-objective optimization problem, the selection tool is used to select the appropriate solution in order to minimize daily energy use and decrease the peak energy demand. Each component of the optimization process is developed and discussed through dissertation content organized as shown in outline of thesis.

Contributions

The original contributions of this work can be summarized the follows:

- Improving the performance of multi-zone HVAC systems using the optimization process proposed and developed in this work.

- Developing a new ventilation control strategy using the supply CO_2 concentration set point. This proposed strategy allows the on-line control of the outdoor air in response to actual building occupancy while ensuring the ventilation requirements of each individual zone, including the critical one.

- Application of artificial intelligence (AI)-based methods to the HVAC system. The component models based on artificial neural networks and genetic algorithm methods are developed. The advantage of AI methods is that they do not require any prior knowledge of specific models to solve problems as is the case with traditional methods based on physical or statistical approaches.

- Evaluation of the performances of several multi-objective GA optimization methods on HVAC system problems. The parameters of selected multi-objective

GAs are adjusted in order to improve its performance on a HVAC system problem.

- Modeling of VAV components using the artificial neural networks. The simplest network architectures that give the best accuracy are implemented. The detailed VAV models as well as the monitored data are used to learn and validate these artificial neural network models.

- Evaluation of the HVAC system performance based on monitored data. Operation and design deficiencies are detected through the monitoring-based evaluation. The necessity of the optimization process to overcome these operation deficiencies is explained and justified.

- Development of strategies of HVAC component model validations. The validation difficulties that are faced due to lack of required measured data are overcome by using these validation strategies.

Outline of the Thesis

The thesis is organized into six chapters. Chapter 1 provides a literature review on global and local optimal control studies. Chapter 2 describes the investigated HVAC system and presents the operational problems observed through the monitoring. The performance of the existing HVAC system is evaluated using monitored data; the chapter also looks at how the proposed optimization process could improve its performance. Chapter 3 introduces the proposed ventilation control strategy using a supply CO_2 concentration set point and shows how this strategy could be integrated into the VAV model used in the optimization process. The detailed and adaptive component models are discussed in Chapter 4, where data acquisition and load prediction tools are also presented. Chapter 5 examines the candidate two-objective optimization methods and evaluates their performances in solving the HVAC system control strategy. Chapter 6 shows the simulation results of applying the proposed optimization process on the existing HVAC system.

CHAPTER 1

LITERATURE REVIEW

Since the energy crisis of the 1970s, great efforts have been invested in minimizing the energy costs associated with the operation of the HVAC system. Computer-aided energy management techniques as well as rigorous applications of the variable air volume (VAV) concept came to be accepted as means of achieving an energy-efficient and comfortable building environment. Not all VAV systems are successful and efficient (Cappellin 1997; Linder and Dorgan 1997). Multiple factors contribute to this unfortunate situation, including system control strategy. Several studies have been reported how the optimization of system control strategy can improve the VAV system performance (ASHRAE 2003). In this chapter, the literature review focuses on the global and local optimization of system control strategy. Since the new ventilation control strategy is also developed in this research, a comprehensive review of ventilation control strategy is discussed. The literature review presents the following (*i*) variable air volume system, (*ii*) global and local optimization of control system, (*iii*) ventilation control strategies, and (vi) optimization methods.

1.1   Variable Air Volume System

Variable air volume systems help to solve energy problems; it can save 20 to 30% in building costs over conventional constant air volume systems. VAV system can also reduce first costs by using smaller equipment such as fans, pumps, boilers, chillers and less costly ductwork and piping distribution systems. VAV systems are described in several HVAC system reference books (Wendes 1991; Kreider and Rabl 1994; Chen and Demster 1995; McQuiston, Parker, and Spitler 2000; Wang 2000). A VAV system controls temperature in a space by varying the quantity of supply air rather than varying the supply air temperature. A VAV terminal device at the zone varies the quantity of

supply air to the space. The supply air temperature is held relatively constant, depending on the season. VAV systems can be applied to interior or perimeter zones, with common or separate fans, with common or separate air temperature control, and with and without auxiliary heating devices (ASHRAE 2003). The greatest energy saving associated with VAV occurs at the perimeter zones, where variations in solar load and outside temperature allow the supply air quantity to be reduced. Humidity control is a potential problem with VAV. If humidity is critical, as in certain research and development laboratories, process work, etc., systems may have to be limited to constant volume airflow. Not all VAV systems are successful and work efficiently. Multiple factors contribute to this unfortunate situation (Cappellin 1997; Linder and Dogran 1997). One of these factors is the control systems and supervisory control strategies (ASHRAE 2003; Kreider and Rabl 1994).

1.2   Optimization of HVAC System Control

The optimal control problem associated with HVAC systems may be thought of as having a two-level control structure. Lower level local-loop control of a single set point is provided by an actuator. The upper control level, supervisory control, specifies the set points and other modes of operation that are time dependent. Set points and operating modes can be adjusted by the supervisor to maximize the overall operating efficiency (ASHRAE 2003). The performance HVAC systems can be improved through better local-loop and supervisory control. At any given time, the HVAC system may be at different modes of operation and set points. However, one set of control set point and modes results in minimum power consumption. This optimal control point results from trade-offs between the energy consumption of different HVAC system components or processes. Chapter 41 of ASHRAE (2003) provides a detailed review of the literature focusing on the global and local optimization of system control strategy.

With a view of local set point of individual system, the supply air temperature set point is reset in purpose to reduce energy use. The benefits of the supply air temperature reset for HVAC systems are not universally accepted. Research has shown that increasing the supply air temperature set point saves both cooling and heating energy for constant-air-volume systems (ASHRAE 2003). For VAV systems, it is not beneficial unless local tempering is required to prevent overcooling rooms served with non-zero minimum setting boxes. Another possible benefit of the supply air temperature set point is that the chiller evaporator temperature could possibly be elevated, with a corresponding improvement in chiller efficiency. In addition, the supply air temperature reset is accompanied by an increased fan energy penalty; it also impacts both the economizer cycle performance and the outdoor air distribution. Ke and Mumma (1997a) investigated the interactions between the supply air temperature reset and ventilation requirements, which dominate the determination of the optimum supply air temperature. This optimization concept simultaneously reduces energy consumption and meets ventilation requirements. The results showed that increasing the supply air temperature set point reduces the humidification energy corresponding to the reduction of the outdoor airflow, but increases the fan energy associated with the growth of the primary airflow. The supply air temperature reset may also have a reduction for the tempering energy partly due to decreasing the heat needed for overcooled spaces, but mainly due to shifting heating loads from the VAV boxes to the system heating coils. Besides, the supply air temperature reset can save cooling energy by reducing reheat of the cold primary air and transferring cooling loads from the coils to the outdoor air as in the economizer cycle. Therefore, the supply air temperature reset will not save cooling energy much in the summer, but is good in mild seasons. However, the penalty of the fan power demand consumes all the benefits for the supply air temperature reset with the highest one. To take advantage of the conflict between the savings and penalty, optimization is the solution (Ke and Mumma 1997a). The optimum supply air temperature reset, most beneficial in mild seasons, ensures that a system will operate in the valley of power demand curve.

The VAV system is based on the principle of matching the load by varying the air volume supplied to each zone rather than varying the temperature, with the intent of saving fan work energy as compared with a constant-volume system. As the individual VAV boxes modulate in response to zone demands, the total volumetric flow rate will vary. If the fan airflow is not controlled, the static pressure in the duct system will increase, resulting in noise, lack of control at the boxes, and possibility of duct blowout. The static pressure sensor located two-thirds to three-fourths of distance from the fan to the most remote box must be used to control the fan speed. Significant fan energy saving are possible if the static pressure set point is reset at least one of the VAV boxes remains open (ASHRAE 2003). With this approach, the flow resistance remains relatively constant. Complete building direct digital control DDC systems allow every box condition to be monitored, which allows the most demanding box to be identified at any time in the day's operation and to be used for a signal (Haines and Wilson 1994). Several different strategies based on this concept are proposed in references (Hartman 1993; Warren and Norford 1993; Englander and Norford 1992). Englander and Norford (1992) used two methods of controlling the supply fan to minimize duct static pressure without sacrificing occupant comfort or adequate ventilation. Both methods make use of feedback from local zone flow control loops. Their technique forms the basis of the following reset strategy. At each decision interval (e.g., 5 minutes), the static pressure set point is increased by a fixed value if any of controller outputs for representative VAV box are greater than a threshold value. However, the static pressure set point is decreased by a fixed value if all of the controller outputs are less than a threshold value. Otherwise, the set point does not be changed. The set point between upper and lower is limited based on upper and lower limits and duct design.

A chiller plant consists of one or more chillers that are typically arranged in parallel with dedicated pumps to provide the primary source of cooling for the system. Individual feedback controllers adjust the cooling capacity of each chiller in order to maintain a specified chilled water supply temperature. Additional chiller control variables include

the number of chillers operating and the relative loading for each chiller. For a given total cooling requirement, individual chiller cooling loads can be controlled by utilizing different chilled water supply set points for constant individual flow or by adjusting individual flows for identical set points. The important aspect of operation mode is the sequencing of chillers and pumps. Sequencing defines the order and conditions associated with bringing equipment online or offline. Braun, et al (1989a) investigated the optimal control to chilled water systems without storage. The results showed that the best performance for different combination of chillers and fixed-speed pumps occurs at about 25% of design load with one chiller and pump operating. As the load increases, the system coefficient of performance (COP) decreases due to decreasing chiller COP and nonlinear increase in the power consumption of cooling tower and air handler fans. A second chiller should be brought online at the point where the overall COP of the system is the same with or without the chiller. For this system, this optimal switch point occurs at about 38% of the total design load or about 75% of the individual chiller's capacity. The optimal switch point for bringing a second condenser and chilled water pump online occurs at a much higher relative chilled load (0.62) than the switch point for adding or removing a chiller (0.38). However, pumps are typically sequenced with chillers (i.e., they are brought on-line together). In this case, the optimal switch point for bringing a second chiller online (with pumps) is about 50% of the overall design capacity of the individual chiller with dedicated pumps.

Individual feedback controllers adjust the cooling capacity of each chiller in order to maintain a specified chilled water supply temperature. One method for determining the optimal chilled water temperature described in (ASHARAE 2003) is to monitor the water control valve positions of "representative" air handlers. Since the valve position data may be unreliable, it should be monitored the discharge air temperatures as the following simple rules. Increase the chilled water set temperature if all water valves are unsaturated or the discharge air temperatures associated with all valves that are saturated are lower than set point. Decrease the chilled water temperature if more than one valve

is saturated at 100% open and their corresponding supply air temperatures are greater than their set points.

The global determination of optimum set points that minimize operating costs has been studied by (Cumali 1994; Braun, Klein, Mitchell, and Beckman 1989b; Cumali 1988). Curtiss, Brandemuehl, and Kreider (1994) used neural networks energy management program to perform on-line set point resets in an actual HVAC system. They found that this energy management system was able to maintain comfort and use less energy than a fixed set point. To optimize the overall system performance, the system approach was utilized in optimal control strategies in a few studies. System-based optimal control and operation studies are examined by House and Smith (1995 and 1991). In House and Smith (1991), the optimal control strategy was applied to an HVAC system with a single zone. Energy saving of 49% was obtained. However, in House and Smith (1995), they proposed a system approach for optimizing multi-zone building systems respecting energy use and without sacrificing the thermal comfort. Energy saving of 24% was obtained.

A system approach was proposed for the on-line control strategy of HVAC in which multiple set points are optimized simultaneously in order to improve the system responses and reduce energy use (Wang and Jin 2000; Zheng and Zaheer-Uddin 1996; Zaheer-Uddin and Patel 1993). Wang and Jin (2000) presented a control strategy using a system approach based on predicting the responses of overall system environment and energy performance to changes of control settings of HVAC system. A genetic algorithm is used by the strategy to solve the optimization problem. The supply air temperature, chilled water temperature, and outdoor air ventilation were optimized. The simulation results of various weather conditions showed that energy saving could be obtained by this strategy while maintaining better thermal comfort.

The optimal control strategy based on steady-state models of HVAC system has been investigated by Zheng and Zaheer-Uddin (1996). These models are interconnected to simulate the responses of the VAV system. The studies based on system approaches showed that an optimal control strategy can improve the system responses and reduce energy use compared to the traditional control strategies (Zaheer-Uddin and Patel 1993, MacArthur and Woessner 1993).

1.3   Ventilation Control Strategy and Economizer Cycle

Air-side economizer cycle control reduces cooling costs when outside air conditions are suitable, that is, when the outdoor air is cool enough to be used as a cooling medium. There are two strategies of air-side economizer cycle control: temperature economizer control, and enthalpy economizer control. The economizer essentially consists of three dampers: an outdoor air damper, a recirculation damper, and a discharge damper. These three dampers are arranged so that the proportion of outdoor air may be modulated between a minimum value and 100 %. Various strategies may be used to control the dampers. The conventional strategy is to couple all three dampers (Zhao 1998). Another strategy is to couple the outdoor air and recirculation dampers and leave the discharge damper open at all operation conditions (Krakow, Zhao, and Muhsin 2000). Another strategy is to leave the outdoor air damper wide open (Seem, House, and Klaassen 1998). When the economizer is at minimum air mode, the outdoor airflow rate varies approximately in proportion to supply air quantity. That means the quantity of outdoor ventilation air supplied to the building at all part-load conditions, when in the minimum air mode, is below that needed to satisfy ASHRAE Standard 62-2001 (ASHRAE 2001). Various ventilation control strategies may be used in variable air volume systems (Wang and Xu 2002; Elovitz 1995; Janu, Wenger, and Nesler 1995). Ke and Mumma (1999) presented eight ventilation control strategies and their annual energy and indoor air quality simulation results for an academic building as if it were situated in each of six geographic locations. The results showed that dynamic minimum outdoor air with

combined primary airflow and supply air temperature reset optimization is the best of reducing total energy consumption than the others (fixed minimum outdoor air percentage and rate, dynamic minimum outdoor air based upon the generalized multiple-spaces equation, etc.).

The CO_2-based demand-controlled ventilation (CO_2-DCV) is one of the strategies that could reduce energy use by reducing the unnecessary over-ventilation of buildings. This strategy is investigated in several studies (Alalawi and Krarti 2002; Persily 1993). The energy consumption reduction benefits derived through the use of this strategy have been demonstrated for many different applications (Schell 1998; Carpenter 1996). ASHRAE Standard 62-2001 (ASHRAE 2001) proposes the multiple space equation, which corrects the fraction of outdoor ventilation air in a supply system in order to minimize energy use while maintaining a proper indoor air quality (IAQ) in all zones, including the critical one. The multiple space equation has been discussed and implemented by several researchers (Kettler 2003; Ke and Mumma 1997b; and Mumma and Bolin 1994).

1.4   Genetic Algorithm

A genetic algorithm GA is a search procedure based on the mechanics of Darwin's natural selection. They combine survival of the fittest among string structures with a structured yet randomized information exchange to form a search algorithm with some of the innovative flair of human search (Holland 1992). GA has been applied to a diverse range of scientific, engineering, and economic search problems (Goldberg 1989). Most of the initial research work can be found in various International Conference Proceedings. However, there exist now several textbooks on GAs (Gen and Cheng 2000; Vose 1999; Mitchell and Netlirary Inc, 1996; and Michalewicz, 1994). Examples of applications of GA in the science and engineering fields include optimization of neural network structure and weights, solution of optimal control problems, design of structures

and image feature recognition (Lee and Lam 1995; and Katz and Thrift 1994). The potential of GA for use in process control and control of air-conditioning systems has also been studied (Lam 1995; and Nordvik and Renders 1991). Lam (1995) found that classifier system with genetic algorithm was applicable to on-line computer control of air-conditioning systems and implementation of a self-learning control system. Huang and Lam (1997) optimized controller parameters for HVAC systems by using genetic algorithms, the results showed that the GA method yields a better performance than that of the traditional Ziegler-Nichols method for controller tuning. The GA is also used to design HVAC systems (Asiedu, Besant, and Gu, 2000; and Wright 1996). Wright (1996) described the performance of a simple genetic algorithm search method instead of using direct search optimization methods, it is concluded that the algorithm exhibits rapid initial progress but that final convergence is slow due to the highly constrained nature of the optimization problem. It is suggested that a more effective use of the constraint functions could improve the convergence and robustness of the algorithm. The performance of the algorithm is also sensitive to the problem formulation. Asiedu and robert (2000) used GA to design an HVAC air duct system with minimum life-cycle cost. Wright and Farmani (2001) investigated the simultaneous optimization of building fabric design, HVAC system size and the supervisory control strategy by using genetic algorithm search method, the results indicated that GA is effective in finding a feasible solution from an initial randomly generated population of solutions and exhibits rapid convergence on a solution.

The principles of multi-objective genetic algorithm optimization are different from that in a single-objective genetic algorithm optimization (Deb 2001). Many researchers have attempted to summarize the studies of multi-objective genetic algorithm optimization (Deb 2001; Veldhuizen and Lamont 1998; and Fonseca 1995). These reviews list many different techniques of multi-criterion optimization that exist to date. Wright and Loosemore (Wright and Loosemore 2001) investigated the application of a multi-objective genetic algorithm (MOGA) search method in the identification of the optimum

pay-off characteristic between the elements of the building design problem. Results were presented for the pay-off characteristics between daily energy cost and zone thermal comfort, and for building capital cost and energy cost. It was concluded that the MOGA was able to find the optimum pay-off characteristic between the daily energy cost and zone thermal comfort, but that the characteristic between the capital cost and energy cost was sub-optimal. However, this study showed that multi-objective genetic algorithm search methods offer great potential for the identification of the pay-off between the elements of building thermal design, and as such can help inform the building design process.

1.5   Summary and Discussion

Several studies have investigated the optimum set points of one or several local-loop controllers. For example, Ke and Mumma (1997a) investigated the interactions between the supply air temperature and ventilation requirement. Englander and Norford (1992) minimized the supply duct static pressure set point without sacrificing occupant comfort or adequate ventilation, and Braun, Klein, Mitchell, and Beckman (1989a) determined the chilled water set point by optimizing chilled systems. With a view of optimizing the overall system performance, the system approach was utilized in optimal control strategies in a few studies. It could be concluded from this literature review that the existing system-based optimal control studies did not address the following points: (*i*) the interaction between the controoler set points and outdoor airflow rate; (*ii*) the interaction between the individual zone temperature set points with other set points; and (*iii*) controlling and varying the thermal comfort during the day as a function of daily energy use by utilizing the two-objective optimization approach, which leads to further energy savings. To date, the on-line optimization of the overall system performance, including individual zone temperature set points, have not been investigated using the two-objective optimization problem. In the next chapter, the performance of the investigated HVAC system is evaluated through the monitored data.

CHAPTER 2

SYSTEM DESCRIPTION AND MONITORING

The performance of the investigated HVAC system is evaluated by analyzing the available monitored data. How the optimization process developed in this thesis could improve performance is also discussed. In processing the monitored data for three years, 2001-2003, many operation and design problems are detected, and are presented and discussed in the references (Kajl, Nassif, and Daigle 2003 and Kajl, Kenné, Paquin, and Daigle 2003). However, only the operation deficiencies related to our optimization task are presented here. The control strategies of the investigated HVAC system are also described in this chapter.

2.1   Control Strategies of Existing System

The investigated HVAC system, which uses variable air volume (VAV), is installed in one of the most advanced "intelligent buildings" in North America today. The system serves the Montreal campus of the École de technologie supérieure (ÉTS). One chilled water cooling system is used to supply water to eleven air-handling units (AHUs). The heating water is supplied from the central heating system installed outside the campus. This central heating system provides hot water for several buildings installed in the same area. Of the eleven AHUs of the HVAC system installed at the ÉTS campus, only the two AHUs (named AHU-6 and AHU-4) are investigated. The AHU-6 meets the load for 70 interior zones on the second floor, while the AHU-4 meets the load for 68 south-west perimeter zones located on the first, second, and third floors. Figure 2 shows the zones at the second floor served by the AHU-6 and AHU-4 units. Figure 3 illustrates the schematic of typical HVAC system AHUs (AHU-6 or AHU-4). The descriptions of the control strategies of the investigated HVAC system are presented below.
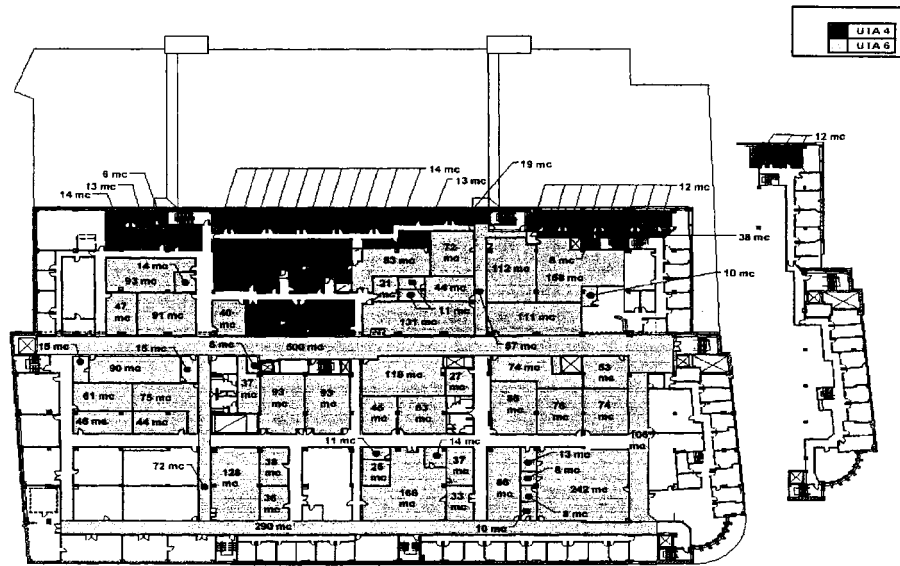
Figure 2   Schematic of zones at second floor served by AHU-6 and AHU-4 units
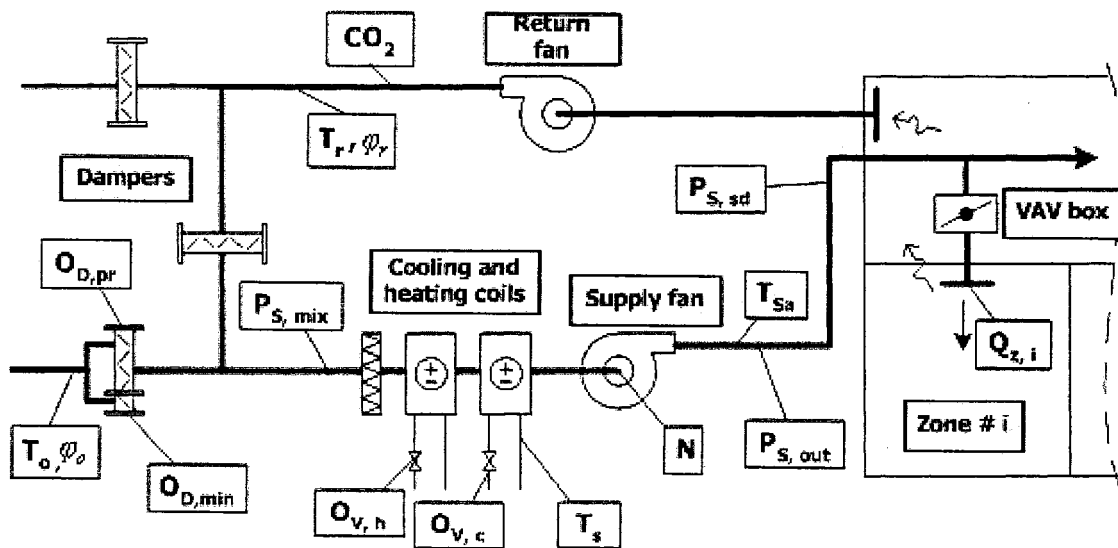
Figure 3   Schematic of AHU-6 or AHU-4 of HVAC systems with the required
           measured variables

2.1.1   Sequencing Control Strategy for AHU

The purpose of the sequencing control strategy for the AHU is to determine the most economical method of using the components of the AHU to maintain the supply air temperature at a set point value. The sequencing control strategy implemented in the AHUs of the HVAC system installed at the ÉTS campus is a "split-range sequencing control strategy". This traditional sequencing control strategy is described in several studies (ASHRAE 2003; Seem, Park, and House 1999).

2.1.2   Dampers Economizer Control Strategy

An economizer is used to control the proportion of outdoor air in the supply air. It consists essentially of three dampers: an outdoor damper, a discharge damper, and a recirculation damper. The conventional strategy coupling all three dampers is used in the HVAC system of the ÉTS campus. The investigated economizer control strategy uses the enthalpy logic, as a result of which the outdoor enthalpy and return enthalpy are compared in order to determine the operation of the economizer.

2.1.3   Ventilation Control Strategy

Several ventilation control strategies are used in the HVAC system in an effort to satisfy the minimum outdoor air requirements at the AHU. However, the ventilation control strategy of the investigated HVAC system could be referred to as the "modified fixed minimum outdoor air percentage". The outdoor damper consists of two parts, one being for the economizer, and called the mixing outdoor and return air damper (*Mix_Damper*), and the other for ventilation, and called the minimum outdoor air damper (*Min_Damper*). When the CO_2 concentration is equal to or less than 600 PPM, this strategy uses a fixed *Min_Damper* position (20% *Min_Damper* and 0% *Mix_Damper*), such that the outdoor air passing through the outdoor damper is approximately equal to a

fixed percentage of the fan airflow rate. When the CO_2 concentration is increased, the *Min_Damper* position is modulated to control the outdoor airflow rate, making the CO_2 concentration less than 800 PPM.

2.1.4   Controller Set Points

The supervisory control strategy of the investigated HVAC system adjusts the controller set points to constant values, or using a particular strategy. The supply air temperature set point is a function of the outdoor air temperature and of the fan airflow rate. The supply air temperature set point changes linearly within the 13 to 18°C range when the outdoor temperature varies between –20 and +20°C. The supply air temperature calculated above is corrected by adding a value which varies linearly from –2 to +2°C, which corresponds to the variation of the fan airflow rate ratio from 50 to 90%. The supply air temperature set point is always limited between 13 and 18°C. The chilled water supply temperature and duct static pressure set points are constant. Zone temperature set points are always fixed within the thermal comfort range for occupied periods.

2.2   Measured and Required Data

The monitoring is performed through a central DDC and data acquisition, taking data from measurements located in different locations of secondary and primary system. Figure 3 shows the schematic of this investigated HVAC system with measured variables required in these studies:

- Outdoor and return air temperatures and relative humidity (T_o, T_r, φ_o and φ_r, respectively);
- Supply air and water temperatures (T_{sa} and T_{sw}, respectively);

- Zone airflow rates $(\dot{Q}_{z,i})$;

- Supply duct, outlet fan, mixing plenum static pressures $(P_{S,sd}, P_{S,out}, \text{and } P_{S,mix}$ respectively);

- Fan speed (N);

- Minimum and principal damper and cooling and heating coil valve positions $(O_{D,min}, O_{D,pr}, O_{V,c}, \text{and } O_{V,h},$ respectively);

- CO_2 concentration in return air duct (Rco_2).

The following are additional required variables that are not measured:

- Fan and outdoor airflow rate $(\dot{Q}_{fan} \text{ and } \dot{Q}_o,$ respectively);

- Inlet and outlet cooling coil relative humidity ($\varphi_{in,c}$ and $\varphi_{ou,c}$, respectively);

- Liquid flow rate through the heating or cooling coils $(\dot{Q}_l)$.

2.3   Monitoring of Existing System

Monitoring serves to: (i) collect and process the data required in the component model and optimization process validations, and (ii) evaluate the performance of the existing HVAC system and the associated operational problems. The following section discusses the performance of the AHU-4 and AHU-6 HVAC systems and how the optimization can improve this performance.

2.3.1   VAV Box Damper

The VAV damper positions for the AHU-4 and AHU-6 are monitored over a period of three years (2001-2003). It was found that they are partially opened during the occupied period. Figure 4 shows the VAV damper positions of the AHU-6 (70 interior zones) for August 8 to 10, 2002. Only the damper position values above 60%, which are based on a

duct static pressure set point of 250 Pa, are illustrated. To save fan energy use, the duct static pressure could be decreased to a given point while maintaining the VAV boxes with the most demand fully open. Even more savings could be obtained by optimizing the air temperature set points of zones with VAV boxes with the most demand as well as the supply air temperature. When the zone air temperature set points are increased or the system supply air temperature is decreased, the zone airflow rates required to meet the loads are decreased, and the damper positions with the highest demand are then moved to lower positions premising a lower system duct static pressure set point. The proposed optimization with the proper constraints (i.e. VAV box positions that are not saturated at full open) offers the best choice among these three set points for minimizing system energy use.

2.3.2   Supply Air Temperature Set Point

Since the supply air temperature set point is determined as a function of the outdoor temperature and the fan airflow rate, without considering individual zone loads, the supply temperature may not be low enough to meet relative high zone loads or not be high enough to prevent overcooling in certain zones under low loads (when reheats are not used, as in the AHU-6).

Figure 5 shows the zone temperatures, damper positions and zone airflow ratios when the supply air temperature is 15°C, while Figure 6 illustrates the case for a supply air temperature of 13°C. In Figure 5, the airflow rate introduced into this selected zone attains the maximum value recorded in the VAV local control loop (the damper, even when open, only reaches 80%). It is clear that because of the high load in this zone, the supply temperature of 15°C is not enough to bring the zone temperature to its set point. In contrast, in Figure 6, after the zone airflow rate reaches the minimum level (30% of maximum value), the air supply temperature of 13°C is not high enough to prevent the overcooling of this selected zone (laboratory zone). It is therefore necessary to have a

proper and optimal determination of the supply air temperature set point with proper constraints to be able to overcome these problems as well as to decrease energy use.
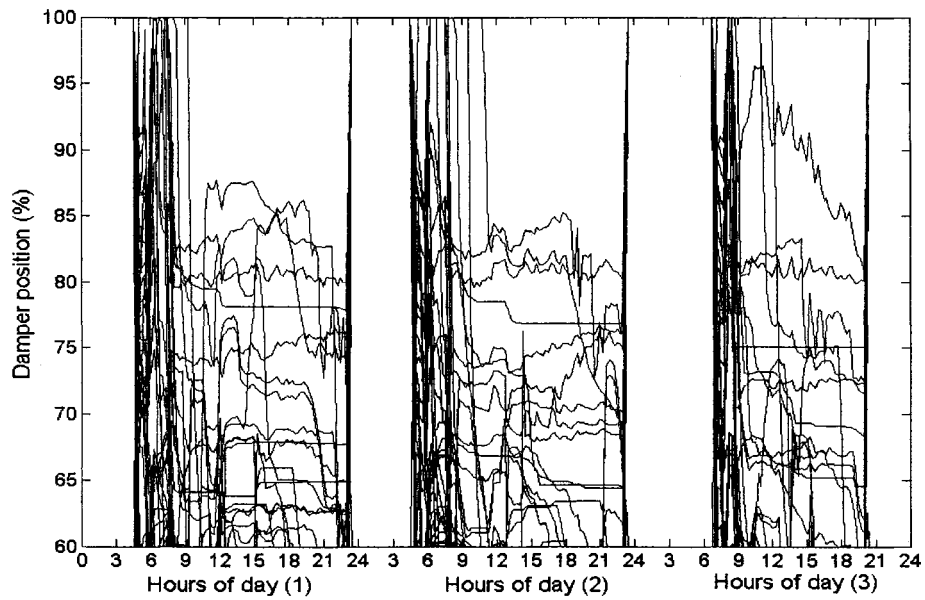
Figure 4   VAV box damper positions of AHU-6 for August 8 to10, 2002

(a)   (b)
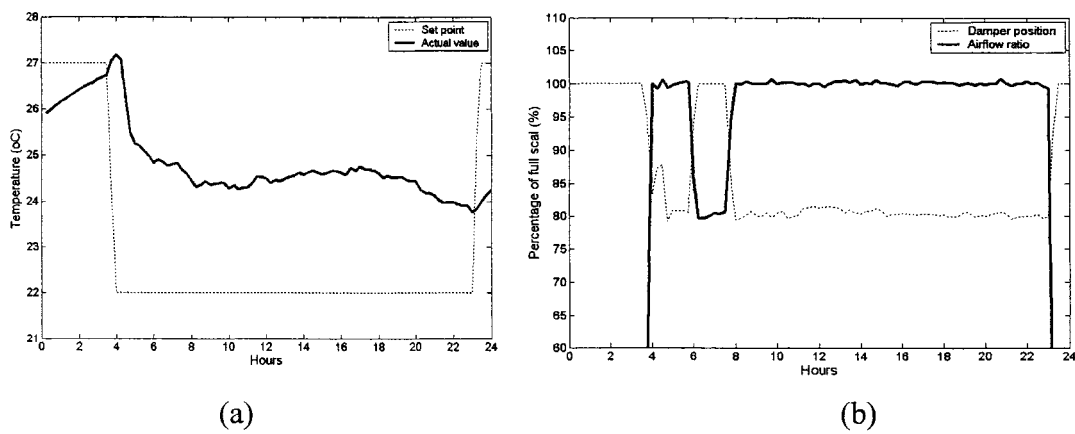
Figure 5   Zone temperatures (a), damper positions and zone airflow ratios (b)
                  when the supply air temperature is 15 °C for one day of August, 2002

(a)   (b)
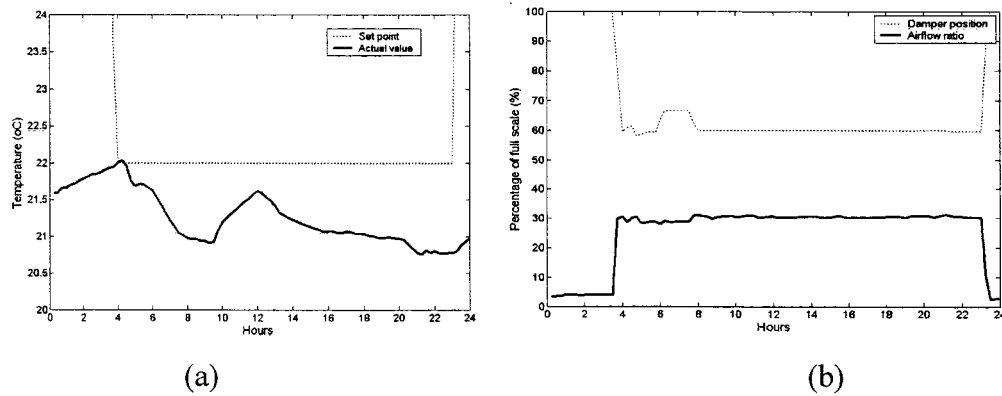
Figure 6   Zone temperatures (a), damper positions and zone airflow ratios (b)
             when the supply air temperature is 13 °C for one day of August, 2002

2.3.3   Economizer Dampers Operation Technique

An air-side economizer is used to control the proportion of outdoor air in the supply air. The economizer consists essentially of three dampers: an outdoor damper, a discharge damper, and a recirculation damper. As mentioned above, the conventional strategy coupling all three dampers is used here. When the outdoor damper is moved to position X%, the recirculation damper is at 1-X%. Given the nonlinearity of these dampers, the amount of decreasing outdoor air when the damper is moved down (X%) is not equal to the increase in the recirculation air at (1-X%). It can be concluded that the static pressure in the mixing plenum is increased when the damper changes its position. Figure 7 shows the mixing plenum static pressure when the outdoor damper is moved down from its full position. At 6:00, when the damper (Mix_Damper) changes its position, the static pressure is sharply increased although the fan airflow rate (building thermal load) does not very significantly. This increase in static pressure leads to a high fan energy use. To decrease fan energy use by decreasing the mixing static pressure, a new strategy should be developed. This could be achieved by linearizing the three damper characteristic (Krakow, Zhao, and Muhsin 2000).
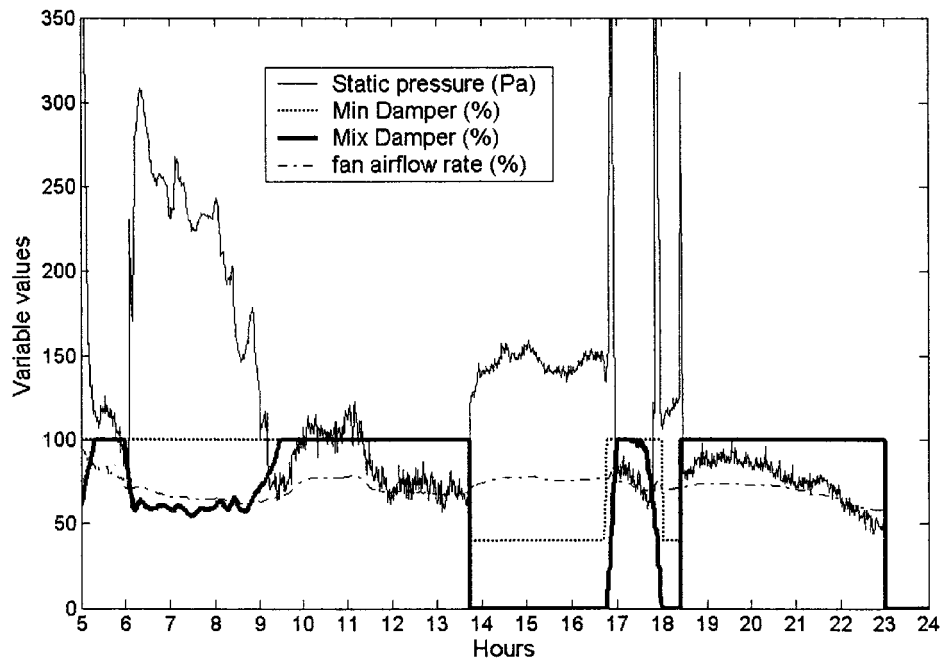
Figure 7   Mixing plenum static pressure when the outdoor damper is moved down from full position.

2.3.4   CO₂ Concentration and Ventilation Control Strategy

Through monitoring, it is observed that the CO_2 concentration in the return duct is just under 500 PPM all year round, which indicates that the outdoor airflow rate is higher than necessary, thus causing high energy use. Figure 8 shows the CO_2 concentration in the return duct for July 2002. Although the outdoor damper is at its minimum position, the CO_2 concentration in the return duct is around 500 PPM. It can be concluded that the outdoor airflow introduced into the system is greater than what is required. The proper ventilation strategy introducing the exact outdoor air requirement is thus developed in Chapter 3 in order to reduce the chiller energy use while meeting ventilation requirements.
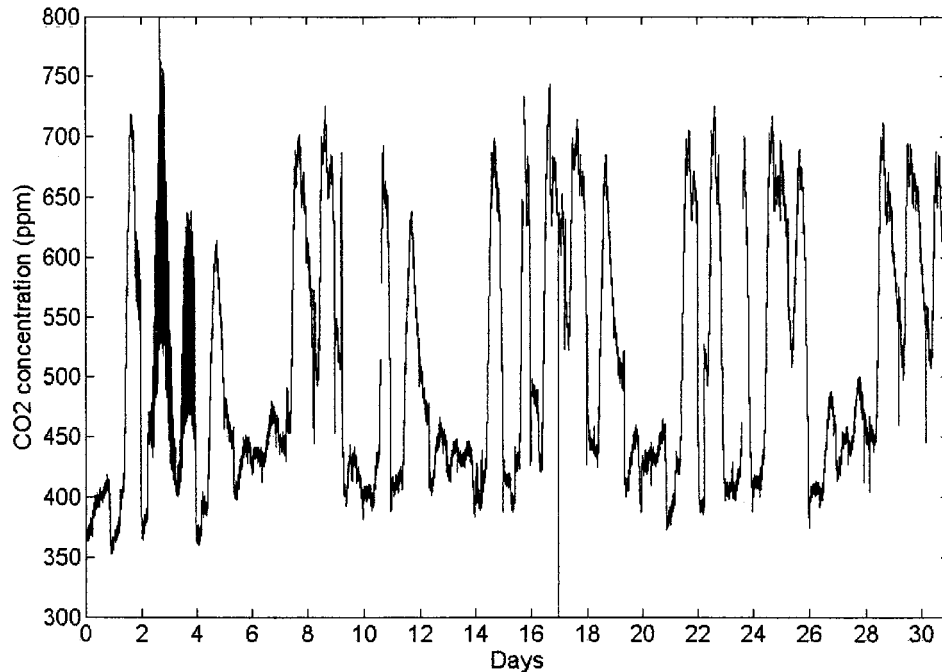
Figure 8 CO_2 concentration in return duct for July 2002

2.3.5   Chilled Water Valve Position

Through the monitoring of the chilled water valve positions, we found they are about 50% during the operation, excluding the cooling down period. Figure 9 shows the chilled water valve positions for July 2002. Although the highest cooling loads exist in this month, the average valve position is about 45%. It should be noted that on the first three days, the chiller was turned off (operational problems). Respecting the zone humidity constraint, the chilled water supply temperature set point can be increased until the valve becomes at full position. Thus, the water flow rate should be verified using the optimization constraint to ensure it is always lower than the maximum water flow rate (33 l/s). Chiller energy saving is obtained by increasing the chilled water supply temperature, thanks to an improved chiller coefficient of performance (COP). The optimization of the chilled water supply temperature set point through the proposed

optimization process, with the proper constraint, could lead to savings in chiller energy use. The chilled water supply temperature and supply air temperature should be limited in order to meet humidity requirements.
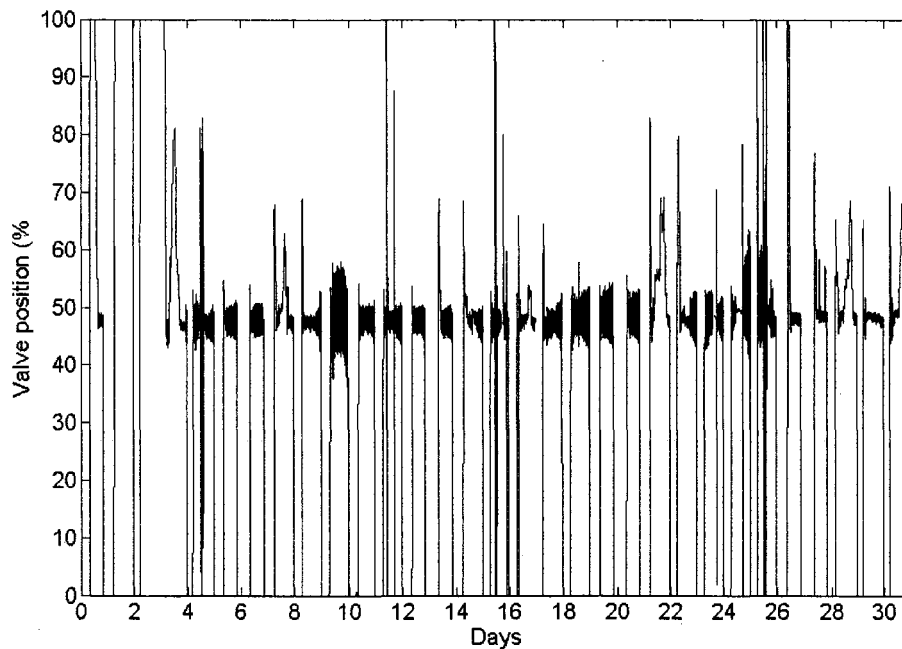
Figure 9   Chilled water valve positions for July 2002

2.3.6   Fan Airflow Rate

The supply fan is controlled to maintain the desired static pressure, while the return fan is controlled to maintain the return and supply flow differential required to space static pressure control. Supply and return airflows ($\dot{Q}_{fan}$) are not measured, but rather, are calculated by the system control, using the monitored fan speed (N) and applying the fan laws:

$$\dot{Q}_{fan} = \frac{N}{N_{design}} * \dot{Q}_{fan,design} \tag{2.1}$$

Figure 10 shows the fan performance curve. The system curve (A) passing through the design point (D) is illustrated. Since the supply fan of the investigated HVAC system is controlled to maintain the desired static pressure of 250 Pa in the supply air duct (Point C), the actual fan airflow rate is therefore represented by the operation fan curve (B), expressed in terms of duct and fan static pressures ($P_{S,sd}$ and $P_{S,fan}$, respectively) determined as follows:

$$\dot{Q}_{fan} = \sqrt{\frac{P_{S,fan} - P_{S,sd}}{P_{S,fan,design} - P_{S,sd}}} * \dot{Q}_{fan,design} \tag{2.2}$$

It is clear that the fan airflow rates calculated through the system control (Equation 2.1) are lower than the actual fan airflow rate, which can be determined by Equation 2.2. There could be a 20% error at a low fan speed. As discussed in section 2.3.3, the mixing plenum static pressure varies with the variation of the outdoor damper, even with the fan airflow rate being the same. Therefore, the actual operation curve also differs from curve (B), and the actual fan airflow rate is close to, but not equal to that calculated by Equation 2.2. The fan model proposed in Chapter 4 and used by the optimization process could be used in order to determine the supply fan airflow rate, and then the flow differential required to space static pressure control. Figure 11 shows the fan airflow rate calculated by Equation 2.1, and implemented in the existing system, as well as the fan airflow rate with the fan developed model (see section 4.2.1). The inaccurate value of the calculated fan airflow rate through the existing control system strategy using Equation 2.1 leads to a malfunction of the building pressurization and outdoor airflow ventilation controls.
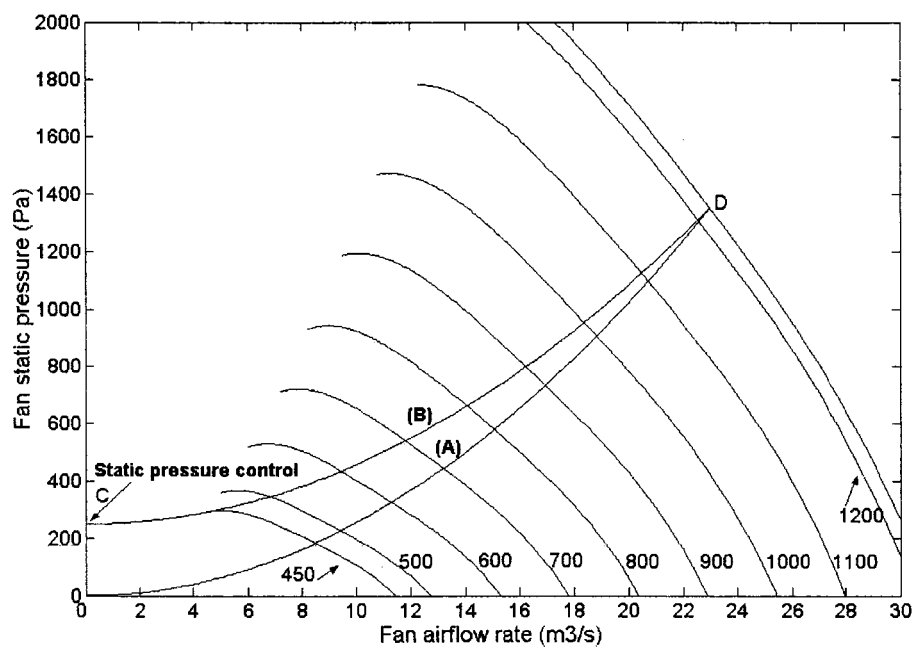
Figure 10   Fan performance curve
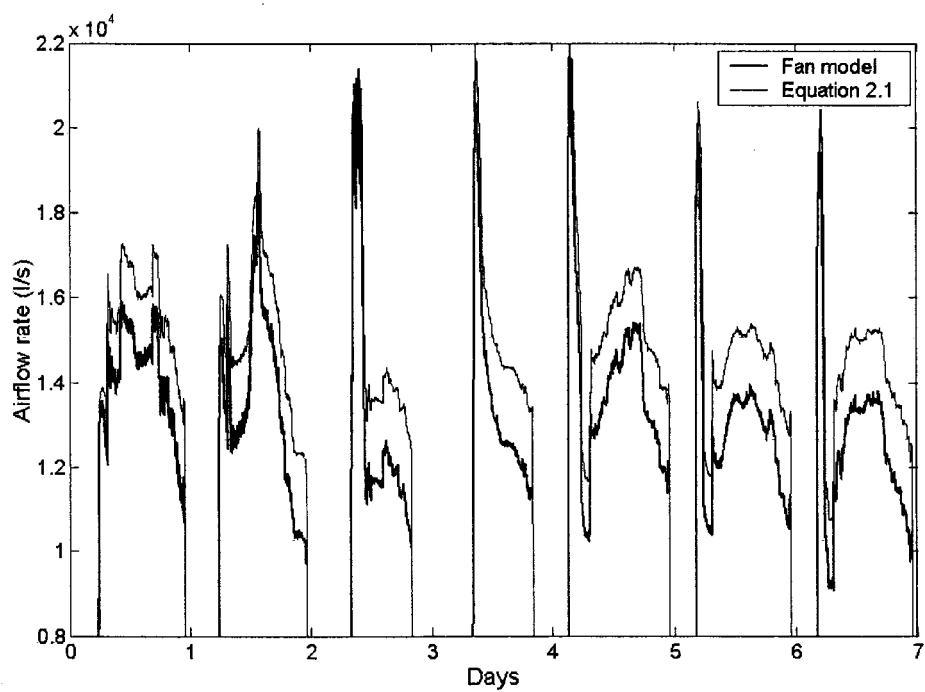
Figure 11   Fan airflow rates determined by fan model and Equation 2.1

2.4 Summary and Discussion

This chapter has presented and discussed the investigated HVAC system and described how the control strategies work. The performance evaluations of this system are conducted using data obtained from monitoring over a three-year period. As discussed in section 2.3, from the monitoring of the HVAC system installed at the ÉTS campus we see that certain operational problems do exist, even though this HVAC system is considered as the "intelligent buildings". Improper operation leads to wasted energy use. The proposed optimization process developed in this thesis improves the performance of both this system and of any others. Through the optimization of the supervisory control strategy, and while considering required constraints, the operation problem indicated above could be overcome and the energy use decreased, while maintaining the required thermal comfort.

As mentioned in section 2.3.4, the outdoor airflow rate introduced into the system is greater than what is required, and therefore leading to high energy use. Thus, the new ventilation control strategy is developed and presented in the next chapter in order to introduce the exact outdoor air requirement.

CHAPTER 3

VENTILATION CONTROL STRATEGY USING THE SUPPLY CO_2 CONCENTRATION SET POINT

This chapter proposes a new ventilation control strategy applied to multiple spaces subject to variable occupancy in order to integrate it in the optimization process. The strategy specified for real-time, on-line ventilation control takes advantage of uninitiated air from some over-ventilated spaces to be used as fresh outdoor air in order to reduce system energy use while maintaining the indoor air quality (IAQ) in each space. This proposed strategy maintains a supply CO_2 concentration set point low enough to dilute CO_2 generated by full occupancy in critical zones. The supply CO_2 concentration set point could be determined on-line using the monitored zone airflow rates. It is tested and evaluated by making comparisons with other known control strategies. The investigated existing VAV system is used to evaluate this new strategy. The outdoor air fraction and associated energy use of investigated ventilation control strategies are calculated using the VAV system component models developed and presented in the chapter 4. This strategy is detailed in the reference (Nassif, Kajl, and Sabourin 2005b).

3.1   Introduction

The quality of the air inside buildings and the associated energy use has been of growing significantly concern over the last 20 years. Many publications have discussed different ventilation control strategies (Janu 1995; Elovitz 1995; Wang and Xu 2002). The CO_2-based demand-controlled ventilation $(CO_2\text{-}DCV)$ is one of the strategies that could reduce energy use by reducing the unnecessary over-ventilation of buildings. This strategy is investigated in several studies (Alalawi and Krarti 2002 and Persily 1993). The energy consumption reduction benefits derived through the use of this strategy have been demonstrated for many different applications (Schell 1998 and Carpenter 1996). When this strategy is applied for multiple spaces by detecting the CO_2 concentration in return air, the poor air quality may result inside certain zones. To overcome this

problem, ASHRAE Standard 62-2001 (ASHRAE 2001) proposes the multiple space equation (*MSE*), which corrects the fraction of outdoor ventilation air in a supply system in order to minimize energy use while maintaining a proper indoor air quality (IAQ) in all zones, including the critical one. Since the amount of outdoor air is based on the design number of occupants, this amount could be more than required by the actual number (off-design), and result in waste in energy use. The *MSE* has been discussed and implemented by several researchers (Kettler 2003; Ke and Mumma 1999; Ke and Mumma 1997b; Mumma and Bolin 1994).

The "supply CO_2-based demand-controlled ventilation" (*S-CO$_2$-DCV*) technique proposed in this paper is a compromise between the *MSE* and the *CO$_2$-DCV*, taking into account: (*i*) the actual occupancy of the building and (*ii*) the critical zone ventilation requirement. This proposed strategy allows the on-line control of the outdoor air in response to actual building occupancy (as in *CO$_2$-DCV*) while ensuring the ventilation requirements of each individual zone, including the critical zone (as in *MSE*). It is tested and evaluated through a comparison with other conventional control strategies. The investigated existing HVAC system is used to evaluate this new strategy. The outdoor air fraction and associated energy use of investigated ventilation control strategies are calculated using the VAV system component models that are developed and presented in chapter 5.

3.2 Ventilation Control Strategies

The ventilation control strategy aims to provide an acceptable IAQ with minimum energy consumption. The two criteria, "the IAQ quality" and "energy use" are used to evaluate the five different control strategies investigated in this chapter. The following are the control strategies studied:

- Strategy S_1: fixed minimum outdoor air percentage;

- Strategy S_2: fixed minimum outdoor air rate;

- Strategy S_3: CO_2-based demand-controlled ventilation (CO_2-DCV);

- Strategy S_4: multiple space equation (MSE);

- Strategy S_5: proposed supply CO_2-based demand-controlled ventilation (S-CO_2-DCV).

All these strategies use the outdoor, return and exhaust dampers to control the proportion of outdoor air in the supply air. Figure 12 shows a schematic diagram of the AHU air distribution system for the investigated VAV system, with the key points used. The symbol of fan airflow introduced in the building ($\dot{Q}_b$) is used here instead of that used in other chapters as ($\dot{Q}_{fan}$) in order to keep the homogenous symbols in this Chapter. The controller output specified by the implemented ventilation control strategy is used to modulate the three-coupled dampers in order to provide an adequate outdoor airflow rate to meet the ventilation requirement.
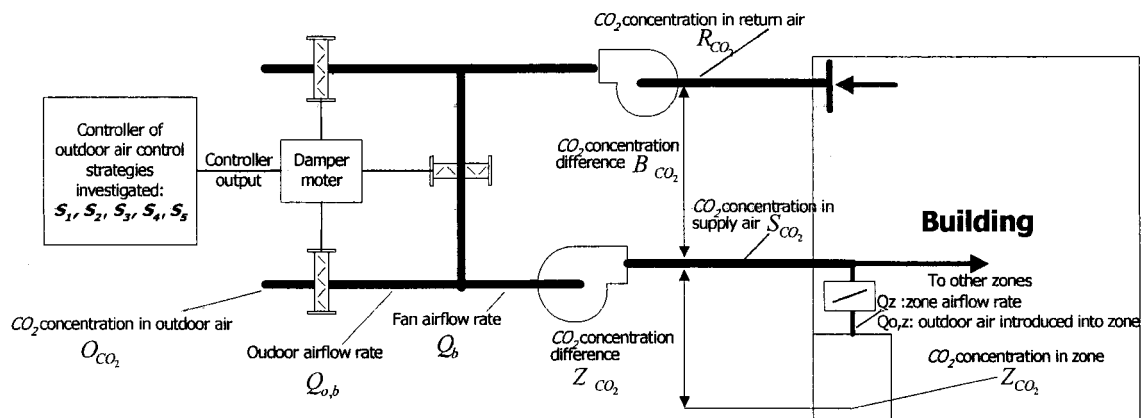
Figure 12   Schematic diagram of the AHU air distribution system for VAV system with the key points used

At the design phase, the amount of outdoor air to be introduced into each zone i ($\dot{Q}_{o,z,dsg,i}$) or whole building ($\dot{Q}_{o,b,dsg}$) is based on providing enough outdoor air to meet the ventilation requirements at full occupancy, i.e., the ventilation rate per person (15 cfm). The fraction of outdoor air introduced into zone i ($Y_{z,dsg,i}$) and building ($Y_{b,dsg}$) at the design phase are given:

$$Y_{z,dsg,i} = \frac{\dot{Q}_{o,z,dsg,i}}{\dot{Q}_{z,dsg,i}} \qquad (3.1)$$

$$Y_{b,dsg} = \frac{\dot{Q}_{o,b,dsg}}{\dot{Q}_{b,dsg}} \qquad (3.2)$$

At design condition, the simple relationship between the occupant-generated CO_2 (ventilation load-VL) and the indoor CO_2 concentration (Z_{CO_2}) and outdoor air ($\dot{Q}_o$) is presented in Appendix C of Standard 62-2001 in the following steady-state mass balance equation:

For zone i:

$$VL_{z,dsg,i} = \dot{Q}_{o,z,dsg,i} \cdot (Z_{CO_2,i} - O_{CO_2}) \qquad (3.3)$$

For the building

$$VL_{b,dsg} = \dot{Q}_{o,b,dsg} \cdot (R_{CO_2} - O_{CO_2}) \qquad (3.4)$$

The last equation can be rewritten for off design in terms of the airflow rate introduced into the building (fan airflow rate-$\dot{Q}_b$) and the CO_2 concentration difference ($B_{\Delta CO_2}$) between the return (R_{CO_2}) and supply (S_{CO_2}) air:

$$VL_b = \dot{Q}_b \cdot B_{\Delta CO_2} \qquad (3.5)$$

where

$$B_{\Delta CO_2} = R_{CO_2} - S_{CO_2} \qquad (3.6)$$

Equation (3.3) could also be represented using the zone airflow rate ($\dot{Q}_{z,i}$) and the CO_2 concentration difference between the zone (Z_{CO_2}) and supply (S_{CO_2}) air:

$$VL_{z,i} = \dot{Q}_{z,i} \cdot (Z_{CO_2,i} - S_{CO_2}) \qquad (3.7)$$

ASHRAE Standard 62-2001 indicates that comfort criteria with respect to human bioeffluents are likely to be satisfied if the ventilation rate is 15 cfm per person. This corresponds to an indoor/outdoor CO_2 differential of 700 ppm. It means that the Standard requires a maximum CO_2 concentration of 1000 ppm in zones, based on the assumption of outdoor air being 300 ppm. Equations 3.3 and 3.4 become, for design conditions (full occupancy and fan airflow rate):

$$VL_{z,dsg,i} = Y_{z,dsg,i} \cdot \dot{Q}_{z,dsg,i} \cdot 700 \qquad (3.8)$$

$$VL_{b,dsg} = Y_{b,dsg} \cdot \dot{Q}_{b,dsg} \cdot 700 \qquad (3.9)$$

Four terms $R_{v,b}$, $R_{a,,b}$, $R_{v,z}$, $R_{a,z}$ are introduced here in order to take into account the on-line operation (off-design conditions). These are defined by the following equations:

$$\left\{ \begin{array}{ll} R_{a,b} = \dfrac{\dot{Q}_b}{\dot{Q}_{b,dsg}} & R_{a,z,i} = \dfrac{\dot{Q}_{z,i}}{\dot{Q}_{z,dsg,i}} \\ \\ R_{v,b} = \dfrac{VL_b}{VL_{b,dsg}} = \dfrac{N_b}{N_{b,dsg}} & R_{v,z,i} = \dfrac{VL_{z,i}}{VL_{z,dsg,i}} = \dfrac{N_{z,i}}{N_{z,dsg,i}} \end{array} \right\} \qquad (3.10)$$

The terms N_b and $N_{z,i}$ represent the actual occupancy in the building and in each zone i, respectively.

The airflow part-load ratios of the building and zone i ($R_{a,b}$, $R_{a,z,i}$, respectively) are defined as the ratio of the actual-to-design airflow rate. The ventilation part-load ratios of the building and zone i ($R_{v,b}$, $R_{v,z,i}$, respectively) are defined as the ratio of the actual - to- design number of occupants.

In order to calculate the actual CO_2 concentration difference between supply and return air ($B_{\Delta CO_2}$), Equations 3.6, 3.9, and 3.10 are used:

$$B_{\Delta CO_2} = \frac{Y_{b,dsg} \cdot 700 \cdot R_{v,b}}{R_{a,b}} \qquad (3.11)$$

The same logic applicable for zones, the actual CO_2 concentration difference between supply and return air in zone i ($Z_{\Delta CO_2,i}$) is given:

$$Z_{\Delta CO_2,i} = \frac{Y_{z,dsg,i} \cdot 700 \cdot R_{v,z,i}}{R_{a,z,i}} \qquad (3.12)$$

Both (CO_2-DCV) and the proposed (S-CO_2-DCV) strategies determine the amount of ventilation outdoor airflow in response to actual building occupancy (real time, on-line ventilation load) by detecting the CO_2 concentration. However, the other control strategies (S_1, S_2, and S_4) do not respond to occupancy change, and the outdoor air is determined according to full occupation. Figure 13 shows the investigated ventilation control strategies, which are described in the following paragraphs.
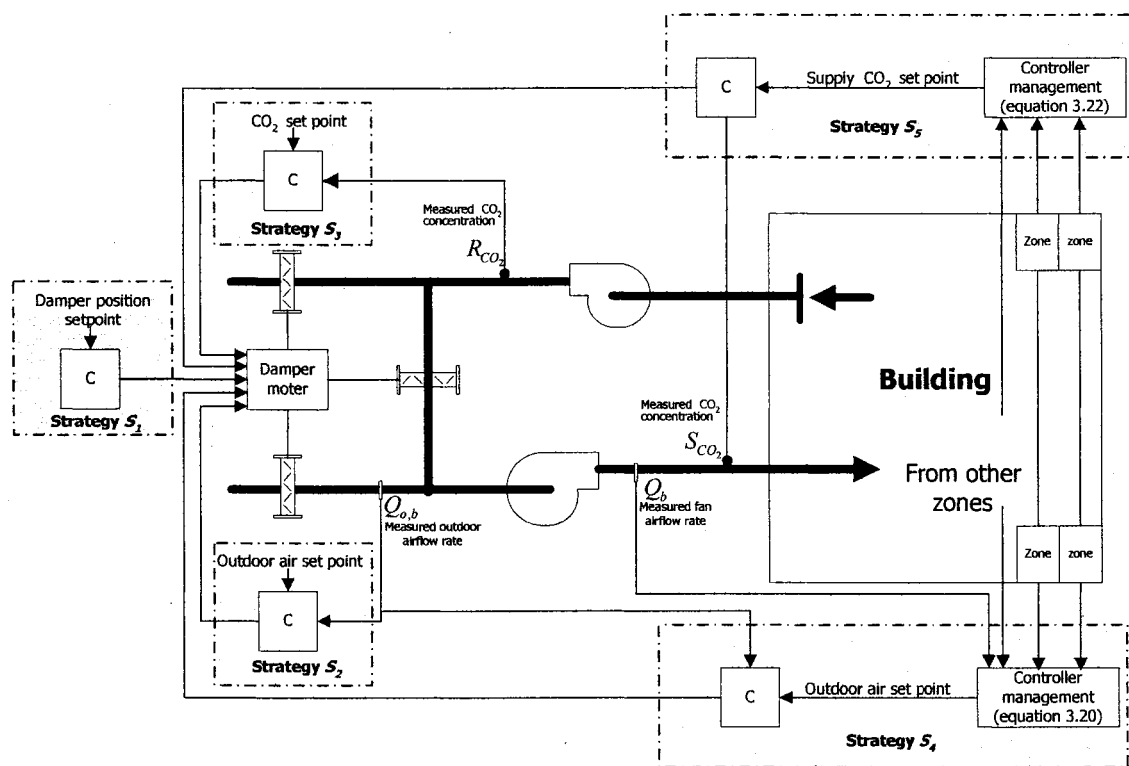
Figure 13   Investigated ventilation control strategies

3.2.1   Fixed Minimum Outdoor Air Percentage (S_1)

This strategy uses a fixed percentage of outdoor air to supply air when the economizer is not activated. This fixed percentage is based on providing enough outside air to meet the requirements of the building at full occupancy ($R_{v,b} = 1$) and at design airflow rate ($R_{a,b}$

$=1$). This strategy is commonly achieved by a fixed minimum outdoor air damper position (Ke and Mumma 1999). The actual fraction of outdoor airflow (Y_b) when the economizer is not activated is always constant and equal to the design value. It is then presented as:

$$(Y_b)_{S_1} = \frac{\dot{Q}_{o,b,dsg}}{\dot{Q}_{b,dsg}} = Y_{b,dsg} \qquad (3.13)$$

Figure 13 shows this control strategy. During the occupied period, and when the economizer is not activated, the controller output is used to maintain the damper at a constant position. The main drawback of this control is the low outdoor air available with low supply air, which leads to a poor IAQ at both the building and individual zone levels

3.2.2 Fixed Minimum Outdoor Air Rate (S₂)

This control strategy maintains a constant amount of outdoor airflow rate determined at full occupancy. The on-line fraction of outdoor airflow (Y_b) becomes:

$$(Y_b)_{S_2} = \frac{\dot{Q}_{o,b,dsg}}{\dot{Q}_b} = \frac{Y_{b,dsg}}{R_{a,b}} \qquad (3.14)$$

This strategy takes into account the actual value of the fan airflow presented by the term $(R_{a,b})$. This strategy is commonly achieved by using the measurement of the outdoor airflow rate as shown in Figure 13. During the occupied period, and when the economizer is not activated, the controller output is used to adjust the position of three-

coupled dampers in order to maintain the measured outdoor airflow rate at its set point value.

3.2.3 CO_2-Based Demand-Controlled Ventilation (S_3)

The CO_2-based demand-controlled ventilation (CO_2–DCV) strategy allows an HVAC system to control the amount of outdoor air supplied to entire system. It detects carbon dioxide in the return duct as an indicator of occupancy density, and adjusts the outdoor air based on this CO_2 concentration. Since this strategy maintains the CO_2 concentration in the return duct at the threshold set point limit while overlooking the individual zone CO_2 concentration, some zones may be over or under-ventilated. The controller output of this strategy, which is determined by comparing the CO_2 concentration in the return air with its set point value, is used to modulate the three-coupled dampers accordingly (see Figure 13). The resulting amount of outdoor airflow should be enough to maintain the return CO_2 concentration set point.

The on-line fraction of outdoor airflow in the supply air could be calculated using the CO_2 concentration balance of return, outdoor and supply air.

$$Y_b = \frac{R_{CO_2} - S_{CO_2}}{R_{CO_2} - O_{CO_2}} \tag{3.15}$$

Using Equations 3.6 and 3.11 while maintaining the return CO_2 concentration at a 1000 ppm set point and with an outdoor CO_2 concentration of 300 ppm, the equation above becomes, for strategy S_3:

$$(Y_b)_{S_3} = Y_{b,dsg} \cdot \frac{R_{v,b}}{R_{a,b}} \tag{3.16}$$

The on-line outdoor air fraction of the CO_2-DCV strategy, which varies with the on-line occupancy and fan airflow rate, is decreased at lower occupancy (decrease in $R_{v,b}$), while it is fixed for strategy S_1, and is only a function of the on-line fan airflow rate for strategy S_2. The decrease in the outdoor airflow rate used in this strategy at low occupancy is due to the term $(R_{v,b})$, which considers the actual on-line occupancy.

When there is wide variance between the ventilation and design loads, the CO_2-DCV ventilation provides a significant energy savings potential, but with possible poor IAQ in certain zones, especially when the multiple spaces are subject to variable profile occupancy and variable load profiles. The multiple space equation described below can provide a good air quality inside all zones, including critical zone, by introducing higher outdoor air determined by the critical zone ventilation requirement at full occupancy.

3.2.4   Multiple Space Equation (S₄)

According to the ASHRAE Standard 62-2001, "Where more than one space is served by a common supply system, the ratio of outdoor to supply air required to satisfy the ventilation and thermal control requirements may differ from space to space". As a result, the critical space requiring the highest percentage of outdoor airflow drives the percentage of outdoor air required by the entire system. The outdoor airflow rate can be reduced by taking advantage of uninitiated air from non-critical spaces to be used as fresh outdoor air. The corrected fraction of outdoor ventilation air in the supply system (Y_b) as given in the ASHRAE Standard 62-2001 is used:

$$Y_b = \frac{X}{1 + X - Z} \tag{3.17}$$

Since the on-line occupancy patterns change arbitrarily from what is originally assumed, the on-line fraction of the outdoor ventilation air in the supply system is always determined at full occupancy.

The term X is the uncorrected fraction of outdoor ventilation air required at full occupancy in the supply system (the ratio of the sum of outdoor ventilation airflow rates for all zones to the fan airflow rate). The term Z is the ratio of the required outdoor air at full occupancy to the primary air in the critical zone.

$$X = \frac{\dot{Q}_{o,b,dsg}}{\dot{Q}_b} = \frac{Y_{b,dsg}}{R_{a,b}} \tag{3.18}$$

$$Z = \left\{\frac{\dot{Q}_{o,z,dsg}}{\dot{Q}_z}\right\}_{critical} = \left\{\frac{Y_{z,dsg}}{R_{a,z}}\right\}_{critical} \tag{3.19}$$

Using Equations 3.18 and 3.19, Equation 3.17 becomes:

$$(Y_b)_{S_4} = \frac{\dfrac{Y_{b,dsg}}{R_{a,b}}}{1 + \dfrac{Y_{b,dsg}}{R_{a,b}} - \left\{\dfrac{Y_{z,dsg}}{R_{a,z}}\right\}_{critical}} \tag{3.20}$$

This strategy takes into consideration the actual values of the fan and critical zone airflow rates by using the $(R_{a,b})$ and $(R_{a,z})$ factors. The strategy is achieved as shown in Figure 13. The controller management determines the outdoor airflow rate set point through Equation 3.20, and using the measured fan and zone airflow rates. The controller output determined by comparing the measured outdoor airflow rate with its set

point value is used accordingly to modulate the three-coupled dampers. The resulting amount of outdoor airflow should be enough to provide the proper IAQ in all zones. Compared to the CO_2-DCV strategy, the MSE strategy needs much higher outdoor airflow– and consequently higher energy use – when the on-line occupancy pattern is significantly decreased from what is originally assumed at design. The main drawback of this control strategy is its inability to respond to changes in occupancy, as does the CO_2-DCV. This seems to be due to the term $(R_{v,b})$ not being included in Equation 3.20. The proposed "supply CO_2-based demand-controlled ventilation" provides a good IAQ in zones, while taking into account the actual building occupancy as described below.

3.2.5   Supply CO2-Based Demand-Controlled Ventilation (S_5)

The supply CO_2-based demand-controlled ventilation strategy (S-CO_2-DCV) maintains the supply CO_2 concentration at a set point value ($S_{CO_2,set}$) determined using the monitored zone airflow rates, which has recently become possible with the use of direct digital control terminal boxes. The supply CO_2-concentration set point is calculated by assuming that full occupancy is faced in the critical zone. This permits the diluting of the highest possible CO_2 generation. Since the set point considers the full occupancy in the critical zone, over-ventilation may occur in the critical as well as in the non-critical zones when the actual occupancy is lower than the full design value. Over-ventilation in the different zones leads to a lower return CO_2 concentration and a resulting lower outdoor flow rate to maintain the required supply CO_2-concentration set point.

Since the supply CO_2 set point must maintain the CO_2 concentration in the critical zone at a lower level than the required threshold ($Z_{CO2,th}$), it could be assumed that the CO_2 concentration in the critical zone is always at the threshold level (i.e., 1000 ppm). This further ensures that the CO_2 concentration in the critical zone does not exceed the threshold level, and the steady state balance in the critical zone could be used to determine the supply CO_2 concentration set point. Thus, by assuming that there is full

occupancy, the steady state balance presented in Equation (3.7) could be rewritten for each zone as:

$$S_{CO_2,set} = \min\left\{Z_{CO_2,th,i} - \frac{VL_{z,dsg,i}}{\overset{\bullet}{Q}_{z,i}}\right\} \tag{3.21}$$

A term within the "min" is calculated for each zone i, representing the required supply CO_2-concentration to dilute the full occupancy CO_2 generation, and the lowest value is used to determine the supply CO_2 concentration set point. The critical zone is the zone requiring the lowest value of supply CO_2-concentration. The resulting on-line CO_2 concentration in the critical zone, which may have either a design or an off-design ventilation load, is equal to or lower than the threshold point. Using Equation 3.8 and threshold ($Z_{CO2,th}$) of 1000 ppm, Equation above becomes:

$$S_{CO_2,set} = \min\left\{1000 - 700 \cdot \frac{Y_{z,dsg,i}}{R_{a,z,i}}\right\} \tag{3.22}$$

The supply CO_2 concentration set point equals the least value of $S_{CO_2,set}$, which is corresponding to the highest value of $Y_{z,dsg}/R_{a,z}$. The supply CO_2 concentration set point is only function of $R_{a,z}$ calculated from measured zone airflow rates.

A comparison of the proposed strategy (S-CO_2-DCV) with the MSE and CO_2-DCV leads to the following conclusions:

1. The S-CO_2-DCV takes into account the on-line over-ventilation that occurs in the building while considering the critical zone ventilation requirement.
2. The CO_2-DCV takes into account the on-line over-ventilation in the building without considering the critical zone ventilation requirement.

3. The *MSE* takes into account the design over-ventilation in the different zones.

At a low building ventilation load, the ventilation flow rate may be lower than the outdoor air required to dilute building-source contaminants and to maintain space pressurization. To overcome these problems, the minimum outdoor airflow rate is limited in order to provide an adequate outdoor air for other occupancy purposes. The building-source contaminant, which does not vary with on-line occupancy variations, could be estimated at the design condition.

In order to satisfy the ventilation requirement in the critical zone (i.e.15 cfm per person), the threshold point ($Z_{CO2,th}$) must be lower than or equal to 1000 ppm, based on the assumption of outdoor air being 300 ppm. Using the assumption above, and inserting Equations 3.8, 3.11, and 3.21 into the CO_2 concentration balance Equation 3.15, it can be concluded that the one-line outdoor fraction for S-CO_2-DCV strategy is given as:

$$(Y_b)_{S_5} = \cfrac{Y_{b,dsg} \cdot \cfrac{R_{v,b}}{R_{a,b}}}{1 + Y_{b,dsg} \cdot \cfrac{R_{v,b}}{R_{a,b}} - \left\{ \cfrac{Y_{z,dsg}}{R_{a,z}} \right\}_{critical}} \tag{3.23}$$

The outdoor fraction is less than that obtained from the multiple space equation (3.20) because of the term $R_{v,b}$ (on-line occupancy). Since the actual number of occupants in each zone is not easy to predict unless there is a CO_2 concentration sensor located in each zone, it is proposed that this strategy maintain a supply CO_2 concentration set point low enough to dilute CO_2 generated by full occupancy in the critical zone. As shown in Equation (3.20), the zone with the highest value of ($Y_{z,dsg}/R_{a,z}$) is considered to be the critical zone.

When it is possible to predict the actual occupancy in critical zone $R_{v,z}$, the outdoor air fraction could be calculated as follows:

$$Y_b = \frac{Y_{b,dsg} \cdot \dfrac{R_{v,b}}{R_{a,b}}}{1 + Y_{b,dsg} \cdot \dfrac{R_{v,b}}{R_{a,b}} - \left\{ Y_{z,dsg} \cdot \dfrac{R_{v,z}}{R_{a,z}} \right\}_{critical}} \qquad (3.24)$$

Since there are difficulties faced in predicting occupancy by measuring the CO_2 concentration in all zones, Equation 3.24 is not investigated in this research. The S-CO_2-DCV strategy can be applied through the following two methods:

S-CO₂-DCV Strategy with the Local Loop

This method employs the local CO_2 control loop to maintain the supply CO_2 concentration below its set point (Equation 3.22) by controlling the outdoor damper. This is the same as with the CO_2-DCV, except that the CO_2 concentration sensor is placed in the supply duct rather than in the return one. Figure 13 shows the S-CO_2-DCV strategy with the local control loop. The controller management calculates the supply CO_2 concentration set point through Equation 3.22, and using the monitored zone airflow rates. The controller output, which is determined by comparing the measured supply CO_2 concentration with its calculated set point value, is used to modulate the three-coupled damper accordingly.

S-CO₂-DCV Strategy with Equation 3.23

The outdoor air fraction in this method is determined by Equation 3.23. However, the actual occupancy in the building ($R_{v,b}$) must be predicted using the methods presented in several studies (Ke and Mumma 1997; Wang and Jin 1998). With these methods, the actual number of occupants in the whole building is calculated using the monitored CO_2 concentration in the return and the supply air.

3.3 Control Strategy Optimization

The proposed supply CO_2-based demand-controlled ventilation could be integrated into the on-line optimization program of the supervisory control strategy such that with each simulation, the set points of the HVAC system, including the supply CO_2 concentration set point, could be optimized. To reduce the outdoor airflow rate, the supply CO_2 concentration set point should be increased by using the higher airflow supplied in the critical zone. This could be achieved by optimizing the zone reheat (supply zone air temperature), system supply and zone air temperature set points. The S-CO_2-DCV as well as the CO_2-DCV could be applied on-line without using the CO_2 control loop, allowing Equations 3.16 and 3.23 to be used. In that case, the actual occupancy in the entire building could be determined based on the measured CO_2 concentrations in the supply and return air.

3.4 Evaluation of Ventilation Control Strategies

The investigated ventilation control strategies are evaluated and tested using the characteristics of the existing HVAC system installed at the ÉTS campus. Only two air handling units (AHU-6 and AHU-4) working alongside several others to provide conditioned air to the ETS campus are investigated. Figure 12 shows a schematic diagram of the investigated VAV system. The AHU-6 meets the thermal loads for 70 internal zones on the second floor, while the AHU-4 meets the thermal loads for 68 south-west perimeter zones. The investigated ventilation control strategies are evaluated and tested for following three cases:

- Evaluation based on three operating conditions of a VAV system. In this evaluation, the potential of the proposed strategy to introduce an exact outdoor air for ventilation comfort are presented.
- Evaluation based on real monitored data of the AHU-6 system. The performances of the VAV system working with the strategies (S_3, S_4 and S_5) are

discussed. How the proposed strategy minimizes the chiller energy use by introducing an exact outdoor air for ventilation comfort is presented and discussed.

- Evaluation based on bin weather data of different locations tested on the AHU-4 system. The effect of the actual occupancy (Rv) and the locations on annual energy use of all investigated strategies are studied.

For these evaluations, the three modeling methodologies (MM) presented below were developed. It should be noted that the ventilation control strategy for the AHU-4 and AHU-6 systems uses a fixed minimum air damper position while the return CO_2 concentration is less than 600 ppm, and otherwise, the damper position is modulated to maintain a return CO_2 concentration set point of 750 ppm. The design outdoor airflow fractions of all zones could be approximated to be the same as 16% ($Y_{z,dsg,i}$ =0.16), and the design building outdoor airflow fraction is 23 % ($Y_{b,dsg}$ =0.23). The two design building and zone fractions are not the same because the sum of the design zone airflow rate equals about 0.76% of the design fan airflow rate (diversity factor).

3.5   Modeling Methodology

To study the energy use and satisfactory zone ventilation of the investigated strategies, the component models required for simulation calculations such as the fan, damper, cooling coil, and chiller models, are developed and validated against the monitored data as will discuss in chapter 6. Three modeling strategies (MM-1, MM-2, and MM-3) required for the three evaluations presented above are used:

MM-1   Modeling strategy for evaluation based on three operating conditions of a VAV system operation. The outdoor air fractions of investigated strategies are determined by Equations (3.13, 3.14, 3.16, 3.20, and 3.23).

MM-2   Modeling strategy for AHU-6 system evaluation. The chiller energy use and indoor air quality index ($CO2$ concentration) are determined using the measured data and validated component models. The fan airflow rate (to meet the thermal load) is calculated from monitored data, whereas the CO_2 concentrations, outdoor air fraction, and chiller energy use are then determined by the detailed and validated component models. This modeling strategy is illustrated in Figure 14, and described below.

MM-3   Modeling strategy for AHU-4 system evaluation. The annual energy use and indoor air quality index (CO_2 concentration) are determined using the weather bin temperature data and validated component models. The thermal loads at given zone temperatures are simplified as a function of outdoor temperature and heat gain from occupants, whereas the CO_2 concentrations, outdoor air fractions, and chiller and heating energy uses are then determined by the detailed and validated component models. This modeling strategy is illustrated in Figure 15, and described below.

3.5.1   Modeling Strategy for AHU-6 System Evaluation (MM-2 Real Monitored Data)

The chiller energy use and outdoor air fraction are determined using validated component models and the measured data for one year (2002) culled from the AHU-6 VAV system. The monitored data is provided at each minute, and saved to a data file throughout the year. The periods of June, July, August, and September are only investigated when the economizer may be at minimum air mode and ventilation control strategy is required for application. This limited period is only investigated for the following reasons, concluded from the monitoring of the AHU-6 (internal zones):

- The outdoor damper is often modulated in winter and mid-season weather (free cooling) in order to maintain supply air temperature set points without ventilation a control strategy requirement.

- The valve position of the heating coil is opened only for a few days a year (during very cold weather). In addition, there are no zone reheats working with the AHU-6 system that provides conditioned air to the internal zones (cooling loads). Thus, the effect of ventilation control strategies on annual heating energy use could be neglected.

The modeling methodology (see Figure 14) is divided into two calculation parts: (i) pre-calculation and (ii) VAV system model. The airflow and ventilation part-load ratios ($R_{a,b}$, $R_{a,z}$, and $R_{v,b}$) are determined in the first one, while the outdoor airflow rate and energy use are obtained in the second.

In the pre-calculation part, the airflow and ventilation part-load ratios ($R_{a,b}$, $R_{a,z}$, and $R_{v,b}$) are determined by Equation (3.10) using: (i) the fan airflow rate and building ventilation loads (VL_b) calculated from the measured data, and (ii) the measured zone airflow rates. The fan airflow rate is not measured, but rather, is calculated by the validated fan model based on the dimensionless coefficients of flow, pressure, and head. The inputs of the fan model consist of the measured static pressures and fan speed. The building ventilation load (VL_b) is determined by Equations (3.5 and 3.15) using the calculated outdoor and fan airflow rates and the measured return CO_2 concentration. The outdoor airflow rate in the existing system is also not measured, but calculated using the damper model based on exponential relations. The inputs of the damper model consist of the measured mixing duct static pressure and damper position. When the airflow and ventilation part-load ratios are determined, the outdoor airflow rate and energy use are determined by VAV system model.
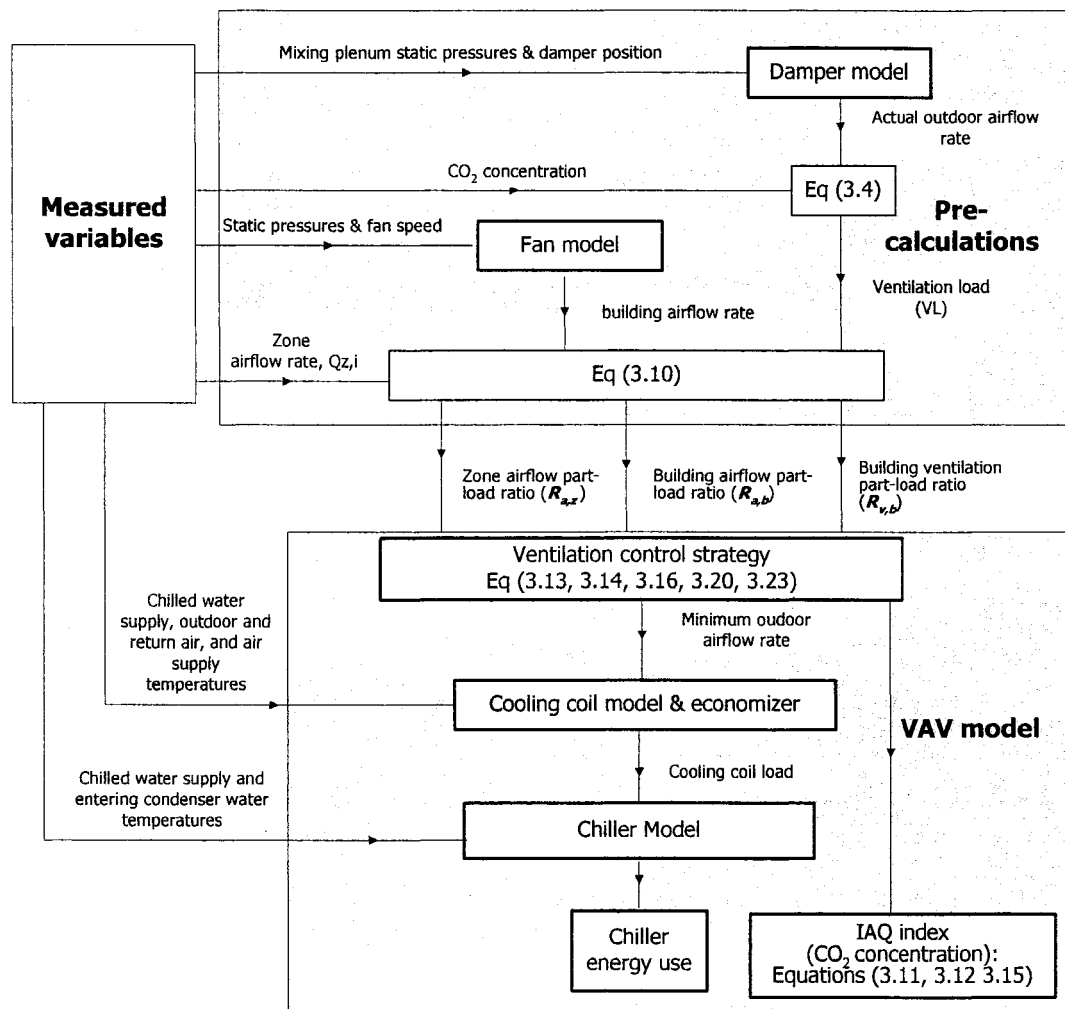
Figure 14   Modeling strategy used for AHU-6 system evaluation

The VAV system model could be presented through the four following main steps:

Step 1. The outdoor airflow fractions are determined for CO_2-DCV (S_3), MSE (S_4), and S- CO_2-DCV (S_5) strategies using Equations (3.16, 3.20, and 3.23), respectively. The highest value of $Y_{z,,dsg}/R_{a,z}$ (critical zone) is used in Equations (3.20 and 3.23).

Step 2. This step represents the iteration process during which the initial value of the cooling coil leaving air humidity ratio is assumed, and the new value is calculated and

reused. This iterative process continues calculating through the loop several times until the values of the cooling coil leaving air humidity ratio stabilize within a specified tolerance. The cooling coil model developed from the ASHRAE HVAC 2 Toolkit (Brandemuel 1993) and presented in chapter 5 is used. The initial value of the cooling coil leaving air humidity ratio is assumed and that for the return air is determined using building latent loads calculated from actual occupancy ($R_{v,b}$). The measured return air temperature can be used because the building thermal cooling load and supply air temperature set point do not vary with changes in the outdoor airflow rate (strategies used). The mixing plenum air temperature and humidity ratio are determined using the energy balance, knowing the outdoor and fan airflow rates and outdoor and return conditions. The cooling coil load and cooling coil leaving air humidity ratio are determined through a detailed cooling coil model using the input variables: the calculated fan airflow rate, calculated mixing plenum air conditions (air condition entering the cooling coil), measured chilled water and air supply temperatures. The cooling coil leaving air humidity ratio is then compared to the previous value. This iterative process continues calculating through the loop several times until the values of the cooling coil leaving air humidity ratio stabilize within a specified tolerance.

Step 3. The chiller energy is determined by the chiller model using the performance curves of electric chillers as functions of variables such as the calculated cooling coil load, measured entering condenser water temperature, and measured chilled water supply temperature (NRCC 1999). This model is presented in chapter 5.

Step 4. The CO_2 concentrations in the critical zones as indexes of indoor air quality are determined. The rise in the CO_2 concentration throughout the building is determined by Equation (3.11). The supply and return CO_2 concentrations are determined using Equation (3.15). The CO_2 concentration in the critical zone is determined by adding the term ($Z_{\Delta CO_2,i}$) calculated by Equation (3.12) to the supply CO_2 concentration.

3.5.2 Modeling Strategy for AHU-4 System Evaluation (MM-3-Weather Bin Temperature Data)

The objective of this evaluation is to study the effect of the actual occupancy (Rv) and the weather locations on annual energy use with the investigated strategies.

The annual energy use (considering the heating period) and indoor air quality in zones are determined at different values of Rv and at different locations. Since the objective is not to obtain accurate predictions of energy use for design purposes, but rather, to be able to make meaningful comparative evaluations of various different control and operating strategies at different ventilation load ($R_{v,b}$) and building locations, the thermal loads are determined as functions of bin weather temperature and actual occupancy. These evaluations are made on an AHU-4 system using the bin temperature data of Montreal, Seattle, and Dallas. Thus, the monitored real data for one year are only used to determine the constant parameters of Equation (3.25) below, which is developed for determining the building and zone thermal loads as a function of outdoor air temperature and occupancy.

The thermal load as a function of the bin weather temperature with the simplified simulation approach (modified bin method) was investigated by Reddy, Liu, and Claridge (1998) in order to obtain sound and meaningful diagnostic insights of actual building performance and operating ventilation control strategies. The results of these control ventilation strategy studies which are based on a simplified HVAC simulation approach are consistent with the conclusions reached by other researchers using more detailed simulation models (Reddy, Liu, and Claridge 1998).

As mentioned above, it assumed that the total sensible thermal building ($q_{s,b}$, %) or zones loads for fixed interior temperatures are functions of internal thermal loads and outdoor temperature. To separate the sensible thermal load from the actual occupants ($c_b.R_{v,,b}$), all internal thermal loads other than occupancy are considered as constant

values during the occupancy period. Thus, the building (or zone) sensible thermal loads are given by:

$$q_{s,b} = a_b \cdot t_o + b_b + c_b \cdot R_{v,b} \qquad (3.25)$$

The building (or zone) sensible thermal loads of the existing VAV system (AHU-4), which are equal to the energy removed from the space, when the space temperature is constant, are calculated, and the parameters of the equations above are determined.
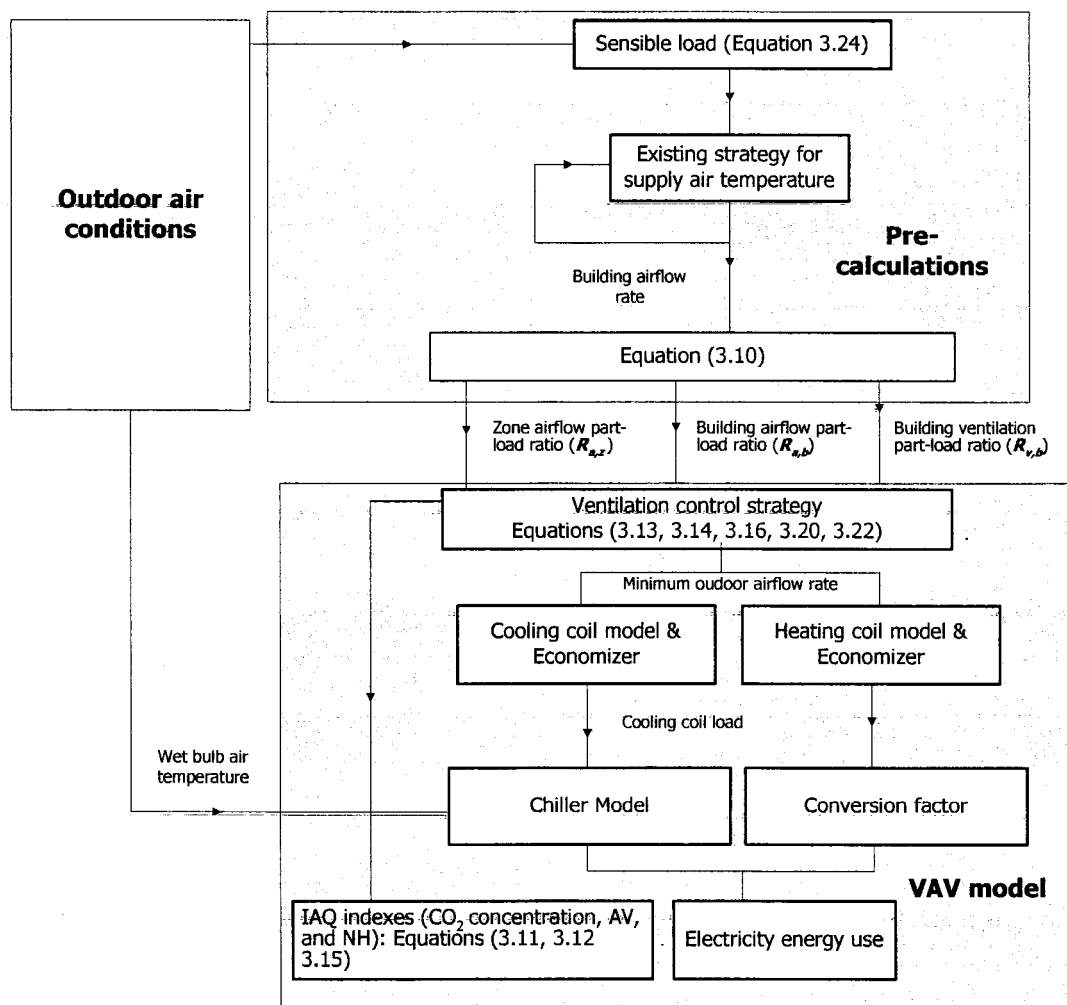
Figure 15   Modeling strategy used for AHU-4 system evaluation

The modeling strategy (see Figure 15) is also divided into two calculation parts: (i) pre-calculation and (ii) VAV system model, which is the same as that described above. The airflow and ventilation part-load ratios ($R_{a,b}$, $R_{a,z}$, and $R_{v,b}$) are determined in the first, and the outdoor airflow rate and energy use are obtained in the second.

In the pre-calculation part, the thermal sensible building or zone loads are determined by Equation (3.25) for each bin temperature. To calculate the fan and zone airflow rates from the sensible thermal loads, the supply air temperature must be known. The supply air temperature set point is determined by the strategy applied in the existing system (it is a function of the outdoor temperature and the fan airflow rate). The strategy is described as follows: the supply air temperature set point changes linearly within the 13 to 18°C range as the outdoor temperature varies within the –20°C to 20°C range. The supply air temperature calculated above is corrected by adding a value which varies linearly from –2 to +2°C, corresponding progressively to the variation of the fan airflow rate ratio from 50 to 90%. The supply air temperature set point is always limited within the 13 to 18°C range. Since the supply air temperature set point is a function of the fan airflow rate, the iteration process is applied using the initial fan airflow rate value.

The building and zone airflow part-load ratios ($R_{a,b}$, $R_{a,z}$) are determined by Equation (3.10) using the calculated fan and zone airflow rates. It should be noted that the $R_{v,b}$ is assumed for each calculation.

In the VAV system model, the energy use and indoor air quality are determined using the VAV model similar to that described above, while taking into account the AHU-4 specifications. The chilled water supply temperature of 7.2°C is assumed as in an actual system. The condensing water temperature higher than the outdoor wet temperature by 3°C is assumed. The summer and winter zone temperatures are 23 and 22°C, respectively. The zone reheats are used and calculated when the zone airflow rates are at their minimum in order to maintain zone air temperature. The heating coil and

dehumidification models are also used. The humidification strategy applied in the existing HVAC system is used. The humidification valve position is modulated to maintain the return air relative humidity set point determined by the control strategy of the AHU-4 system. The conversion factor of non-electrical energy consumption (heating coil and humidifiers) to electricity was assumed to be 0.21 (Ke and Mumma, 1997a). The fan energy use calculated by the fan model is considered for annual energy use. The inputs of the fan model are thus the calculated fan airflow rate and the fan static pressure. The fan static pressure is determined by an equation representing the operation curve (B) in Figure 10 (see Equation 4.33), which is a function of the fan airflow rate and the supply duct pressure set point of 300 Pa.

3.6   Evaluation Results

3.6.1   Results of Evaluation Based On Three Operating Conditions (MM-1)

In order to evaluate the ventilation control strategies, the outdoor air fraction and CO_2 concentration in the return, supply and critical zones of each investigated ventilation control strategy are determined and presented in Table I for three operating conditions:

A. *Design fan airflow rate and occupancy.* In this case, all part-load factors ($R_{a,b}$, $R_{v,b}$, $R_{a,z}$, $R_{v,z}$) are equal to 1.

B. *Off-design fan airflow rate and full occupancy.* In this case, the following are assumed: (*i*) full occupancy (design building ventilation load, $R_{v,b}$ =1), (*ii*) off-design fan airflow rate assumed to be 50% of design rate ($R_{a,b}$ =0.5), and (*iii*) airflow rate introduced into critical zone falls to its minimum limit (30% of design); at full occupancy, that means $R_{a,z}$=0.3 and $R_{z,v}$=1.

C. *Off-design fan airflow rate and occupancy.* In this case, the following are assumed: (*i*) off-design occupancy ($R_{v,b}$ =0.5) and off-design fan airflow rate ($R_{a,b}$ =0.5), and (*ii*) airflow rate introduced into critical zone falls to its minimum limit (30% of design) at full occupancy, that means $R_{a,z}$ =0.3 and $R_{z,v}$ =1.

Table I

Results of the evaluation based on three operating conditions

	Strategy	Design fan airflow rate and occupancy	Off-design fan airflow rate and full occupancy	Off-design fan airflow rate and occupancy
		A	B	C
Part-load ratios	System	$R_{a,b}=1$, $R_{v,b}=1$	$R_{a,b}=0.5$, $R_{v,b}=1$	$R_{a,b}=0.5$, $R_{v,b}=0.5$
	Critical zones	$R_{a,z}=1$, $R_{v,z}=1$	$R_{a,z}=0.3$, $R_{v,z}=1$	$R_{a,z}=0.3$, $R_{v,z}=1$
Outdoor air fraction Y	S_1	10	10	10
	S_2	10	20	20
	S_3	10	20	10
	S_4	10	23.1	23.1
	S_5	10	23.1	13
CO_2 concentration in critical zone, ppm	S_1	1000	1733.3	1163.3
	S_2	1000	1093.3	813.3
	S_3	1000	1093.3	1163.3
	S_4	1000	1000	766.3
	S_5	1000	1000	1000
CO_2 concentration in supply air, ppm	S_1	930	1560	930
	S_2	930	860	580
	S_3	930	860	930
	S_4	930	766.6	533
	S_5	930	766.6	766.6
CO_2 concentration in return air, ppm	S_1	1000	1700	1000
	S_2	1000	1000	650
	S_3	1000	1000	1000
	S_4	1000	906	603
	S_5	1000	906	836.6

The design building and zone outdoor airflow fractions in this evaluation are assumed to be 10% ($Y_{z,dsg,i}$ and $Y_{b,dsg}$ are 0.1). The outdoor air fraction is determined using the Equations (3.13, 3.14, 3.16, 3.20, and 3.23). The CO_2 concentration rise throughout the building is determined by Equation (11). The supply and return CO_2 concentrations are determined using Equation (3.15). The CO_2 concentration in the critical zone is determined by adding the term ($Z_{\Delta CO_2,i}$) calculated by Equation (3.12) to the supply CO_2 concentration.

At design conditions (Case A), all the strategies perform similarly, as shown in the third column of Table I. At off-design fan airflow rate and full occupancy (Case B), strategies S_4 and S_5 perform similarly, as shown in the fourth column. Although strategies S_1, S_2 and S_3 introduce less outdoor air fraction, the fraction is not sufficient to meet the ventilation requirements in all zones. At off-design fan airflow rate and occupancy (Case C), S_5 introduces a much lower outdoor air fraction than S_4 while maintaining good indoor quality in all zones.

A comparison of the three strategies S_3, S_4 and S_5 shows for Case C that S_3 (CO_2-based demand-controlled ventilation) introduces the least – but inadequate – outdoor air fraction to meet ventilation requirements, causing poor indoor air quality in certain zones (CO_2 concentration is 1163.3 ppm). However, the multiple space equation (S_4) introduces an unnecessarily high outdoor air fraction required for actual occupancy. In this case, the over-ventilation is seen in both the critical (CO_2 concentration is 755 ppm) and non-critical zones, and consequently unnecessary energy is used to ventilate this high outdoor air. The supply CO_2-based demand-controlled ventilation (S_5) introduces an exact outdoor air fraction to meet ventilation requirements in the critical zone based on on-line occupancy in the building (CO_2 concentration is 1000 ppm), thus minimising the energy use required for better indoor air quality. To enhance the indoor air quality (compared to strategy S_3 in Case C), the supply CO_2 demand-controlled ventilation

provides only 3% additional outdoor air to satisfy all zones, whereas the multiple space equation provides 13.1%.

3.6.2 Results of Evaluation Based On Real Monitored Data of AHU-6 System (MM-2)

The CO_2-DCV (S_3), MSE (S_4), and S- CO_2-DCV (S_5) strategies are evaluated and compared with the actual operation scenario, using real monitored data for one year (2002) culled from the AHU-6 of the VAV system.

As mentioned above, the outdoor air fraction and associated chiller energy of the three investigated strategies are determined for the period of June, July, August, and September. The airflow and ventilation part-load ratios are first determined using the modeling strategy shown in Figure 14. The VAV system model is then used to calculate the system performance response due to theses values and the ventilation control strategy used. Figure 16 shows the building airflow and ventilation part-load ratios of the AHU-6 for July 25 to 31, 2002. It is clear that the ventilation part-load ratios (actual occupancy) for Saturday and Sunday are lower than those for other days. The outdoor airflow fractions of the investigated strategies tested on the AHU-6 are calculated by the VAV system model and illustrated for July 25 to 31 in Figure 17. In the first three days (Thursday, Friday, and Saturday), the outdoor air enthalpy is close to the return one, and the outdoor damper resulting from the economizer strategy thus varies between the full and minimum positions. Since strategies S_3 and S_5 consider the actual occupancy, their outdoor fractions are lower for Saturday and Sunday than for other days. The actual outdoor fractions (close to strategy S_1), are calculated by the damper model and shown in Figure 17. The fan energy use is not considered because the fan airflow rate and static pressure of all the investigated strategies have the same values. The chiller energy demands are calculated by the VAV system model, and illustrated for July 27 to 31 in Figure 18.
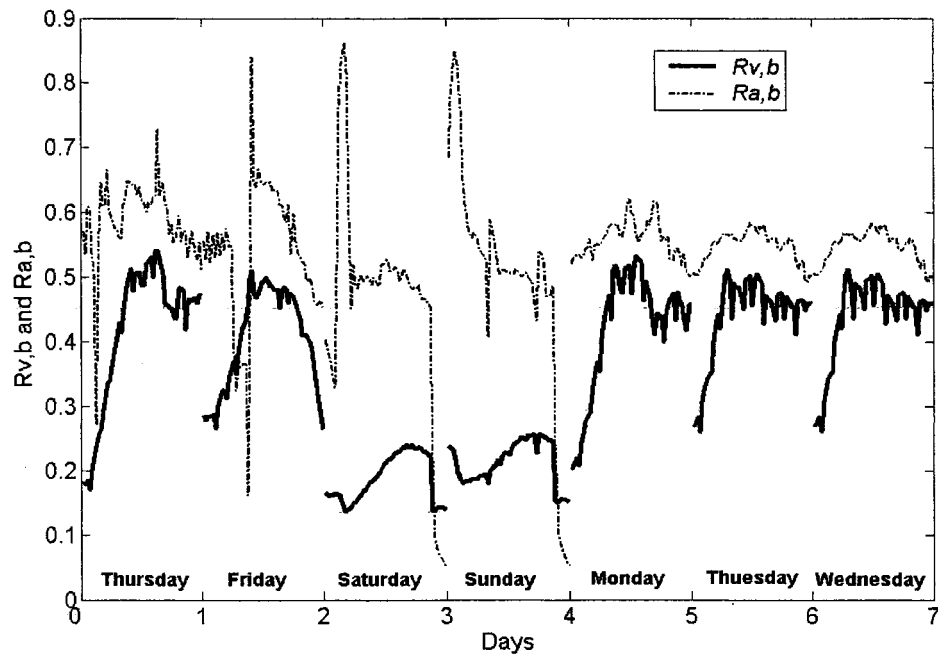
Figure 16   Building airflow and ventilation part-load ratios of AHU-6 for July
25 to 31, 2002
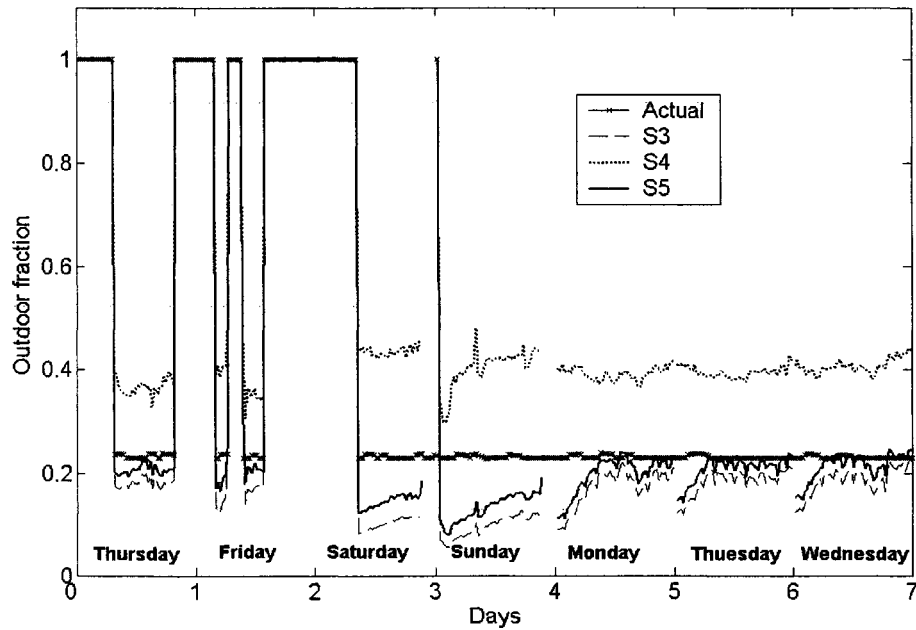
Figure 17   Outdoor airflow fractions of investigated strategies tested on
AHU-6 for July 25 to 31, 2002
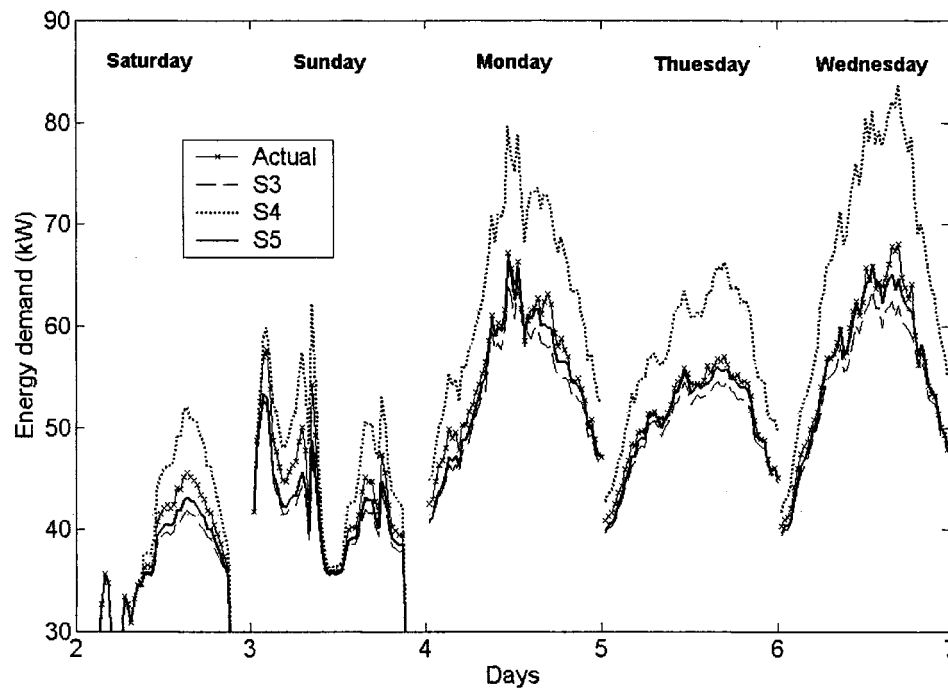
Figure 18   Chiller energy demands of investigated strategies tested on AHU-6
                 for July 27 to 31, 2002

The chiller energy demands required for Thursday and Friday are not shown in Figure 18 because the outdoor air enthalpy is quite close to the return one, and the chiller energy demands for all investigated strategies are about the same.

The CO_2 concentrations in critical zones, representing the indoor air quality of each strategy, are calculated using step 4 of the VAV system model. The critical zone is the zone with the highest value of $Y_{z,dsg}/R_{a,z}$. Since the design outdoor airflow fractions of all zones could be approximated to be the same as 16% ($Y_{z,dsg,i}$=0.16), the critical zone in this case is the zone with the lowest value of ($R_{a,z}$), which is limited for the investigated system to $R_{a,z}$=0.3. There are several zones having ($R_{a,z}$=0.3), and are considered as the critical zones. Figure 19 shows the CO_2 concentration in the critical zones of the investigated strategies for July 25 to 31, 2002.
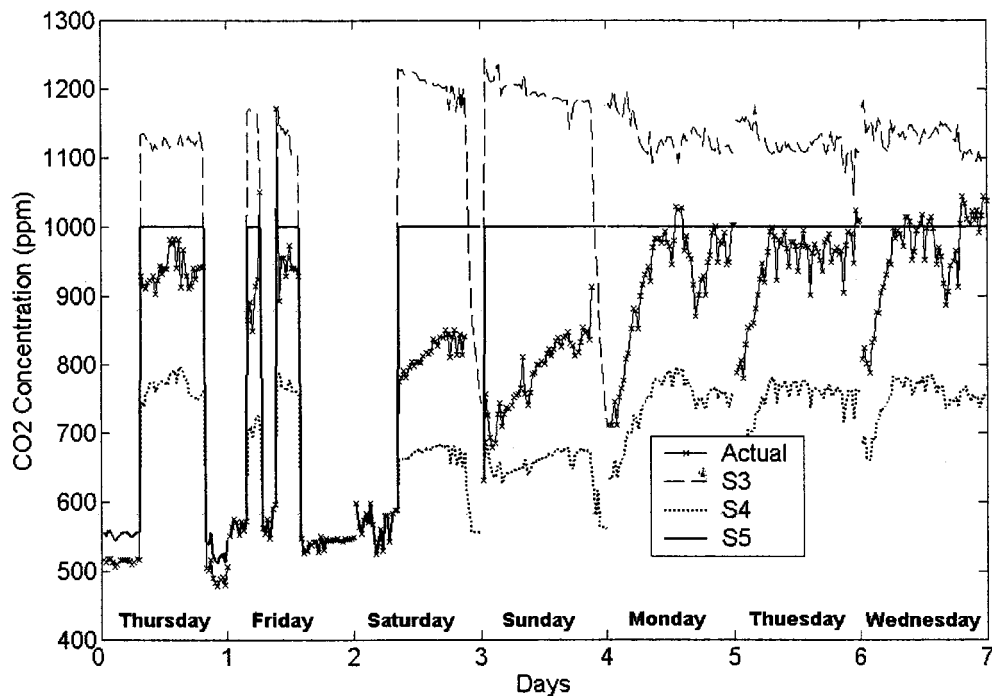
Figure 19 CO_2 concentration in the critical zones of investigated strategies tested on AHU-6 for July 25 to 31, 2002

Strategy S_3 employs the least outdoor air, and uses the least chiller energy, but the poor indoor air quality in the critical zones (1100-1300) is obtained most of the time. To improve the indoor air quality in the critical zones, strategy S_4 proposes an unnecessarily high outdoor air fraction. In this case, we are faced with over-ventilation and high chiller energy demands. Strategy S_5 proposes an exact outdoor fraction to meet the ventilation requirement (1000 ppm).

For the period of June, July, August, and September, the chiller energy use when strategy S_4 is used is 18% higher than that for strategy S_3, but only 2.5% higher than for strategy S_3, when the strategy S_5 is used while meeting the ventilation requirements in the critical zones. However, the actual chiller energy use is 6% higher than S_3.

It is concluded that strategy S_5 can potentially minimize chiller energy use while respecting indoor quality in all zones, including the critical ones. However, further savings could be obtained by S_3 but with scarifying the ventilation in certain zones. In Figure 16, the building airflow part-load ratios ($R_{a,b}$) are close to the ventilation values ($R_{v,b}$), for Monday, Tuesday, and Wednesday. From Equations (3.13 and 3.16), it is shown that the outdoor air fractions of strategy S_3 are close to that for the actual strategy (as in S_1) as well as to that for strategy S_5 (see Figure 17), and their chiller energy demands are not widely different for these days (see Figure 18). Although the actual strategy performs well in the AHU-6 system, it poses a considerable problem for the AHU-4 system (perimeter zones), as will be discussed in the next section.

3.6.3 Results of Evaluation Based on Weather Bin Temperature (MM-3)

The objective is to compare the differences in annual energy and ventilation airflow rates supplied to different zones in the building situated in different locations. The cooling and heating building thermal loads are determined for different bin temperature data for Montreal (cold locations), Seattle (mild and less humid locations), and Dallas (moderately hot and humid locations). The concurrent wet-bulb temperatures are also used. These bin temperature data are presented by Reddy et al (1998), and taken originally from Degelman (1984). The investigated strategies are tested on the AHU-4 for different assumed values of $R_{v,b}$ and selected weather locations. To study the effect of $R_{v,b}$ on annual energy use, the assumed actual building occupancy pattern ($R_{v,b}$) for the occupied period (from 8:00 to 22:00) is considered to be constant during the occupied day and year. The outdoor air fraction, the CO_2 concentration in the critical zones, and the annual energy use for the investigated strategies are determined through the modeling strategy shown in Figure 15. Figures 20 and 21 show the outdoor air fractions and CO_2 concentrations in the critical zones for the Montreal location and when the $R_{v,b}$ is 0.6, respectively.
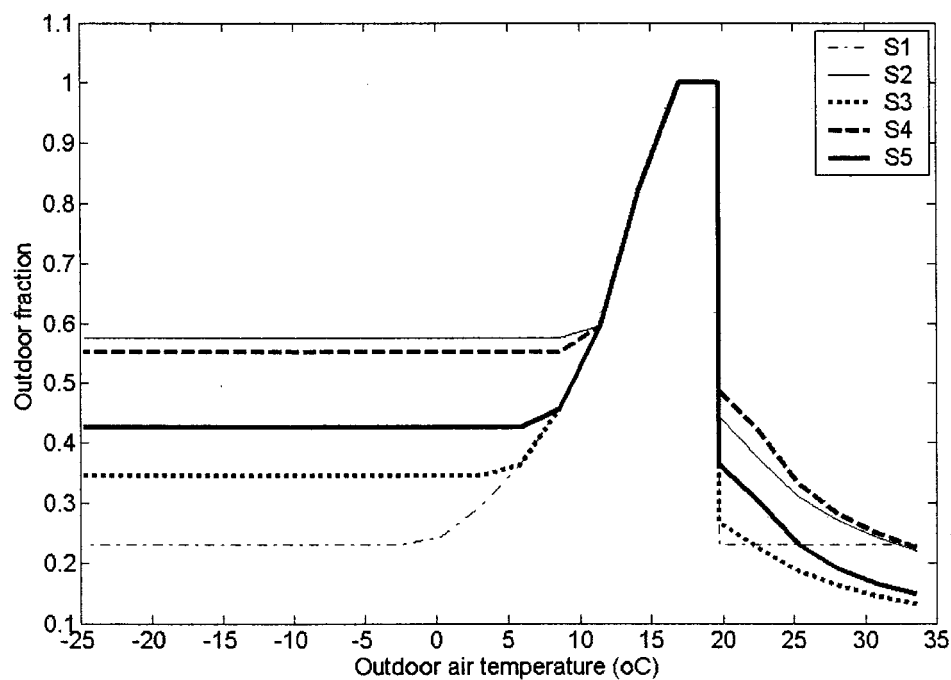
Figure 20   Outdoor air fraction of investigated strategies for each Montreal bin temperature and when the $R_{v,b}$ during the occupied period is 0.6
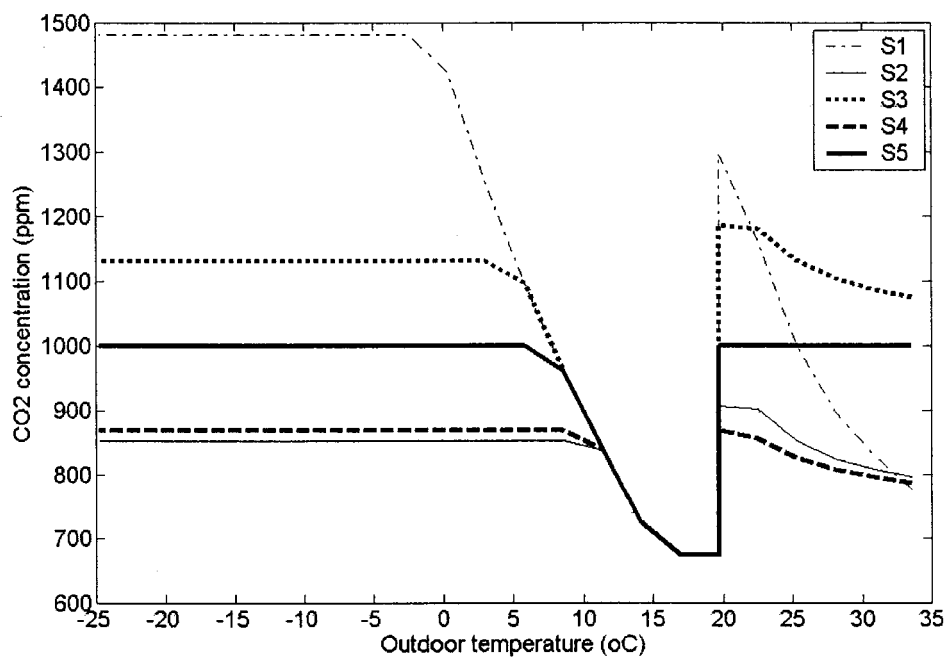
Figure 21 CO_2 concentration in the critical zones of investigated strategies for each Montreal bin temperature

Below a 0°C bin temperature, the values for the outdoor air fractions and CO_2 concentrations in critical zones do not vary due to non-variations of $R_{v,b}$, $R_{a,b}$, and $R_{a,z}$. The fan and zone airflow ratios ($R_{v,b}$, $R_{a,b}$) freeze at their minimum values (40% and 30%, respectively). Around 15°C, the economizer is used, introducing the outdoor air flow rate required for free cooling.

In order to evaluate the indoor air quality (IAQ) in the critical zones, two indexes are used: (i) the number of hours (NH) when the critical zones are above 1000 ppm, and (ii) the average value (AV) of CO_2 concentration in critical zones for the period when the CO_2 concentration is above 1000 ppm. As mentioned above, ASHRAE Standard 62-2001 requires a maximum CO_2 concentration of 1000 ppm in zones. Thus, the indexes measure how long (NH) and how much (AV) the critical zones could be under-ventilated. The NH is calculated as the percentage of the total investigated time. The total investigated time is the number of annual hours for occupied period. The AV is the average CO_2 concentration in critical zones for the NH period. For instance, when strategy S_1 is used in the Montreal location and $R_{v,b}$ is 0.8, the average CO_2 concentration in critical zones, as presented in Table 2, is 1450 ppm during 75.4 % of the total investigated time.

Taking the annual energy use of strategy S_3 as a reference, the ratios of annual energy use for the investigated strategies at different occupancy ($R_{v,b}$) and different locations are calculated and illustrated in Figure 22.

As shown in Figure 20, when the $R_{v,b}$ equals 0.6 for Montreal, the S_1 introduces very low outdoor air in winter days, when the building airflow rate is low and frequently at a minimum level. Certain zones, including critical ones, are under-ventilated by an average CO_2 concentration value of 1334.3 ppm during 61% of the total investigated time (see Table II). There could be some improvement of the IAQ in the critical zone when this strategy works in hot weather (Dallas) due to high thermal loads (and $R_{a,b}$),

and consequently, outdoor air. In Dallas, the critical zones are under-ventilated for 64.6% of the total investigated time, but the average value of CO_2 concentration in critical zones is 1190.1 ppm. Thus, the annual energy uses of strategy S_1 are not at their lowest when $R_{v,b}$ is 0.6 at the Dallas location. For this location, the annual energy uses are 96.7, 98.7, and 100.6 % of the reference strategy, S_3 for $R_{v,b}$ values of 1, 0.8, 0.6, respectively. However, for other investigated locations, strategy S_1 causes very poor IAQ but consumes the least annual energy uses, which are 92.9, 95.7, and 98.2% of reference strategy S_3 for Montreal and 94, 97.2, and 99.3% for Seattle at $R_{v,b}$ values of 1, 0.8, and 0.6, respectively.

At full occupancy ($R_{v,b}=1$), strategy S_2 performs exactly the same as S_3 (see Equations 3.13 and 3.14) and strategy S_4 performs the same as S_5 (see Equations 20 and 23). The performance of strategies S_2 and S_3 differs slightly from that for strategies S_4 and S_5 due to thermal load diversity ($R_{a,b}$ is not the same value of $R_{a,z}$). When strategies S_2 and S_3 are used, the NHs are 28.4, 11.6, and 57.5 and the AVs are 1060.3, 1064.6, and 1068.2 ppm for the Montreal, Seattle and Dallas locations, respectively. If the thermal load distributions between zones vary significantly (high difference between $R_{a,b}$ and $R_{a,z}$), then when strategies S_2 and S_3 are used, the critical zones will be very under-ventilated for long periods.

Respecting the IAQ criteria, strategies S_4 and S_5 are the best. There are no zones that are under-ventilated for all locations and values of $R_{v,b}$. Strategy S_5 performs much better than S_4 respecting the two criteria: IAQ and energy use. Annual energy savings of 3.1, 2.6, and 3% are respectively obtained using strategy S_5 instead of S_4 for Montreal, Dallas, and Seattle when the actual occupancy ($R_{v,b}$) is 0.6. Annual energy savings is decreased when the actual occupancy is increased, and no saving is obtained when the actual occupancy is still the same as the design value ($R_{v,b}=1$).

Table II

IAQ indexes for the investigated ventilation control strategies

			S_1	S_2	S_3	S_4 and S_5
Montreal	$R_{v,b}=1$	NH*	78.4	28.4	28.4	0
		AV**	1604.3	1060.3	1060.3	0
	$R_{v,b}=0.8$	NH	75.4	0	80	0
		AV	1450	0	1070.6	0
	$R_{v,b}=0.6$	NH	61	0	72.5	0
		AV	1334.3	0	1139.3	0
Seattle	$R_{v,b}=1$	NH	70.6	11.6	11.6	0
		AV	1392.2	1064.6	1064.6	0
	$R_{v,b}=0.8$	NH	70	15	76	0
		AV	1306	1016	1099	0
	$R_{v,b}=0.6$	NH	53.8	0	74.7	0
		AV	1184.6	0	1104.5	0
Dallas	$R_{v,b}=1$	NH	76.2	57.5	57.5	0
		AV	1400.6	1068.2	1068.2	0
	$R_{v,b}=0.8$	NH	54	0	54.7	0
		AV	1340	0	1064.4	0
	$R_{v,b}=0.6$	NH	64.6	0	76	0
		AV	1190.1	0	1146.5	0

* Number of hours: Percentage number of hour of investigated time, when the CO_2 concentration is above 1000ppm, %. Investigated time is the number of annual hours for occupied period.

** Average value: Average value of CO_2 concentration for the period when the CO_2 concentration is above 1000ppm, ppm
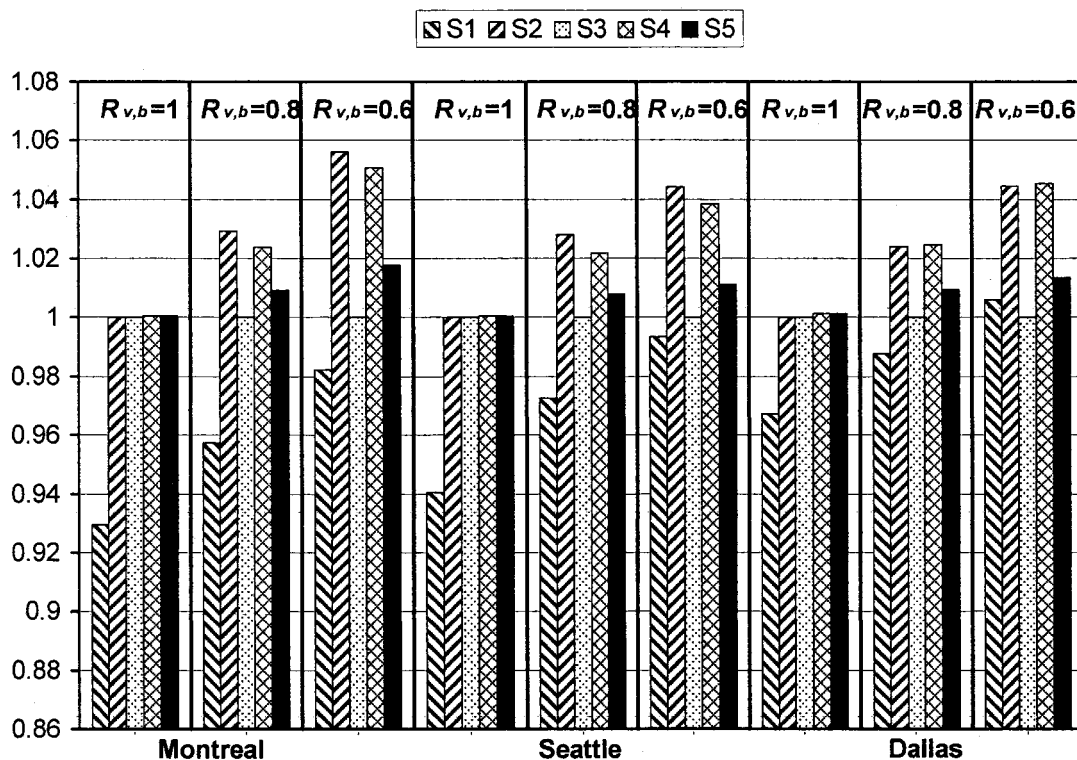
Figure 22   Ratio of annual energy use of investigated strategies to reference strategy S_3

Comparing S_3, S_4, and S_5, shows that S_3 introduces the least outdoor air and consumes the least annual energy use for all cases, but that leads to a very poor IAQ in critical zones. In this case, when $R_{v,b}$ is 0.6, the NHs are 72.5, 74.7, and 76 % and the AVs are 1139.3, 1104.5, and 1146.5 ppm for the Montreal, Seattle, and Dallas locations, respectively. However, when $R_{v,b}$ is 0.8, the NHs are 80, 76, and 54.7% and the AVs are 1070.6, 1099, and 1064.4 ppm. To improve the IAQ, S_4 and S_5 could be used. The annual energy uses of S_4, when $R_{v,b}$ of 0.6, are 5%, 3.8%, 4.5% respectively higher than that for strategy S_3 for Montreal, Seattle, and Dallas, whereas the annual energy uses of S_5 are only 1.7%, 1.1% , and 1.3% than that for strategy S_3. That confirms that strategy S_5 consumes lower additional energy than strategy S_4 in improving the poor IAQ of strategy S_3. S_5 performs better than S_3 respecting the IAQ criteria, and better than S_4 respecting two criteria: energy use and IAQ.

3.7   Summary and Discussion

The new supply CO_2-based demand-controlled ventilation strategy is proposed in order to minimize energy use while ensuring proper indoor air quality in all zones, including in critical zone(s). This proposed strategy maintains a supply CO_2 concentration set point that is low enough to dilute CO_2 generated by full occupancy in the critical zone. The supply CO_2 concentration set point could be determined on-line using the monitored zone airflow rates, which has recently become possible with the use of direct digital control terminal boxes. The strategy is a compromise between the multiple-space equation and the CO_2-based DCV, taking into account: (*i*) the building's actual occupancy and (*ii*) the critical zone ventilation requirement. Thus, the S-CO_2-DCV (S_5) takes into account the on-line over-ventilation occurring in buildings, while considering the critical zone ventilation requirement. The CO_2-DCV (S_3) takes into account the same, but without considering the critical zone ventilation requirement, and the MSE (S_4) takes into account only design over-ventilation in the different zones. The simulation results applied to two existing AHU systems showed that the S-CO_2-DCV (S_5) needs less outdoor air, and consumes less energy than the MSE (S_3) by taking greater advantage of on-line over-ventilated spaces. Although the CO_2-DCV strategy uses the lowest outdoor air and energy, there is poor indoor air quality in some zones. The simulation results also show that energy use could be saved as compared to the actual ventilation control strategy by implementing the proposed S-CO_2-DCV strategy while ensuring a good indoor air quality in all zones, including the critical one.

As discussed in section 3.3, the proposed supply CO_2-based demand-controlled ventilation could be integrated into the on-line optimization process of the supervisory control strategy such that with each simulation, the set points of the HVAC system, including the supply CO_2 concentration set point, could be optimized. This optimization process is illustrated in Figure 1. For the VAV system performance calculation required

by optimization process, the VAV models should be developed and validated. The detailed and adaptive component models are discussed in next chapter.

CHAPTER 4

MODELLING AND VALIDATION OF INVESTIGATED HVAC SYSTEM

4.1   Introduction

In simulation and optimization calculations, the mathematical model of the HVAC system must include all the individual component models that influence energy use and thermal comfort. For that reason, component models are developed and validated against measured monitored variables or the variables calculated through other validated models. This chapter shows also the validation difficulties that are faced due to lack of required measured data. Since our research is developed the optimization process for investigated existing system (ETS), the component models based on detailed information of this system are developed. For the future HVAC system applications when the detailed information may not be available, the on-line adaptive component models could be used instead. With adaptive system modeling, the optimization process could work with most existing building energy management control systems. Since neural networks have been shown to be able to approximate many continuous non-linear functions to a pre-specified accuracy, they can be used here to express the unknown non-linear function. An infinite variety of network architectures can be used for this purpose, but in the interest of conserving computer time the simplest structure is used here. These models with 'self-tuning' based artificial neural networks are developed and proposed for the future applications. The advantage of these methods is that they do not require detailed information of the model parameters. The reader could also review for more detailed our references (Nassif, Kajl, Sabourin 2004a and Nassif, Kajl, Sabourin 2003a).

4.2 Modeling and Validation of HVAC Components

The component models that are developed and validated against the monitored variables are (*i*) fan model, (*ii*) damper model, (*iii*) cooling and heating coils and valves, and (iv) chiller model. Figure 23 shows the input and output variables of the component models for purposes of validation. However, certain component models used for optimization process are inverted, e.g., the fan airflow rate for the fan model and the supply air temperature for the cooling coil are the inputs rather than the fan speed and water flow rate, respectively. Each component model, as well as its input and output variables are shown in Figure 23. The variable inputs of the cooling coil model are not measured, but are determined using the fan, cooling coil valve, and damper models. The output variables (validation variables in Figure 23) could then be validated against reference variables which are available measured variables (e.g., Figure 24) or the variables calculated through other validated models (e.g., Figure 25). The error of the validation models is determined as the absolute ratio of difference between the output (V_{out}) and reference (V_{ref}) variables to the reference variable:

$$Error = \frac{abs\left(V_{out} - V_{ref}\right)}{V_{ref}} \qquad (4.1)$$

4.2.1 Fan Model

Two fan models are developed and used in this research: (*i*) Detailed fan model (DFM) based on manufacturer's information and (*ii*) adaptive fan model (AFM) based on artificial neural network. The first one is used for actual energy use simulations and optimization of existing system. The second is proposed for the investigated and future HVAC system optimizations.
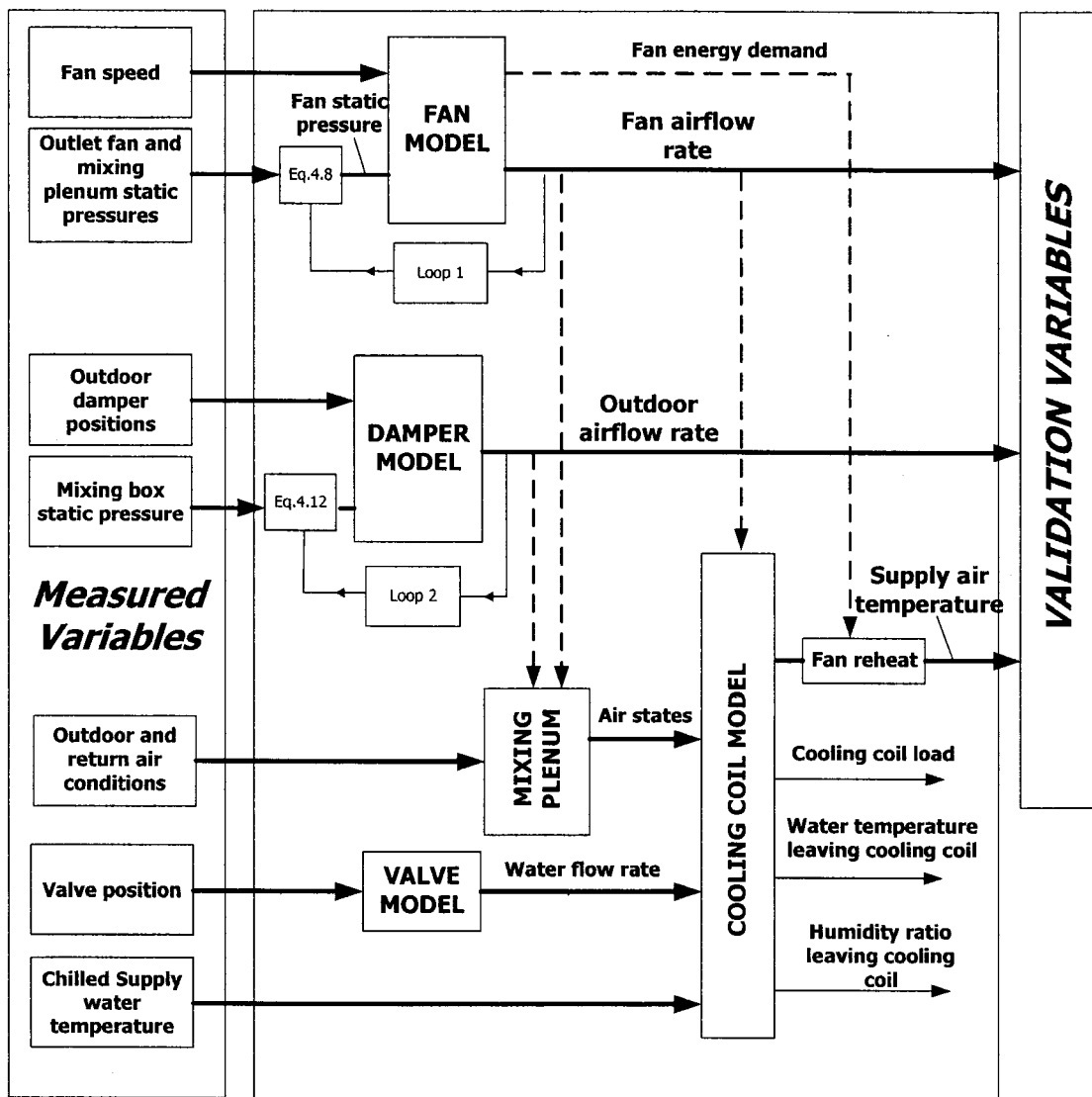
Figure 23   The input and output variables of component models for validation
purpose

4.2.1.1   Detailed Fan Model

The detailed fan model (DFM) is used to calculate the power consumption over a wide
range, using data acquired from the manufacturer. This model was introduced by Clark
(Clark, 1985) to estimate airflow rates as a component of fluid flow networks. It uses the

dimensionless coefficients of flow (Φ), pressure head (Ψ), and shaft power (η_f), as in the following.

$$\Phi = \frac{\dot{Q}_{fan}}{N \cdot d^3}$$ (4.2)

$$\Psi = \frac{P_{S,fan}}{\rho \cdot N^2 \cdot d^2}$$ (4.3)

$$\eta_f = \frac{\dot{Q}_{fan} \cdot P_{S,fan}}{\dot{W}_s}$$ (4.4)

where (d) is the diameter of fan wheel and (ρ) is the air density. The performance of a fan is represented by a polynomial regression of the manufacturer's data using these dimensionless coefficients.

$$\Psi = a_0 + a_1\Phi + a_2\Phi^2 + a_3\Phi^3 + a_4\Phi^4$$ (4.5)

$$\eta_f = b_0 + b_1\Phi + b_2\Phi^2 + b_3\Phi^3 + b_4\Phi^4$$ (4.6)

The coefficients, a_i and b_i are determined from the manufacturer's data and presented in Table V in Appendix 1, while the fan power ($\dot{W}_{fan}$) is determined using the shaft power ($\dot{W}_s$) and the motor efficiency (η_m):

$$\dot{W}_{fan} = \frac{\dot{W}_s}{\eta_m}$$ (4.7)

Since the fan is mounted in the air stream and motor losses directly affect the air temperature rise, the heat transferred to the air is equal to the fan power.

For validation purposes (see Figure 23), two variable inputs are used in the fan model: the fan static pressure ($P_{S,fan}$) and the fan speed (N). The fan speed is measured while the fan static pressure is determined through the following equation:

$$P_{S,fan} = P_{S,mix} + P_{S,out} + \Delta P_{comp} \tag{4.8}$$

It should be noted that the mixing plenum static pressure $P_{S,mix}$ and the static pressure at the fan outlet $P_{S,out}$ are measured. The static pressure drops ΔP_{comp} in the cooling and heating coils, in the filter, and in the humidifier are calculated:

$$\Delta P_{comp} = C_{comp} \cdot \dot{Q}_{fan}^{2} \tag{4.9}$$

The coefficient, C_{comp}, is determined from the known components pressure drops at rating. In calculating the fan airflow rate through the fan model, the initial value of the fan airflow rate is assumed to be used in Equation 4.9; the value calculated through the fan model is then reused in Equation 4.9, and so on until the calculated and used values converge (loop 1 in Figure 23).

Since the fan airflow rate is not measured for the investigated existing system, the sum of the measured airflow rates of the VAV box in different zones are used for comparison with the airflow rate calculated through the investigated fan model. The error obtained by Equation 4.1 for July 2002 is 2.9%. Figure 24 shows the comparison of the sum of the measured zone airflow rates and the fan airflow rate obtained through the fan model for July 25 to 31.

The fan performance curve, including the system curve (*A*) and operation curve (*B*) are illustrated in Figure 10 and discussed in section 2.3.6. The formula representing the

operation curve (*B*) can be expressed in terms of the known design point (*D*) and the measured duct static pressure ($P_{S,sd}$).

$$\dot{Q}_{fan} = \sqrt{\frac{P_{S,fan} - P_{S,sd}}{P_{S,fan,dsg} - P_{S,sd}}} * \dot{Q}_{fan,dsg}$$
(4.10)

The fan airflow rate calculated through the fan model is also validated against the airflow rate calculated by Equation 4.10. In this case, the error obtained by Equation 4.1 for summer 2002 does not exceed 1.3%. Figure 25 shows a comparison of the airflow rates obtained through the fan model and by Equation 4.10 for July 29-31(2002).
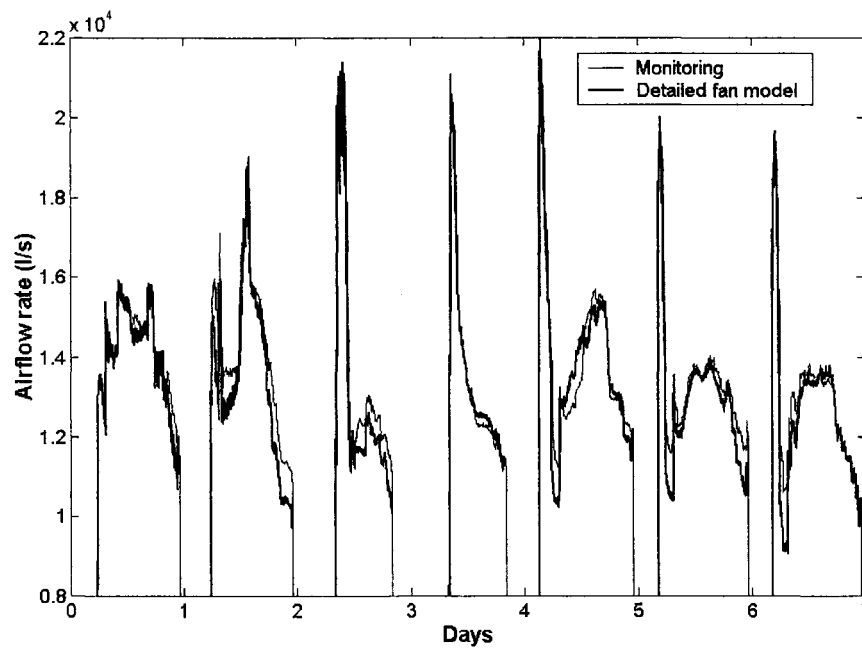
Figure 24   Comparison of the sum of measured zone airflow rates and fan airflow rate obtained by fan model for July 25 to 31, 2002
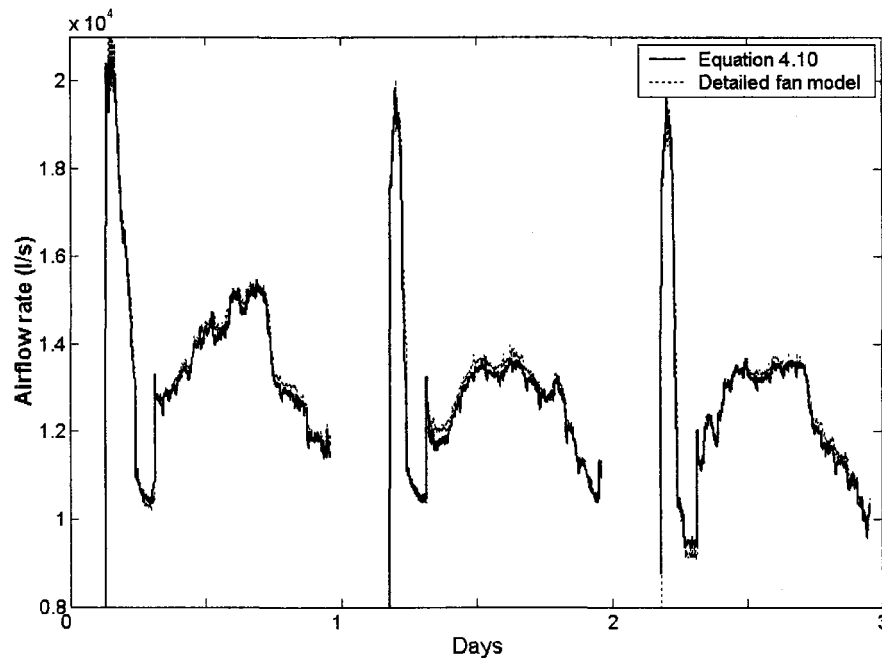
Figure 25   Comparison of airflow rates obtained through fan model and by
             Equation 4.10 for July 29 to 31, 2002

In the optimization process calculations, the fan model should determine the energy use. The required fan airflow rate, based on the zone airflow rates for meeting the loads, and the fan static pressure presented next in Equation 4.33 (determined by rearranged Equation 4.10) are the input variables in the fan model.

4.2.1.2   Adaptive Fan Model

The adaptive fan model (AFM) using an artificial neural network can also be used in place of the detailed model described above for the existing system or for the other investigated VAV system. This network is initially trained using the wide range of data created by the validated fan model. However, in the on-line optimization of the HVAC system, the calculated fan energy could be compared with the measured value in order to perform an on-line retraining of the network.

Since neural networks have been shown to be able to approximate many continuous non-linear functions to a pre-specified accuracy, they can be used here to express the unknown non-linear function. An infinite variety of network architectures can be used for this purpose, but in the interest of conserving computer time the simplest structure with a good accurate result is used. The structure and the activation functions used and tested by Mei and Levermore (2002) for modeling the fan are used here. The fan airflow rate and static pressure representing the input layer (two neurons) are the inputs to the hidden layer based on nine neurons with a hyperbolic activation function (tanh). The output layer consists of one neuron with an activation function based on the sum of the weighted hidden layer neurons. Each neuron also has a bias. The weights and biases (37 variables) are determined using genetic algorithm optimization methods in order to minimize the error between the calculated and the real values. Seventy different operation points are used in training the artificial neural network. The fan energy use is predicted by using this neural network for operation points, as illustrated in curve (B) of Figure 10. A comparison of the values obtained by the neural and by the validated models indicates that the energy demand obtained by adaptive fan model based on neural network is very close to that obtained by the validated detailed fan model, as shown in Figure 26. The error obtained is 0.8% within operation range of the fan airflow rate (9-20 m^3/s).
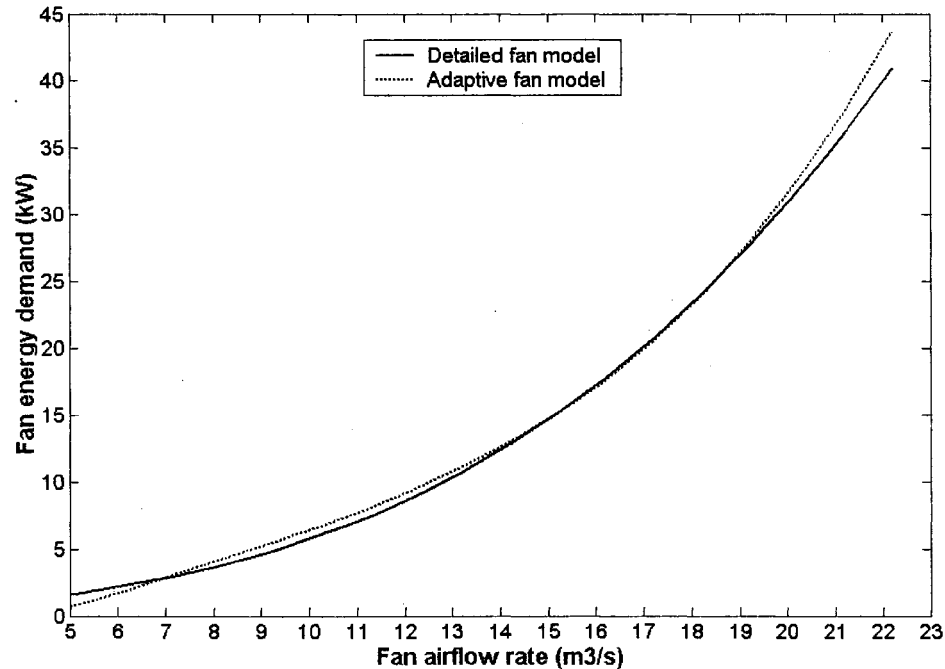
Figure 26   Energy demands obtained by artificial neural network and validated fan
            models

4.2.2   Damper Model

The damper model (DM) is based on an exponential relation, which leads to the outdoor

airflow rate $(\dot{Q}_o)$ being given as the following formula

$$\dot{Q}_o = C_{damper} * \Delta P_{damper}^x \tag{4.11}$$

The coefficients (C_{damper} and x), which are functions of the damper position (O_D, %) are
determined from the manufacturer's data and presented in Table VI in Appendix 1. In
the optimization process, the damper model could be used to determine the damper
position required to provide the optimal outdoor airflow set point (it depends on the
outdoor air ventilation strategy).

In this chapter, the damper is modeled for validation and optimization of existing system. In the optimization, the damper is determined outdoor airflow rate to determine the ventilation load presented in Equation 4.29 as will discuss later. In the HVAC component validations of existing system, the outdoor airflow rate and the relative humidity entering the coil are not measured, while the damper position and the air temperature entering the coil are. Thus, to validate the cooling coil model, the damper model is required for determining the air states entering the cooling coil. Since the damper pressure drop ΔP_{damper} is not measured, it is calculated using the measured mixing plenum static pressure as:

$$\Delta P_{damper} = P_{S,mix} - C \cdot \dot{Q}_o^2 \qquad (4.12)$$

The pressure drop coefficient C in the duct where the outdoor damper is installed is determined using the manufacture's data at full damper position.

To determine the outdoor airflow rate using the damper model, the initial value of the outdoor air is assumed to be used in Equation 4.12, and the value calculated through the damper model is reused in Equation 4.12, and so on until the calculated and used values converge (loop 2 in Figure 23).

The damper model is validated against the monitored data for two operation modes: (*i*) when the damper is fully opened, and (*ii*) when the damper modulates. When the damper is fully opened, the outdoor airflow rate calculated through the damper model is compared with the fan airflow rate calculated through the fan model.

Figure 27 shows the comparison of the outdoor airflow rate obtained through the damper model (DM) with the fan airflow rate obtained through the detailed fan model (DFM) for May 3 to 5. When the damper modulates, the outdoor airflow rate calculated through the damper model (DM) is compared with the outdoor airflow rate calculated through

the temperature balance method (TBM), taking into account only the data when this method is applicable, such that the difference between the return and outdoor air temperature is sufficiently large (Schroeder, krarti, and Brandemuel 2000). Figure 28 shows a comparison of the outdoor airflow rate obtained through the damper model and through the temperature balance method. The validation results indicate that the errors of these two operation modes are 4 and 5%, respectively. Since the outdoor airflow rate is not measured, the adaptive damper model could not be used in this system.
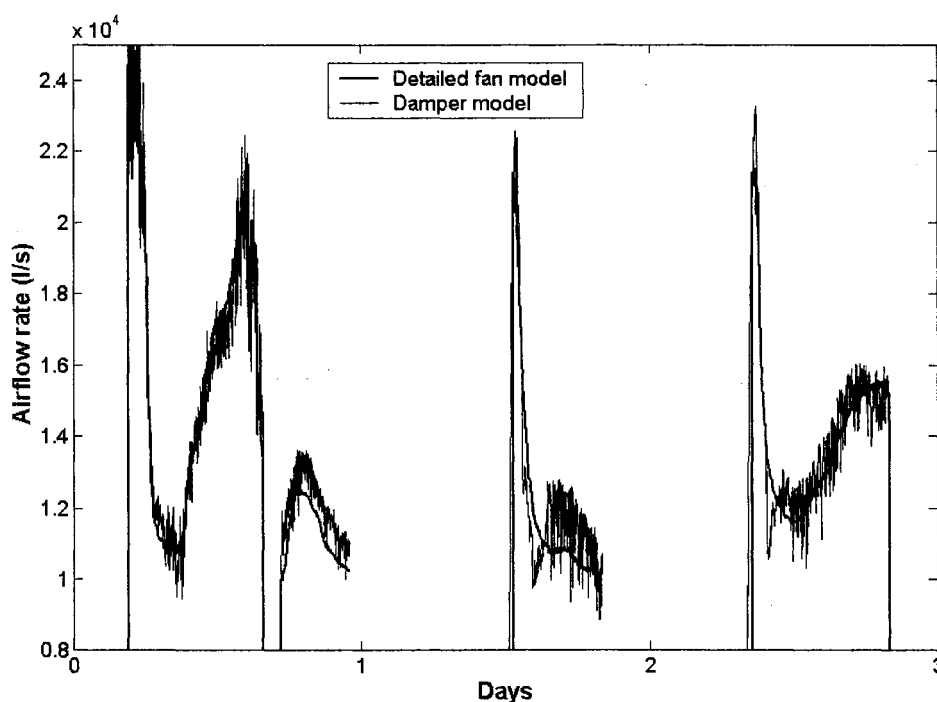
Figure 27   Comparison of airflow rate obtained through fan model and damper model (damper wide open) for May 3-5

4.2.3   Cooling Coil and Valve Models

Two kinds of models are developed in this research: (*i*) detailed cooling coil models and (*ii*) adaptive cooling coil models.
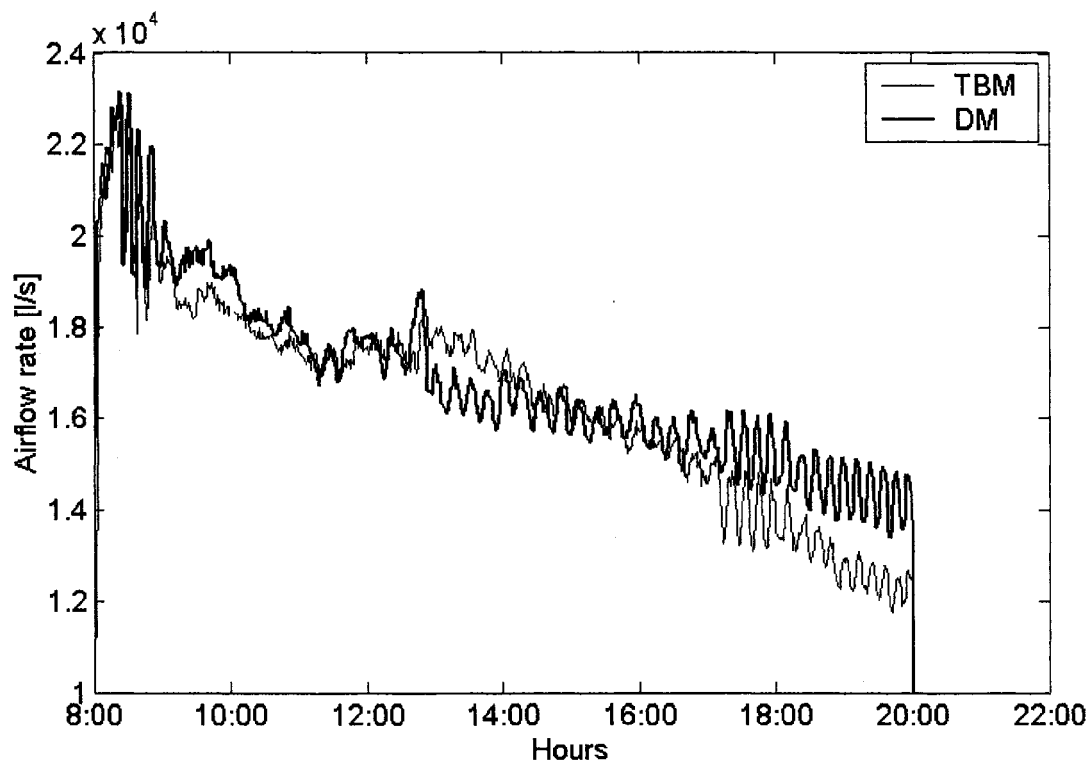
Figure 28   Comparison of outdoor airflow rate obtained through damper model
(DM) and by temperature balance method (TBM)

4.2.3.1   Detailed Cooling Coil Model

The detailed cooling coil model (CCDET) was developed based on the detailed model presented in the ASHRAE HVAC 2 Toolkit (Brandemuel, Gabel, Andersen 1993). Internal and external heat transfer coefficients for this model are determined from detailed information about the coil geometry (Table VII in Appendix 1). The simple cooling coil model (CCSIM) is also presented for comparison. The internal and external heat transfer coefficients for the (CCSIM) are determined from the performance of the coil at a single rating point, and assumed to be constant.

Since the opening of the cooling coil valve is measured rather than the water flow rate, the valve model (Valve and Actuator Manual 1994) is also combined with the cooling

coil model. The inherent flow rate $\dot{Q}_{l,inh}$ through the valve is calculated for each valve position ($O_{V,c}$) through the following equation:

$$\dot{Q}_{l,inh} = \dot{Q}_{l,dsg} \cdot R^{(O_{V,c}-1)}$$

(4.13)

where $\dot{Q}_{l,dsg}$ is the liquid maximum flow rate (design), and R is the valve rangeability defined as the ratio of the maximum to the minimum controllable flow through the valve.

This inherent flow rate is calculated by considering the pressure drop across the valve as being constant. This does not reflect the actual performance of the valve once it is installed within a system. The pressure drop varies with the flow and with other changes in the system. As the valve closes, the pressure drop shifts to the valve and away from the other system components. This has a significant impact on the actual flow rate of the installed valve, which is a function of the valve authority (A), defined as following:

$$A = \frac{\Delta P_{valve}}{\Delta P_{system}}$$

(4.14)

where ΔP_{valve} is the full flow valve pressure drop, and ΔP_{system} is the system pressure drop, including the valve.

The actual flow rate ($\dot{Q}_l$), when the valve is installed, is given by the following equation:

$$\dot{Q}_l = \dot{Q}_{l,dsg} * \sqrt{\frac{\frac{1}{A}}{\frac{1}{A} - 1 + \frac{1}{k^2}}}$$

(4.15)

The inherent flow rate factor (K) is defined as the ratio of the inherent flow rate to the maximum flow rate (at rating).

The CCDET and CCSIM models are validated by comparing the supply air temperatures obtained through the models with the measured temperatures. In this case, the fan and duct air heat up are added to the leaving cooling coil air temperature simulated through the cooling coil model in order to calculate the supply air temperature. The errors obtained by Equation 5.1 for July 2002 are 1.8% for the CCDET and 23% for the CCSIM. Figure 29 shows the supply air temperature measured and obtained through the cooling coil models for July 29.
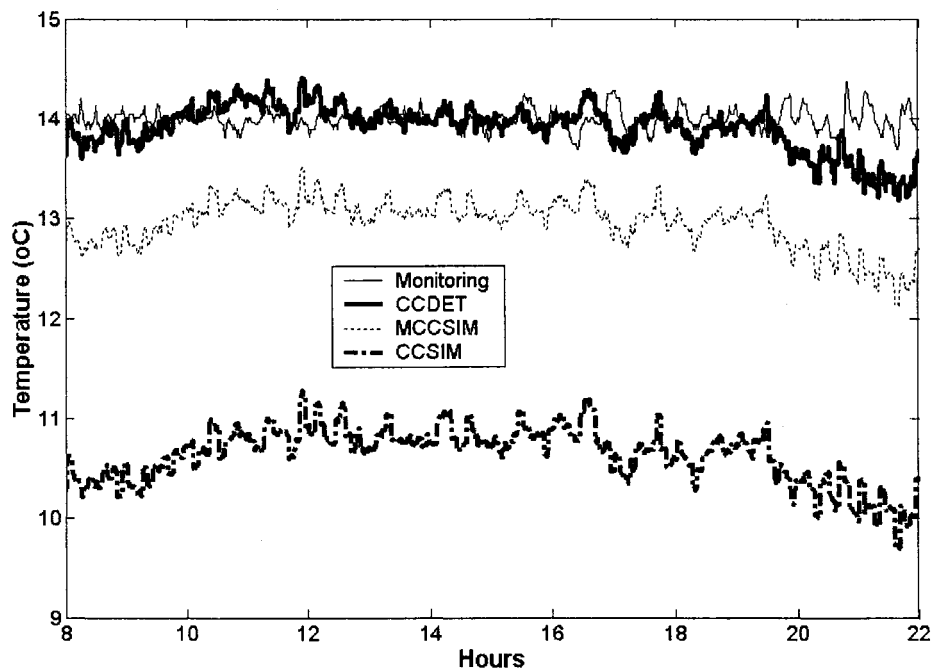
Figure 29   Comparison of measured supply air temperature and that obtained through CCDET, CCSIM, and MCCSIM models for July 29

Note that the fan airflow rate and humidity ratio (or relative humidity) and temperature entering the cooling coil used to validate the cooling coil model are determined using the fan and damper models, respectively. Since the CCSIM is not quite accurate for the

existing system, the detailed cooling coil model is only used. The inverse form of this detailed cooling coil model, presented in the HAVC 2 Toolkit as INVCCDET, is used in the VAV system performance calculations required by the optimization process. In this inversed model, the input used is the supply air temperature set point, which is the optimization variable, rather than the water airflow rate.

4.2.3.2 Adaptive Cooling Coil Model

The adaptive cooling coil model can also be used instead of the INVCCDET for the existing system or for other investigated systems. This model is based on the modification of the simple cooling coil model (CCSIM). Internal and external heat transfer coefficients (UA_{int} and UA_{ext}, respectively) are determined from the performance of the coil at a single rating point, and assumed to be functions of the liquid and airflow rates as follows:

$$UA_{int} = UA_{int,dsg} \left(\frac{\dot{Q}_l}{\dot{Q}_{l,dsg}} \right)^{C_{in}} \tag{4.16}$$

$$UA_{ext} = UA_{ext,dsg} \left(\frac{\dot{Q}_{fan}}{\dot{Q}_{fan,dsg}} \right)^{C_{ex}} \tag{4.17}$$

This modified simple cooling coil model (MCCSIM) is investigated by Morisot, Marchio, Srabat (2002). The authors propose the values of the parameter model (C_{int}=0.8 and C_{ext}=0.77). Using these values, the MCCSIM model is also validated against the monitored value. The supply air temperature obtained by the modified simple cooling coil model is compared with the measured values as shown in Figure 29. The error obtained for this model is 6.5%. During the optimization process, the model parameters could be updated on-line in order to improve the accuracy. Through previous on-line performance data of the cooling coil (outlet and inlet air states and air and liquid airflow

rates), the internal and external heat transfer coefficients are determined using the method presented in the CCSIM, and the model parameters (C_{int} and C_{ext}) could be calculated using Equations 4.16 and 4.17. These parameters could be used in the next time step. When the fan air and water flow rates are not measured, as in the investigated system, the fan model and valve cooling coil models are used in determining them. Although the adaptive VAV system uses the adaptive MCCSIM, the adaptive cooling coil model based on artificial neural network is proposed and presented below.

The adaptive cooling coil model based on the artificial neural network (ANNCCM) is developed for optimization purpose. However, it could be also useful for HVAC system identification and control (Ahmed, Michell, and Klein 1996). The inputs for the neural network are the air conditions entering the cooling coil, the valve cooling coil position, and the fan airflow rate. The controlled variable output is the supply air temperature. Figure 30 shows the supply air temperature calculated through the CCDET as a function of the valve position at different airflow rates and at design air states entering the cooling coil and chilled water supply temperature.

Different neural network architectures with one and two hidden layers and different activation functions are tested and studied. Two different neural network architectures with (tanh) as activation function are presented here. The first has only one hidden layer with eight neurons, and the second has two hidden layers with four neurons each. The output layer of these architectures consists of one neuron with an activation function based on the sum of the weighted hidden layer neurons. The weights and biases are determined using genetic algorithm optimization methods in order to minimize the error between the calculated and the real values. To train the neural network, the two hundred different operation points are selected. Figure 30 shows the supply air temperature determined through the ANNCCM and CCDET models. It is clear that the ANNCCM with two hidden layers is able to trace the detailed cooling coil model curve except during the transition from laminar to turbulent flow in tubes. When the adaptive VAV

system model is used, the ANNCCM is used to verify that air supply temperature set point is met.
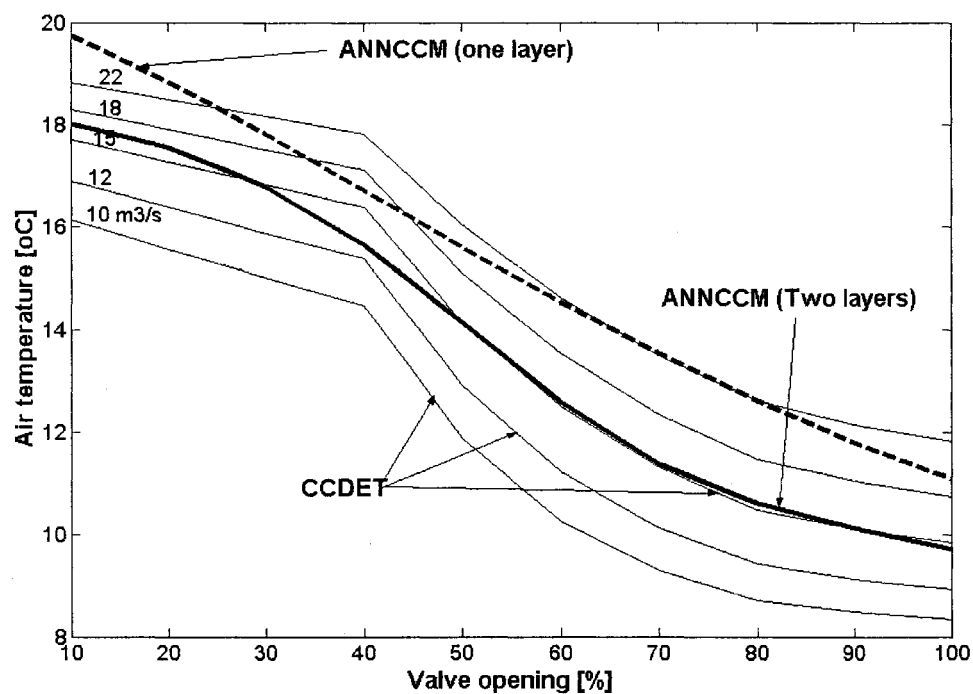
Figure 30   Comparison of supply air temperature obtained through detailed cooling coil models and neural network models

4.2.4   Chiller Model

Two chiller models are developed and used in this research: (*i*) detailed chiller model (DCHM) and (*ii*) adaptive chiller model (ACHM).

4.2.4.1   Detailed Chiller Model

The detailed chiller model DCHM (compared to that in Chapter 5) calculates the power as the function of load, entering condenser water temperature (T_{cws}), and chilled water

supply temperature (T_{sw}). The chiller power ($P_{operation}$) is then determined as the following (NRCC 1999).

$$P_{operation} = P_{rated} \cdot RE\_PLR \cdot RE\_FT \cdot CAP\_FT \tag{4.18}$$

Where:

$P_{operation}$	Power draw at specified operating conditions, kW
P_{rated}	Rated power draw at ARI conditions, kW
ER_PLR	Adjustment to rated efficiency due to change in load calculated by Equation 4.19
ER_FT	Adjustment to rated efficiency due to environmental variables calculated by Equation 4.20
CAP_FT	capacity factor calculated by Equation 4.21

The Equations 4.19, 4.20, and 4.21 are given as the following.

$$ER\_PLR = a_1 + b_1 \cdot PLR + c_1 \cdot PLR^2 \tag{4.19}$$

$$ER\_FT = a_2 + b_2 \cdot T_{sw} + c_2 \cdot T_{sw}^2 + d_2 \cdot T_{cws} + e_2 \cdot T_{cws}^2 + f_2 \cdot T_{sw} \cdot T_{cws} \tag{4.20}$$

$$CAP\_FT = a_3 + b_3 \cdot T_{sw} + c_3 \cdot T_{sw}^2 + d_3 \cdot T_{cws} + e_3 \cdot T_{cws}^2 + f_3 \cdot T_{sw} \cdot T_{cws} \tag{4.21}$$

The part load ratio PLR, which is based on available capacity (not rated capacity), is the present load on chiller to chiller available capacity at present evaporator and condenser. The coefficients of equations above are taken from the default curves of *ER_PLR*, *ER_FT*, and *CAP_FT* presented in (NRCC 1999). These coefficients are tabulated in Tables V, VI, and VII in Appendix 1.

4.2.4.2   Adaptive Chiller Model

The adaptive chiller model (ACHM) using an artificial neural network can also be used in place of the detailed model described above for the existing system or for the other investigated VAV system. This network is initially trained using the wide range of data created by the detailed chiller model described above. The cooling coil load, chilled water supply temperature, and the entering condenser water temperature representing the input layer (three neurons) are the inputs to the hidden layer based on four neurons with a hyperbolic activation function (*tanh*). The chiller energy use representing the output layer consists of one neuron with an activation function based on the sum of the weighted hidden layer neurons. Each neuron also has a bias. The weights and biases (21 variables) are determined using genetic algorithm optimization methods in order to minimize the error between the calculated and the real values. Figure 31 shows the comparison of chiller energy demand obtained through detailed model and neural network chiller models (ACHM). In this figure, the energy demands are represented as the function of part load ratio *PLRr* (based on rated capacity) at two values of chilled water supply temperatures and entering condenser water temperature of 33 °C.
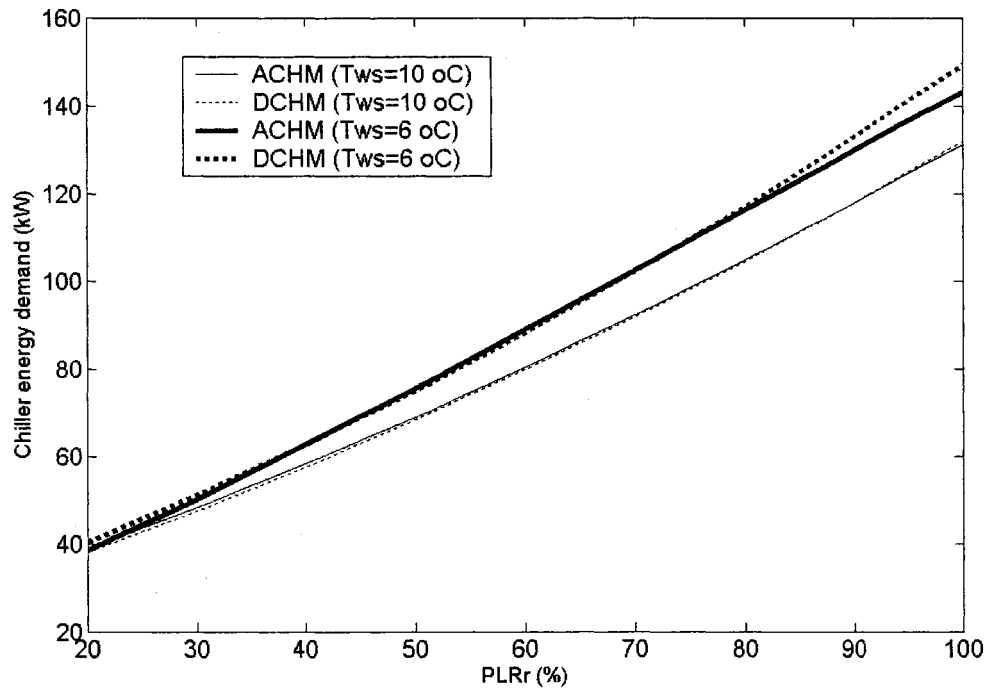
Figure 31   Comparison of chiller energy demand obtained through detailed and adaptive chiller models

4.3   Duct Static Pressure Calculation

The design maximum airflow rate ($\dot{Q}_{z_{max,drg}}$) introduced into each zone at design duct static pressure ($P_{S,sd,dsg}$) can be expressed in the following formula:

$$P_{S,sd,dsg} - \Delta P_{duct,dsg} = C \cdot \dot{Q}_{z_{max,drg}}^2 \qquad (4.22)$$

The new maximum airflow rate ($\dot{Q}_{z_{max}}$) introduced into each zone at new duct static pressure ($P_{S,sd}$) can be expressed in the following formula

$$P_{S,sd} - \Delta P_{duct} = C \cdot \dot{Q}_{z_{max}}^2 \qquad (4.23)$$

The term ΔP_{duct} represents the pressure drop between the static pressure sensor location and the zone VAV box inlet. The term C represents the flow coefficient of VAV damper at certain position (In Figure 5 (b), it is at 80%).

The optimal duct static pressure set point should be at minimum possible value while maintaining the actual zone airflow rates are less (or equal to) than the maximum airflow rate at this optimal set point. Using Equations 4.22 and 4.23 (with actual zone airflow rate equal to maximum one), the optimal duct static pressure set point is given:

$$P_{S,sd} = \left(R_{a,z}^2\right)_{cr} \cdot P_{S,sd,dsg} + \left(\Delta P_{duct} - \left(R_{a,z}^2\right)_{cr} \cdot \Delta P_{duct,dsg}\right) \qquad (4.24)$$

The $\left(R_{a,z}\right)_{cr}$ is the ratio of actual to design maximum airflow rate. This value is determined for each zone and the high one (corresponding to critical zone) is considered in the equation above. When the VAV box of the critical zone exists in the air duct, the term at the right of the equation above become zero. In the existing system, there are several zones with VAV boxes installed at the same branch. In this case, the term ΔP_{duct} is not easy to determine. Therefore, the equation above could be simplified as the following:

$$P_{S,sd} \approx \left(R_a^2\right)_{cr} \cdot P_{S,sd,dsg} \qquad (4.25)$$

Since the zone airflow rate into the non-critical zones are less than or equal to design one, the term ΔP_{duct} is always less than the product of $\left(R_a^2\right)_{cr}$ and $\Delta P_{duct,\ dsg}$. Thus, the optimal duct static pressure determined by simplified equation (Equation 4.25) is high enough than required to ensure that the actual airflow rate introduced into the critical zone is always less than the new maximum airflow rate determined at this optimal set point.

For the adaptive model, the following equation could be used:

$$P_{S,sd} = \left(R_{a,z}^2\right)_{cr} \cdot P_{S,sd,dsg} + a_{cr}$$

(4.26)

Where a_{cr} is adaptive value determined from the on-line data of the previous period. When the VAV damper position is still less than 95%, the a_{cr} could be decreased by a fixed value. As mentioned earliest, the maximum airflow rate attaint ($Ra=1$) while the VAV damper is less than 100% (In Figure 5 (b), at 80%). To decrease the fan energy use, the supply duct static pressure (250 Pa) could be decreased until the VAV position become 100%. By applying the adaptive strategy with the Equation 4.26, the optimal duct static pressure set point at the next time optimization step will be less than the actual one by a fixed value presented by the term a_{cr} while the VAV damper position is less than 95%. In this research, the only Equation 4.25 is used to determine the optimal duct static pressure set point.

4.4   Load Prediction Tool

The sensible zone, building latent, and system ventilation loads ($q_{s,i}$, $q_{l,b}$, and $R_{v,b}$, respectively) are predicted by the load prediction tool (see Figure 1). They are all normalized by dividing at the design loads. The design sensible load is determined by the design maximum airflow rate and the difference between the zone temperature of 23 °C and supply air temperature of 13 °C. The latent building load is determined by assuming the supply relative humidity of 100% (supply air temperature of 13 °C) and the return relative humidity of 50% (return air temperature of 23°C). The difference between the supply and return humidity ratios is then 6.10^{-6} kg/kg$_{dry\ air}$. The design ventilation load is determined using Equation 3.4 (the term ($R_{CO2}-O_{CO2}$) is 700 ppm). ASHRAE Standard 62-2001 indicates that comfort criteria with respect to human bioeffluents are likely to be satisfied if the ventilation rate is 15 cfm per person. This corresponds to an indoor/outdoor CO_2 differential of 700 ppm.

The loads for next time step (k) are determined from data at the previous time (k-1) and they are considered to be constant during a sampling step (ΔTs) .

$$(q_{s,i})_k = (R_{a,z})_{k-1} \cdot \frac{(T_{z,i} - T_s)_{k-1}}{10} + (q_{s,i})_{k-1} - (q_{s,i})_{k-2} \tag{4.27}$$

$$(q_{l,b})_k = (R_{a,b})_{k-1} \cdot \frac{(w_r - w_s)_{k-1}}{6 \cdot 10^{-6}} + (q_{l,b})_{k-1} - (q_{l,b})_{k-2} \tag{4.28}$$

$$(R_{v,b})_k = \left(\frac{\dot{Q}_{o,b}}{\dot{Q}_{o,b,dsg}}\right)_{k-1} \cdot \frac{(R_{CO_2} - O_{CO_2})_{k-1}}{700} + (R_{v,b})_{k-1} - (R_{v,b})_{k-2} \tag{4.29}$$

4.5   Thermal Comfort Model

The Fanger comfort model based on steady-state balance is used here. The "Predicted Percentage of Dissatisfied" (PPD) used as index of the comfort is calculated using the following equation:

$$PPD = 100 - 95 \cdot EXP[- (0.03353 \cdot PMV^4 + 0.2179 \cdot PMV^2)] \tag{4.30}$$

The predicted mean vote (PMV) is an index devised to predict the mean response of a large group of people according to the ASHRAE thermal sensation scale. Fanger related the PMV to imbalance between the actual heat flow from the body in a given environment and the heat flow required for optimum comfort at a specific activity level.

$$PMV = (0.303 EXP(- 0.036M) + 0.028)L \tag{4.31}$$

where L is the thermal load on the body that is defined as the difference between the internal heat production and the heat loss to the environment for a human hypothetically

kept at the comfort values of the mean skin temperature and sweat secretion rate for the actual activity level. In a practical situation, the PMV values tabulated can be used to predict the performance of a VAV system for a combination of variables (Fanger 1970). For example, for a combination of 1 clo (I_{cl} clothing insulation), an ambient temperature of 24°C and a velocity of 0.3 m/s, the PMV value from Table III is -0.09.

Table III

Predicted mean vote (PMV)

Clo (I_{cl})	Temperature (°C)	Velocity (m/s)			
		0.1	0.2	0.3	0.4
0.75	21	-1.11	-1.44	-1.66	-1.82
	23	-0.47	-0.78	-0.96	-1.09
	24	-0.15	-0.44	-0.61	-0.73
	25	0.17	-0.11	-0.26	-0.37
1.00	21	-0.57	-0.84	-0.99	-1.11
	22	-0.30	-0.55	-0.69	-0.80
	23	-0.02	-0.27	-0.39	-0.49
	24	0.26	0.02	-0.09	-0.18
	25	0.53	0.31	0.21	0.13

In this study, Table III is used by considering: (*i*) the rate of metabolic heat product (M) is constant, (*ii*) the zone temperature is equal to radiant temperature, (*iii*) the I_{cl} clothing insulation is 1, and (*vi*) the air velocity is determined as function of zone airflow rate by the following.

$$V_z = V_{z,dsg} \cdot \frac{\dot{Q}_z}{\dot{Q}_{z,dsg}} \qquad (4.32)$$

where the $V_{z,dsg}$ is the design air velocity that is assumed to be 0.3 m/s.

4.6 Detailed and Adaptive VAV System Model

The detailed or adaptive component models presented above are interconnected to form the detailed or adaptive VAV system model. The VAV model determines the energy use and thermal comfort using the trial set points supplied by the genetic algorithm, and using the outdoor condition and predicted loads. Figure 32 shows the flow diagram for the VAV system performance calculations required by the optimization process.

There are nine steps presented as blocks labeled with the names of the calculated variables.

Step 1: The zone and supply air temperature set points and indoor sensible load are used to calculate the zone airflow rates. The reheat is considered if it is used as in AHU-4 system.

Step 2: The fan airflow rate is calculated as the sum of the zone airflow rates.

Step 3: Using the supply duct static pressure set point and fan airflow rate, the fan static pressure is determined by rewriting Equation 4.10 as the following.

$$P_{S,fan} = \left(\frac{\dot{Q}_{fan}}{\dot{Q}_{fan,dsg}}\right)^2 \bullet \left(P_{S,fan,dsg} - P_{S,sd}\right) + P_{S,sd} \qquad (4.33)$$

Step 4: The fan static pressure and airflow rate are used by the fan model in calculating the fan energy demand. The detailed VAV system model uses detailed fan model, whereas the adaptive VAV system model uses adaptive one.
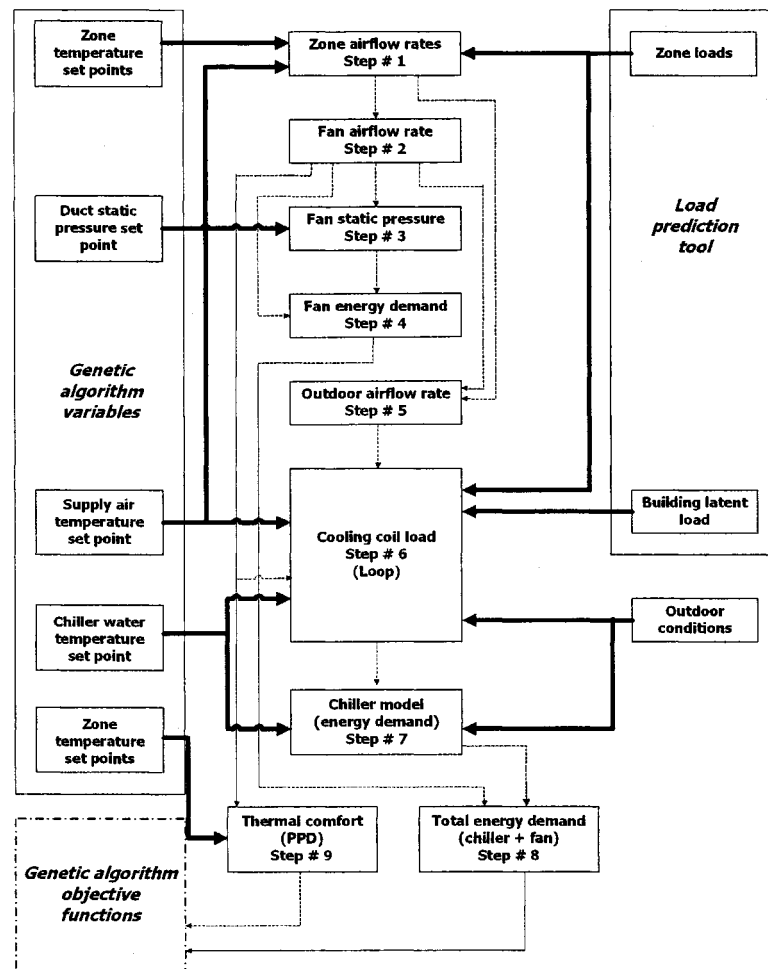
Figure 32   Flow diagrams for VAV system performance calculations required by optimization process

Step 5: The outdoor airflow fraction (Y_b) is determined by Equation 3.23 to satisfy the zone ventilation requirement, using input variables: zone and fan airflow rate and zone ventilation requirements. However, when the local supply CO_2 concentration control loop is used, the optimal supply CO_2 concentration set point is determined by Equation 3.21.

Step 6: The inverse form of CCDET model (INVCCDET) is used for detailed VAV model, whereas the adaptive MCCSIM is used for adaptive VAV system model. In this case, the coefficients (C_{in} and C_{ext}) are determined using the previous data as discussed

in Section 4.2.3.2. The step 6 represents the iteration process during which the initial value of the cooling coil leaving air humidity ratio is assumed, and the new value is calculated and reused until the converge is obtained. The following are all the required calculations in this step:

- The initial value of the cooling coil leaving air humidity ratio is assumed to be equal to the saturated humidity ratio corresponding to the cooling coil leaving air temperature (calculated from trial supply air temperature set point and the fan and duct heat up).

- The return air temperature and humidity ratio are calculated using the building latent and sensible loads, fan airflow rate, and supply air temperature and humidity ratio.

- The mixing plenum air temperature and humidity ratio are determined using the energy balance and economizer logic, knowing the minimum outdoor and fan airflow rate and outdoor and return conditions.

- The chilled water supply temperature and supply air temperature set points provided by the genetic algorithm, the outdoor airflow rate, the mixing plenum condition (cooling coil inlet conditions) are the inputs of the inverted detailed cooling coil model (INVCCDET), allowing calculations of a new value of the cooling coil leaving air humidity ratio to verify the assumed value as well as the cooling coil load, water flow rate, and cooling coil load.

It is noted that the calculated water flow rate from the cooling coil model should be less than design one (33 l/s).

Step 7: The chiller power is calculated through the chiller model, using as inputs the cooling coil load, chilled water supply temperature, and entering condenser water temperature that is assumed to be 3 °C higher than measured outdoor wet bulb temperature. The detailed VAV system model uses detailed chiller model, whereas the adaptive VAV system model uses adaptive one

Step 8: The total energy use is calculated as the sum of the fan and chiller energy use. The zone reheats are also added if it used as in AHU-4 system.

Step 9: The zone thermal comforts presented by the PPDs index are determined using Equation 4.30.

4.7   Summary and Discussion

The detailed and adaptive VAV systems that are required to energy and thermal comfort calculations are developed. The detailed VAV system consists of component models that are developed using the detailed information of existing VAV system. The fan, damper, cooling coil and valve, and chiller models are developed and validated against the monitored data or the variables calculated through other validated models. The detailed VAV system is used for optimization calculations of investigated existing HVAC system. The adaptive VAV system consisting of the component models is also proposed for future HVAC system. Since artificial neural networks have been shown to be able to approximate many continuous non-linear functions to a pre-specified accuracy, the HVAC component models are developed using the artificial neural networks, which do not require a prior knowledge of specific models to solve problems. An infinite variety of network architectures can be used for this purpose, but the simplest structures with good accurate results are used.

As mentioned earliest (see Figure 1), the proposed optimization includes (*i*) the adaptive or detailed VAV model, (*ii*) the two-objective genetic algorithm optimization program, and (*iii*) three main tools, namely, data acquisition, load prediction, and optimal solution selection tools. The VAV model and load prediction tool are developed and discussed in this chapter. However, the two-objective genetic algorithm optimization programs will discuss in next one.

CHAPTER 5

EVOLUTIONARY ALGORITMS FOR MULTI-OBJECTIVE OPTIMIZATION IN HVAC SYSTEM CONTROL STRATEGY

The goal of this chapter is to evaluate and test the candidate optimization method on HVAC control strategy problem. The potential of selected evolutionary algorithm method to find the set of optimal solutions closed to Pareto-optimal front is investigated and presented. Thus, to evaluate the optimization method, Pareto-optimal solutions should be known. For that reason, the VAV model was simplified in this chapter in order to be able to predict the Pareto-optimal front. Keep in mind that the simplifications applied here are only for the purpose in this chapter, but the detailed VAV model are applied for the optimization of existing HVAC system studied in Chapter 6. The detailed studies are presented in our reference (Nassif, Kajl, and Sabourin 2004b). Prior to this study, the real and binary non-dominated sorting genetic algorithm (NSGA) and elitist non-dominated sorting genetic algorithm (NSGA-II) are also evaluated on mathematical problem (Nassif 2002). The results of this previous study and genetic algorithm operators are presented in Appendix 3.

5.1   Introduction

As mentioned earlier, the performance of the heating, ventilating, and air conditioning (HVAC) system can be improved through the optimization of control set points. The set points that should be optimized could account for more than 70 variables. The high number of variable problems makes the traditional optimization methods require a sequential, and therefore computationally intensive, approach to find the optimal set of solutions (Wright, Loosmore, and Farmani 2002). In addition, since the optimization of a supervisor control strategy should be run on-line at a specific interval (e.g., 15 minutes), the computation must be quite rapid. Using a two-objective optimization algorithm, such as energy use and thermal comfort, could also provide an opportunity to control the thermal comfort and energy use according to the day or month, thereby

bringing about further energy savings as will discuss in chapter 6. Thus, the optimization of a supervisory control strategy requires a set of solutions put through a single simulation run; in this case, the multi-criterion optimization method is required.

From a large number of multi-objective optimization methods, Srinivas and Deb (1994) investigated Goldberg's notion of non-dominated sorting in genetic algorithms to find multiple Pareto-optimal points simultaneously. The results of this study showed that the non-dominated sorting genetic algorithm (NSGA) performs better than other investigated methods among three two-objective problems. Deb introduces an elitist non-dominated sorting genetic algorithm (NSGA-II) (Deb, Agrawal, Pratap, and Meyarivan 2000). The simulation results showed that the NSGA-II performs better than nine other investigated methods. Therefore, the NSGA and NSGA-II are selected and evaluated to solve the HVAC optimization problem. These evaluations are done using the simplified VAV model. However, the optimization of the existing HVAC system is conducted using the detailed and validated VAV model.

The goals of the two-objective optimization are: (*i*) to find solutions close to true Pareto-optimal solutions and (*ii*) to find solutions that are widely different from each other. To evaluate the candidate evolutionary algorithms, the solutions obtained should be compared with known Pareto-optimal solutions. For that reason, the VAV model was simplified in order to be able to predict the Pareto-optimal front. It was verified that the energy use (objective function) obtained by the simplified model is close to the energy use obtained by the detailed model. In addition, it should be noted that the thermal comfort (second objective function) is the same as in the detailed model.

At each optimization period (e.g., 15 minutes), the genetic algorithm program sends the trial investigated controller set points to the VAV system model, where the energy use and thermal comfort (objective functions) are simulated and returned back to the genetic algorithm. The VAV model determines the energy use and thermal comfort resulting

from the change in outdoor conditions and indoor loads (independent variables) and controller set points (dependent variables or problem variables). The independent variables (identified in this chapter by index IV) are: the (*i*) the enthalpy of outdoor air $(Ho)_{IV}$, *(ii)* the indoor sensible loads at each zone i $(q_{s,i})_{IV}$, and *(iii)* the total load of the building $(q_t)_{IV}$. However, the dependent variables or problem variables (identified in this chapter by index PV) are: (*i*) the zone temperatures $(T_z)_{PV}$, (*ii*) the supply duct static pressure $(P_{s,sd})_{PV}$, (*iii*) the supply air temperature $(T_{sa})_{PV}$, and (*iv*) the chilled water supply temperature $(T_{sw})_{PV}$.

5.2   Simplified VAV System Model

In order to evaluate different evolutionary algorithm methods, the water flow rate constraint and energy use calculations (first objective function), including the fan and chiller energy uses, are determined as follows.

5.2.1   Fan Energy Use

The fan energy use is calculated as a function of the fan airflow rate ($\dot{Q}_{fan}$, l/s) and total static pressure (fan efficiency equals 0.68). The total static pressure is equal to the static pressure set point $((P_{S,sd})_{PV}$, Pa) plus the remaining duct pressure drop, which is a function of the fan airflow rate (sum of the zone airflow rates, $\dot{Q}_z$). Applying existing system characteristics, the fan energy use ($\dot{w}_{fan}$, kW) could be simplified as:

$$\dot{W}_{fan} = \frac{\dot{Q}_{fan}}{680000} \cdot \left((Ps_{sd})_{PV} + 2 \cdot 10^{-6} \cdot \dot{Q}_{fan}^2 \right) \tag{5.1}$$

where:

$$\dot{Q}_{fan} = \sum \dot{Q}_{z,i} = \sum \frac{(q_{s,i})_{IV}}{\rho \cdot c_p \cdot ((T_{z,i})_{PV} - (Ts)_{PV})}$$ (5.2)

The error obtained by comparing the fan energy uses calculated by Equation 5.1 with that calculated by detailed model described in Chapter 4 is 4% within the normal fan operation.

5.2.2 Chiller Energy Use

The chiller energy, which is determined as a function of cooling coil load and COP, is given as the following:

$$\dot{W}_c = \frac{\left[Y_b \cdot \dot{Q}_{fan} \cdot ((Ho)_{IV} - Hs) + (qt)_{IV} \cdot (1 - Y_b) \right]}{COP}$$ (5.3)

The outdoor air fraction in the supply air Y_b is determined using the standard economizer logic:

$$if \ (Ho)_{IV} \geq \left(\frac{(q_t)_{IV}}{\dot{Q}_{fan}} + Hs \right) \text{then} \ Y_b = 0.2 \ else \ Y_b = 1$$ (5.4)

$$if (Ho)_{IV} \leq Hs \quad \text{then} \quad \dot{W}c = 0$$

To simplify (5.3), the following assumptions are made:

- The air leaving the cooling coil is saturated and its enthalpy (Hs) is calculated a function of supply air temperature $(T_{sa})_{PV}$.
- The coefficient of chiller performance (COP) could be determined as:

$$COP = 7.9275 \cdot PLR^3 - 21.194 \cdot PLR^2 + 16.485 \cdot PLR + 2.2139 + 0.1 \cdot \left((Tw)_{PV} - 6 \right) \qquad (5.5)$$

where the *PLR* is the part load ratio, which is equal to the ratio of the cooling coil load ($\dot{Q}c$) to the design load (722 kW). The parameters of the equation above is taken from (Kreider and Rabel 1994) It is assumed in the equation above that the *COP* is increased by 0.1 as the chilled water supply temperature $(T_{sw})_{PV}$ is increased by 1°C. It should be noted that the chilled water supply temperature is limited within [6-11].

5.2.3 Water Flow Rate Constraint

The water flow rate, which is used in the constraint verifications (5.10) presented below, could be determined as follows:

$$\dot{Q}_l = \dot{Q}_{l,dsg} \cdot \left(\frac{\dot{W}_c \cdot COP}{UA_{int} \cdot \left((T_{sa})_{PV} - (T_{sw})_{PV} \right)} \right)^{1.25} \qquad (5.6)$$

The water flow rate at rating ($\dot{Q}_{l,dsg}$) is 33 l/s. The equation above is obtained by assuming that the water heat transfer coefficient (UA_{int}) is a function of the water flow rate ($\dot{Q}_l$) as follows:

$$UA_{int} = UA_{int,dsg} \left(\frac{\dot{Q}_l}{\dot{Q}_{l,dsg}} \right)^{0.8} = \frac{\dot{W}_c \cdot COP}{\left((T_{sa})_{PV} - (T_{sw})_{PV} \right)} \qquad (5.7)$$

5.3 Problem Formation

The optimization seeks to determine the set point values of the supervisory control strategy of the ÉTS system. These set points should be optimized for the energy use and

the thermal comfort of building occupants. The optimization problem is formed by determining the problem variables, the constraints, and the objective functions.

5.3.1   Problem Variables

The problem variables are the zone temperatures (70 variables) set points, the supply duct static pressure, the supply air temperature, and the chilled water supply temperature. The resulting problem variables consist of 73 variables.

5.3.2   Objective Function

The problem variables should be determined on-line at each optimization period in order: (*i*) to reduce energy use, and (*ii*) to improve thermal comfort. During the optimization process, the chiller and fan energy uses are determined using the detailed and validated VAV component models. However, in order to evaluate the evolutionary algorithm methods, the energy use is calculated as the sum of the fan and chiller energy uses and using the simplifications presented above.

$$\dot{W}_t = \dot{W}_{fan} + \dot{W}_c \qquad (5.8)$$

Using (5.1) and (5.3), the energy use ($\dot{W}t$) can be determined at each independent variable (*IV*) and proposed problem variable (*PV*).

The zone comfort is represented as the "Predicted Percentage of Dissatisfied" (PPD), and calculated using Equation 4.30. The two-objective functions and the constraints could then be represented as follows:

$$Min(\dot{W}t) = f_1\left((Ts)_{PV}, (Tz_i)_{PV}, (Ps_{sd})_{PV}, (Tw)_{PV}\right) \qquad (5.9a)$$

$$Min(PPD) = f_2\left((Tz_i)_{PV}\right) \qquad (5.9b)$$

The function f_1 is simplified for this Chapter (Evaluation of GA methods) by 5.1, 5.3, and 5.8 or detailed by the VAV model. The function f_2 is determined by Equation 4.30.

5.3.3 Constraints

The constraints result from restrictions on the operation of the HVAC system. They cover the lower and upper limits of problem variables: (*i*) the supply air temperature (13–18 °C), (*ii*) the zone air temperature (21–25 °C), (*iii*) the chilled water supply temperature (6–11 °C), and (*iv*) the static pressure (150–250 Pa). The constraints also cover the design capacity of components. The constraints could be written as the following:

$$0.3 \cdot \dot{Q}_{z,max,i} \leq \frac{(qs)_{PV}}{\rho \cdot c_p \cdot \left((Tz_i)_{PV} - (Ts)_{PV} \right)} \leq \dot{Q}_{z,max,i} \qquad (5.10a)$$

$$0.3 \cdot \dot{Q}_{fan,dsg} \leq \dot{Q}_{fan} \leq \dot{Q}_{fan,dsg} \qquad (5.10b)$$

$$\dot{Q}_l \leq \dot{Q}_{l,dsg} \qquad (5.10c)$$

Low limits ≤ *Problem variables* ≤ *High limits* $\qquad (5.10e)$

The fan airflow rate is restricted within the design ($\dot{Q}_{fan,dsg} = 2300 \, l/s$) and minimum limit ($0.4 \cdot \dot{Q}_{fan,dsg}$). The zone airflow rates are also restricted within the maximum ($\dot{Q}_{z,max}$) and minimum limits, which are equal to 30% of design airflow rate ($0.3 \cdot \dot{Q}_{z,max,dsg}$). The maximum limit could be determined as follows:

$$\dot{Q}_{z,max,i} = \dot{Q}_{z,max,dsg,i} \cdot \sqrt{\frac{(P_{s,sd})_{PV}}{P_{s,sd,dsg}}} \qquad (5.11)$$

The design static pressure $(P_{s,sd,dsg})$ of the investigated system is 250 Pa and the design airflow rate at each zone i ($\dot{Q}_{z,max,dsg}$) is known.

5.4   Optimization Algorithm

Although there are several optimization methods, the genetic algorithm (GA) is used for the following reasons:

- The ability of genetic algorithm to find multiple optimal solutions in one single simulation run makes the genetic algorithm unique in solving multi-objective optimization problems (Deb 2001).

- Many traditional methods scalarize the objective vector into a single objective. In those cases, the obtained solution is highly sensitive to the weight vector used in the scalarization process and demands the user to have knowledge about the underlying problem. However, the multi-objective GA find set of solutions (Srinivas and Deb 1994).

- The big number of variable problems (more than 140 variables for Unit-4) makes the traditional methods require a sequential and therefore computationally intensive approach to find the optimal set of solution (Wright and Loosemore 2001).

- The genetic algorithm using a multi-objective approach has the potential to find the trade-off between the HVAC problem functions (Wright and Loosemore 2001).

- Genetic algorithm has been proved to be robust and efficient in finding near-optimal solutions in complex problem spaces (Huang and Lam 1997).

- Genetic algorithm has been applied to a diverse range of scientific, engineering, and economic search problem (Deb 2001). GA optimization methods have been also used in HVAC problem (Lam 1995; Huang and Lam 1997; Wright 1996;

Wright and Farmani 2001). The results indicated that the GA is able to find the optimal solution in HVAC problem space.

Since no research has evaluated the multi-objective genetic algorithm optimization in HVAC system control strategy, the goal of this chapter is to examine the performance of selected optimization method as will discuss in Section 5.5 below.

5.4.1   Genetic Algorithm

In this study, a genetic algorithm (GA) search method based on the mechanics of Darwin's natural selection theory was developed in order to solve the optimization problem. Since energy use and thermal comfort are the objective functions, the multi-objective optimization must be investigated. In this paper, the NSGA and NSGA-II are investigated and evaluated for solving the HVAC system control strategy optimization problem. The reader could refer to the Appendix 3 for detailed information about NSGA and NSGA-II.

The NSGA-II uses the elite-preserving operator, which favors the elites of a population by giving them an opportunity to be directly carried over to the next generation. After two offsprings are created using the crossover and mutation operators, they are compared with both of their parents to select two best solutions among the four parent-offspring solutions. The NSGA-II employs the crowded tournament selection operator (Deb 2001). As a result of the constraint functions, a penalty must be imposed on the objective functions. The constraint violation is calculated using the penalty function approach (see Equation A3.8 in Appendix 3). The penalty parameters are set at 100 and 5 for energy use and thermal comfort objective, respectively. The simulated binary crossover operator (*SBX*) is used here to create two offspring from two-parent solutions. The random simplest mutation operator is applied in order to randomly create a solution

from the entire search space. The GA operators used in this study are detailed in Appendix 3.

The NSGA uses both the non-dominated sorting strategy and the sharing strategy (niche method) before the reproduction operator. The crossover and mutation operators remain as usual (as in the NSGA-II described above). The idea behind the non-dominated sorting procedure is that a ranking selection method is used to emphasize good solutions while a niche method is used to maintain stable subpopulations of good points.

5.4.2 Comparison of Two-Objective Optimization Methods

Since many two-objective optimization methods are available, it is natural to ask witch of them performs better when compared to other algorithms on the investigated problem (HVAC problem). The performance of these optimization methods is evaluated through the HVAC problem presented in Equations 5.9 and 5.10. In these evaluations, the following two performance metrics are used: (*i*) metric evaluating the closeness to the Pareto-optimal front, and (*ii*) metric evaluating diversity among non-dominated solutions. In the first metric, the distances of the solutions obtained from the Pareto-optimal solutions are calculated and divided by the number of solutions. In the second one, the *Spread* metric (Deb 2001) is used, considering the distance between neighboring solutions and extreme solutions located on the Pareto-optimal front. Equations (A3.9 and A3.11) in Appendix 3 represent these metrics.

5.4.3 Pareto-Optimal Solutions

In order to compare the different optimization methods, the Pareto-optimal solutions, which vary with the independent variables, should be known. At each optimization period, the Pareto-optimal solutions corresponding to these independent variables (*IV*) are obtained. For example, at hot summer day (Case # 1), the optimal supply air

temperature set point, which has the greatest effect on the energy use objective function, is at its minimum possible value while all constraints in Equation 5.10 are respected. The optimal zone temperatures vary within the range [23.1 - 25°C]. The optimal static pressure should be at its lowest possible level while constraint 2 in Equation 5.10 is respected. The optimal chilled water supply temperature is at its highest possible value while the water flow rate is less than 33 l/s (Equation 5.10c).

5.5   Comparison Results and Algorithm Selected

The optimization process presented in Figure 1 is applied for existing AHU-6 system under three different optimization periods (summer, midseason, and winter) using the real monitored data. The energy use and thermal comfort are determined using the simplified VAV models described in this Chapter.

- **Case#1:** Hot and humid summer day, outdoor temperature of 28°C and a relative humidity of 70% (the enthalpy of outdoor air is 71.25 kJ/kg). The fraction of outdoor air in the supply air (Y_b) is 0.2.

- **Case # 2:** midseason day, outdoor temperature of 12°C and a relative humidity of 70% (the enthalpy of outdoor air is 27.6 kJ/kg). The fraction of outdoor air in the supply air (Y_b) is 1.

- **Case # 3:** Winter day, outdoor temperature of -10°C and a relative humidity of 90% (the enthalpy of outdoor air is -6.4 kJ/kg). The fraction of outdoor air in the supply air (Y_b) is 0.2.

Prior to this study, the real and binary NSGA-II and NSGA optimization programs are evaluated on mathematical problem using the two performance metrics mentioned above (Nassif 2002). The results of these studies, which are summarized in Appendix 3, showed that the real NSGA-II performs better than other methods.   Different GA parameter settings are used in these evaluations.

For this study (evaluation based on HVAC problem), the NSGA and NSGA-II program is executed for 100 generations, with a population size of p_z= 50, and with different parameters. The best parameters, which are: crossover probability p_c=0.9 and distribution index η_c =4, mutation probability p_m=0.04, and NSGA sharing value σ_{share} 0.15, are only presented. Figure 33 and 34 show respectively the optimal solutions obtained by NSGA and NSGA-II after 100 generations for case # 1 of HVAC problem. The Pareto-optimal solutions front is presented in the two figures. The spread and the distance are determined for two programs and for three cases, as shown in Table IV. The NSGA-II performs better for this HVAC problem with the parameters mentioned above.
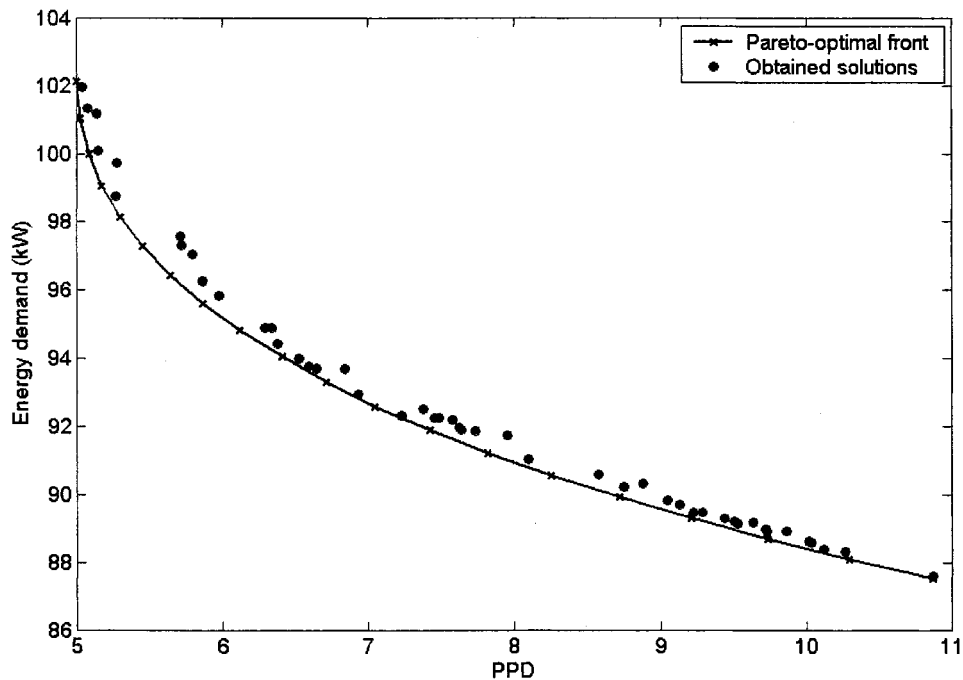
Figure 33   Optimal solutions obtained by NSGA after 100 generations for case # 1 of HVAC problem
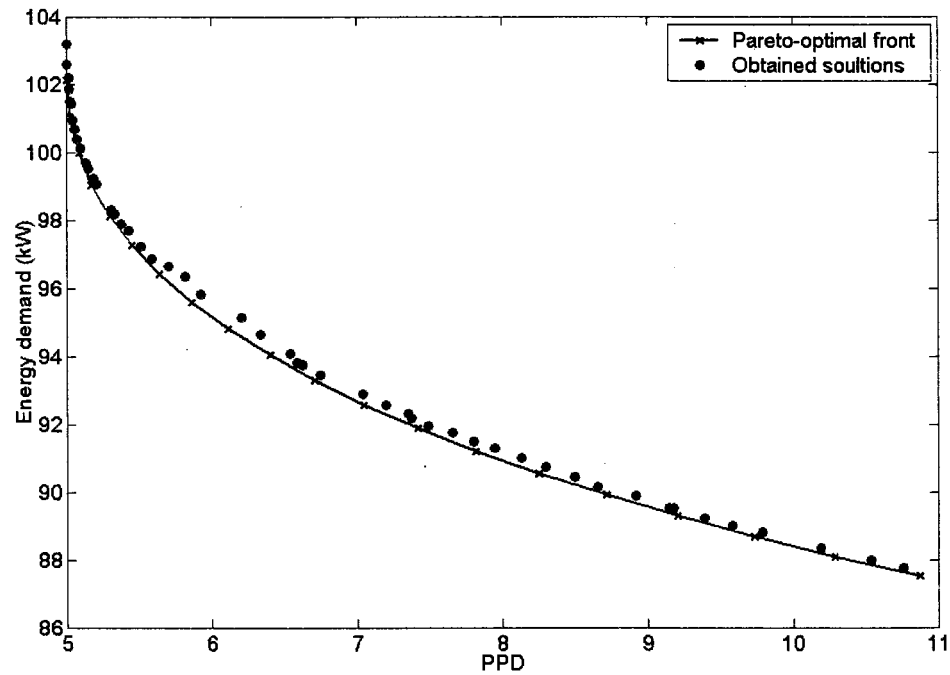
Figure 34   Optimal solutions obtained by NSGA-II after 100 generations for case # 1 of HVAC problem

Table IV

Metric performance for investigated GA methods

Periods	Metric	NSGA-II	NSGA	C-NSGA-II
Case #1	Spread	0.431	1.265	0.411
	Distance	0.346	0.727	0.341
Case #2	Spread	0.521	1.132	0.511
	Distance	0.361	0.778	0.362
Case #3	Spread	0.413	1.211	0.401
	Distance	0.361	0.662	0.362
Average	Spread	0.455	1.202	0.421
	Distance	0.356	0.722	0.345

If the initial solutions are not properly selected, premature convergence may occur. Assuming that all initial supply air temperatures values are higher than 14°C, with high exploitation, the crossover operator may not be able to find the new solution in the supply air temperature direction as shown in Figure 35 and Figure 36, and premature convergence is observed. In order to overcome this problem, the mutation operator probability could be increased, but the good solutions obtained could be deteriorated. Deb proposes the NSGA-II with a controlled elitist operator for better convergence (Deb and Goel 2001). By applying the controlled elitist operator, the NSGA-II produces a better convergence and distribution of solutions. Table II shows also the spread and distance for controlled NSGA-II (C-NSGA-II) tested on HVAC problem after 100 generations.
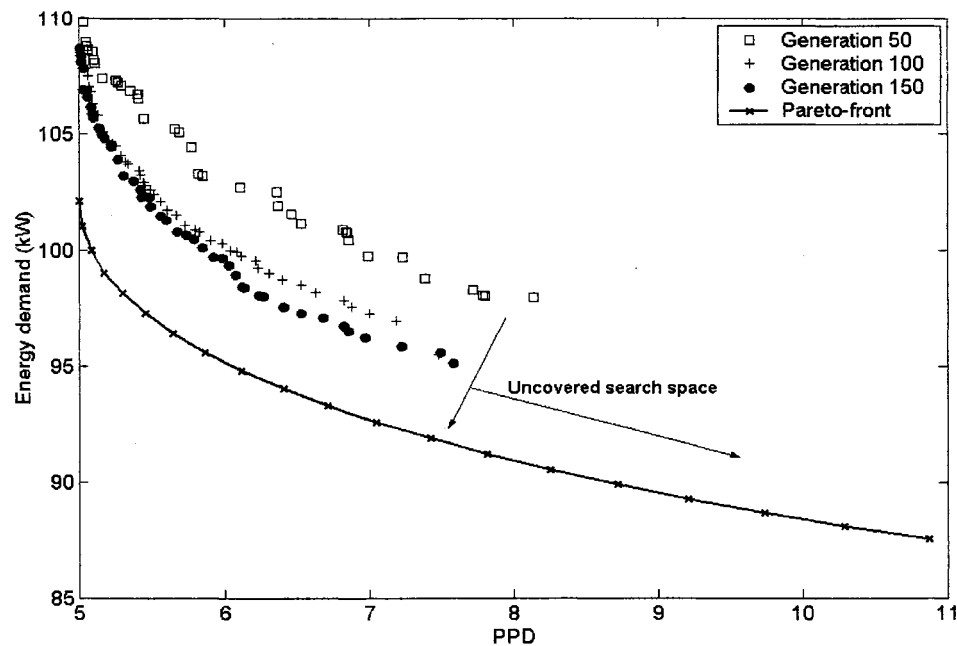
Figure 35   Search for optimal Pareto-optimal front in objective space using NSGA-II when the initial solutions are not properly selected, and with low probability of mutation.
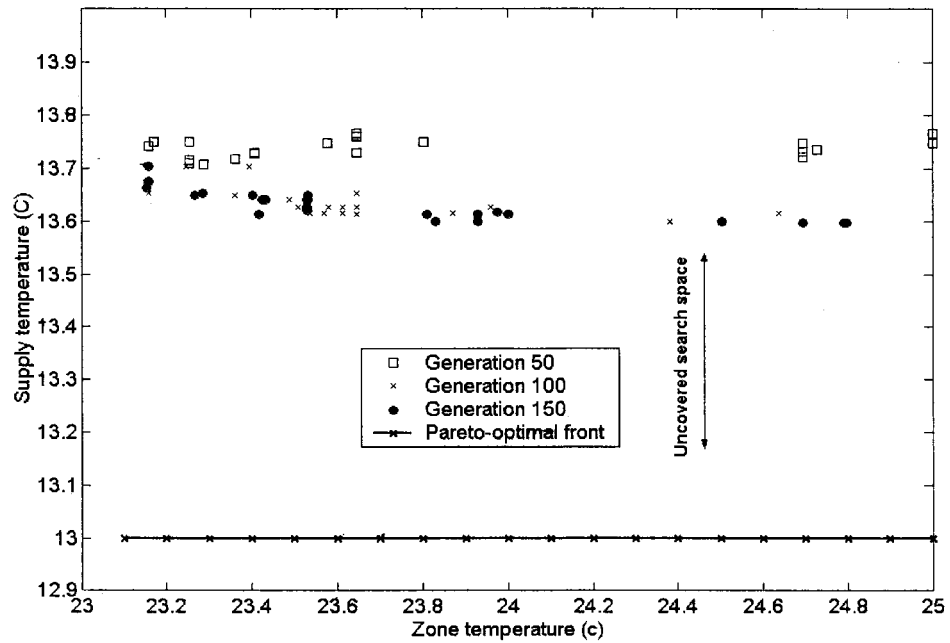
Figure 36   Search for optimal supply air temperature (13°C) in decision space using
NSGA-II, the crossover with low probability of mutation operator
cannot find real optimal solution

Figure 37 shows the solutions obtained by a controlled elitist NSGA-II. The true optimal
solutions are found using a controlled elitist NSGA-II with higher than 200 generations.
The controlled NSGA-II is therefore used to solve the investigated HVAC problem.
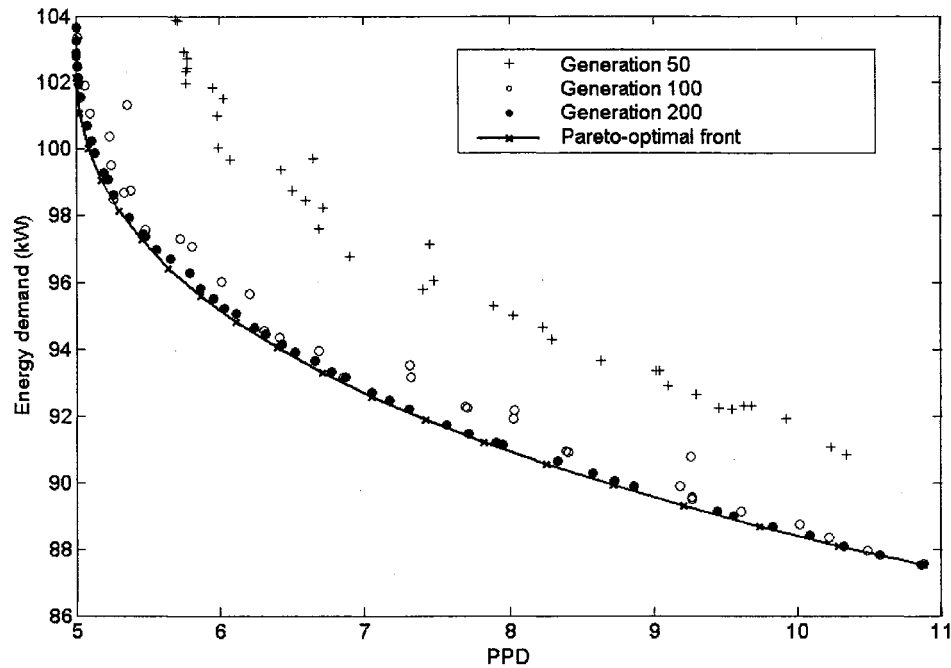
Figure 37   Search for optimal Pareto-optimal front in objective spaces using controlled NSGA-II when the initial solutions are not properly selected, and with low probability of mutation

5.6   Summary and Discussion

Since many two-objective optimization methods are available, it is natural to ask witch of them performs better when compared to other algorithms on investigated problem. The performance of these optimization methods is evaluated through the HVAC problem at three different optimization periods. In these evaluations, the following two performance metrics are used: (i) metric evaluating the closeness to the Pareto-optimal front, and (ii) metric evaluating diversity among non-dominated. To predict Pareto-optimal front, the VAV model is developed and simplified exclusively for this chapter.

The results showed that the controlled elitist NSGA-II with higher than 200 generations has a good potential to find the set of optimal solutions closed to Pareto-optimal front and to find solutions that are widely different from each other. Controlled elitist NSGA-II is then used in the optimization process proposed in this research.

Each component of the optimization process proposed in this thesis and illustrated in Figure 1 is completed through dissertation content organized in chapters 4 and 5. In the next chapter, the evaluation of this optimization process will be made and discussed.

CHAPTER 6

EVALUATION OF OPTIMIZATION PROCESS ON EXISTING HVAC SYSTEM

The supervisory control strategy set points for the existing HVAC system are optimized with respect to energy use and thermal comfort. The existing HVAC system, which is installed at École technologie supérieure, is used. The air handling unit, abbreviated AHU-6, which provides conditioned air to internal zones is only investigated among ten existing AHUs. Since the adaptive model of this existing system is trained using the detailed model, the results of both models are almost similar, and so only those of the detailed model are presented. The optimization is done for the three different weather weeks taken from July 2002, February 2003, and May 2003, respectively. The simulation results of the optimization are discussed and presented below. To allow a study of a typical multi-zone HVAC system using zone reheats, the HVAC system modified from the AHU-6 is also investigated. The detailed discussions of these simulation results are presented in our reference (Nassif, Kajl, and Sabourin 2005a), and resumed in Appendix 2.

6.1 Optimization Process

The optimization of the set points of the existing HVAC system is achieved through the optimization process shown in Figure 38. The optimization process includes: (*i*) a detailed VAV model, (*ii*) a controlled elitist non-dominated sorting genetic algorithm (C-NSGA-II), and (*iii*) three main tools, namely, data acquisition, load prediction, and optimal solution selection tools. Since we evaluate the optimization process using monitoring data, Equations (4.27, 4.28, and 4.29) of the load prediction tool are modified using this monitoring data of time k:

$$\left\{ \begin{array}{l} (q_{s,i})_k = (R_{a,z})_k \cdot \dfrac{(T_{z,i} - T_s)_k}{10} \\[3mm] (q_{l,b})_k = (R_{a,b})_k \cdot \dfrac{(w_r - w_s)_k}{6 \cdot 10^{-6}} \\[3mm] (R_{v,b})_k = \left(\dfrac{\dot{Q}_{o,b}}{\dot{Q}_{o,b,dsg}} \right)_k \cdot \dfrac{(R_{CO_2} - O_{CO_2})_k}{700} \end{array} \right\} \qquad (6.1)$$

The indoor sensible loads are then determined (Equation 6.1) by assuming that they are exactly the same as the product of the monitored zone airflow rate and the difference in the monitored temperature between the supply and air zones. The latent load of the building is calculated using the product of the fan airflow and the difference in supply and return humidity ratios. The ventilation loads are determined as a product of the outdoor airflow rate calculated by the damper model and the difference in the monitored return CO_2 concentration and outdoor air concentration (300 ppm). The monitored data are averaged for 15 minutes and saved in a data file by the data acquisition tool. The VAV model and the controlled elitist non-dominated sorting genetic algorithm (C-NSGA-II) were discussed in Chapters 4 and 5, respectively. The VAV model is shown in Figure (32), while the elitist non-dominated sorting genetic algorithm is shown in Figure (39). The optimal solution selection will be introduced later.

6.2   Zone Temperature Set Points

Typically, zone air temperatures are maintained at constant set points in the comfort zone during occupied periods. However, during unoccupied times, the set points are set up for cooling and set back for heating in order to reduce energy use. A strategy using the optimization of individual zone temperature set points combined with other controller set points during occupied periods could further reduce system energy use. The variation of individual zone air temperature set points has an effect on the system

controller set points, such as outdoor airflow rate, supply air temperature, and supply duct static pressure.
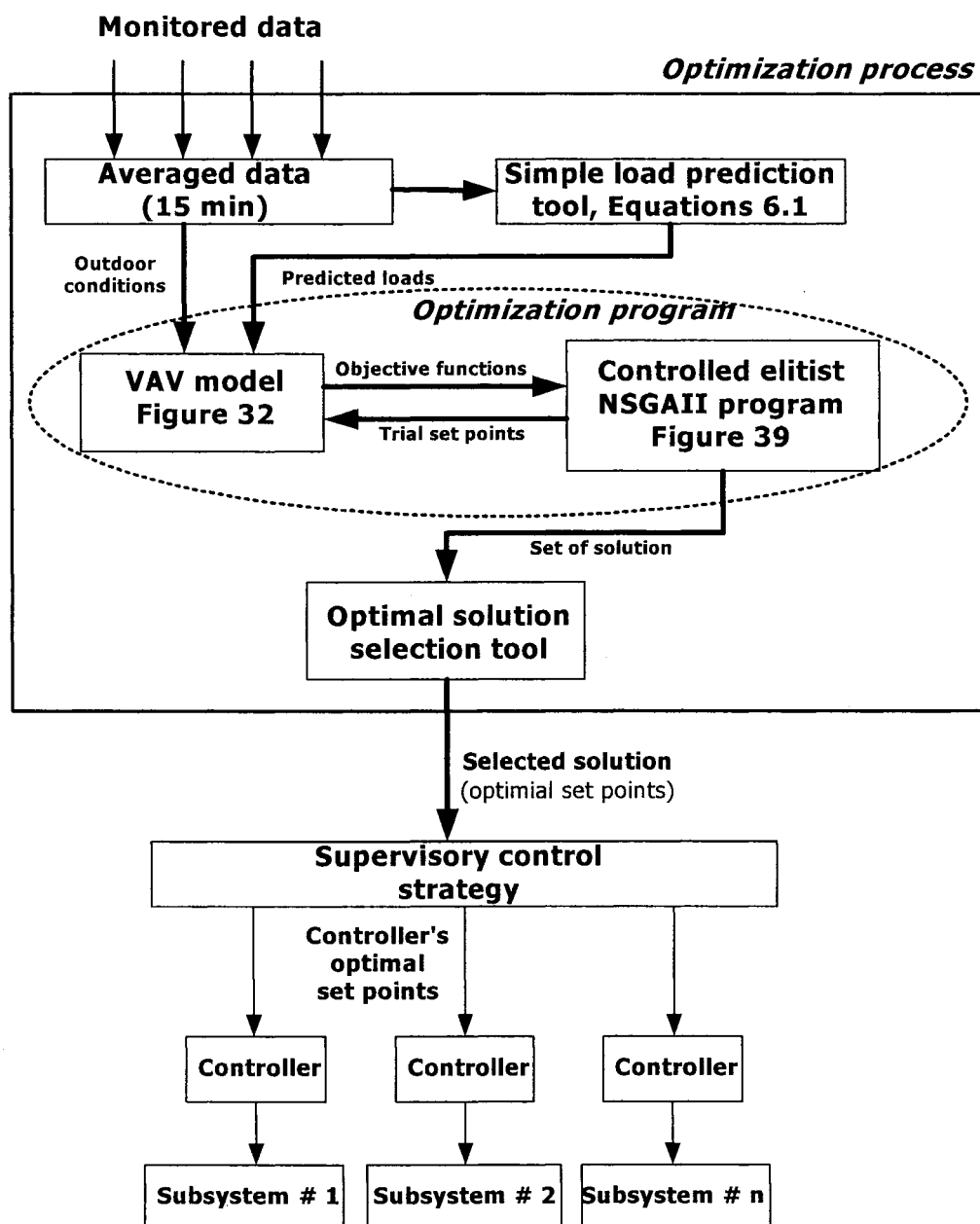
Figure 38   Schematic of optimization process of on-line optimization of supervisory control strategy

6.2.1 Optimization of Critical Zone Temperatures

Zones with relative high loads (high airflow rate) and those with relative low loads (low airflow rate) are considered as the critical zones in this research project. The system controller set points, such as supply air temperature, outdoor airflow rate, and supply duct static pressure should be optimized while ensuring thermal comfort and proper ventilation within these critical zones. The variation of air temperature set points within the comfort zone inside the critical zones could increase the possible range for selecting the system controller set points, resulting in less system energy use, as described below.

To evaluate the effect of critical zone air temperature on supply duct static pressure, the zone with a highest Ra must be examined because the set point is determined according to this zone airflow rate by Equation 4.25; for instance, if the duct static pressure set point $(P_{S,sd})$ is 200 Pa at zone temperature set point (T_z) 22.8°C, the new duct static pressure set point $(P_{S,sd})_{new}$ will be 158.7 Pa by increasing the temperature to 24°C $(T_z)_{new}$. Since the zone airflow rate at certain loads is a function of the difference between the zone and supply air temperatures, the value of this new duct static pressure is determined by the following equation:

$$\left(P_{S,sd}\right)_{new} = \left(P_{S,sd}\right)\left(\frac{\left(T_z\right)_{new} - T_{sa}}{T_z - T_{sa}}\right)^2 \tag{6.2}$$

Assuming that the fan airflow rate $(R_{a,b})$ is at 50% of the design rate, the fan energy use of the existing HVAC system will be decreased by 10% through the optimization of the critical zone air temperature (changes from 22.8 to 24°C).

In order to evaluate the effect of the individual zone temperature on the outdoor airflow rate set points, the individual zone with a relative low load must be examined. The temperature set point of this zone could be decreased in order to increase the zone

airflow required to satisfy the zone load, and consequently, to decrease the outdoor airflow rate (see Equation 3.22).

Since the supply air temperature set point is determined such that the airflow rates of critical zones remain within the *restricted range*, the airflow rate should be (i) higher than the minimum level, and (ii) lower than the maximum airflow rate introduced at full VAV damper open. The variation of the zone air temperature set point will increase the *restricted range*, allowing more freedom to choose a supply air temperature set point. For more details, please refer to 'Discussion of results' section of the reference (Nassif, Kajl, Sabourin, 2005a) summarized in Appendix 2.

6.2.2   Optimization of Non-Critical Zone Temperatures

As mentioned above, the optimization of the critical zone temperature set points combined with other controller set points during occupied periods could further reduce system energy use. The non-critical zone temperatures could all take the same value and be optimized in order to control comfort and energy use. Selecting high zone temperature set points will decrease the thermal comfort and energy use. If the daily or monthly energy use is limited, thermal comfort is only improved when the energy use penalty is low enough to lead to a cumulative daily or monthly energy use that is lower than the upper limit. That is why the two-objective optimization problem is used. Energy use savings obtained using the two-objective problem compared to those with the one-objective problem will be discussed later in this chapter.

6.2.3   Number of Critical Zones

The highest or lowest ratios of zone airflow rates to maximum design rates are first considered as the critical zones; in this case, two critical zone temperature set points are the optimal variables. When the temperature set points inside these zones are optimized,

and the zones are still at their highest or lowest ratio values, these zones are only the critical zones. Otherwise, the next highest or least are also optimized as the critical zones, and so on. The air temperatures into all the remaining zones have the same value corresponding to the required thermal comfort at this optimization time.

6.3   Problem Formation

Optimization seeks to determine the set point values of the supervisory control strategy of the HVAC system. These set points should be optimized for the operating consumption energy and the building thermal comfort. The optimization problem is formed through the determination of the problem variables, the objective functions, and the constraints.

6.3.1   Problem Variables

The following are the problem variables for the existing AHU-6 and modified HVAC systems:

- Zone temperature set points (the critical as well as the remaining zones; it counts 5 variables for modified HVAC system and 70 variables for AHU-6 one);
- Supply air temperature set point;
- Chilled water supply temperature set point;
- Required reheat applied to perimeter zones or zone supply air temperatures. This applies only to the modified HVAC system (it counts 5 variables).

The VAV model determines the optimal supply duct static pressure and CO_2 concentration (outdoor air) set points using Equations 4.25 and 3.22, respectively. The resulting problem variables consist of 74 for the AHU-6 and 14 for the modified HVAC system.

6.3.2 Objective Function

The set points of the supervisory control strategy are optimized in order: (*i*) to reduce energy use, and (*ii*) to maintain thermal comfort. The energy use, including the reheat, chiller, and fan power, is calculated using the VAV system model, as shown in Figure 32. The thermal comfort for each zone is presented as the "Predicted Percentage of Dissatisfied" (PPD), and calculated using Equation 4.30. Since the adaptive model of this existing system is trained by the detailed model, the results of both models are almost similar, and thus only those of the detailed model are presented.

6.3.3 Constraints

Constraints result from restrictions on the operation of the HVAC system. They cover the lower and upper limits of variables, such as supply air temperature, zone air temperatures, etc. The constraints also cover the design capacity of components. The fan and zone airflow rates, for instance, are restricted within the maximum and minimum limits:

- The fan airflow rate must be less than the design rate (23000 l/s), and higher than 40% of the design value.
- The zone airflow rates must be higher than the minimum limits given in the operation manual for the existing HVAC system (about 30% of the design value).

The maximum PPD of each zone is limited at 12 %, and the chilled water supply temperature is limited at 11.5 °C. The water flow rate calculated through the detailed cooling coil model must be equal to or lower than the design value when the valve is wide open (33 l/s). However, if the adaptive VAV system is used, the output of the adaptive cooling coil model based on a neural network (supply air temperature) should

be less than the supply air temperature set point required when the valve position is wide open.

6.4   Genetic Algorithm Optimization Method

The controlled elitist NSGA-II developed by Deb (Deb 2001) is used in the optimization process. This algorithm uses the elite-preserving operator, which favors the elites of a population by giving them an opportunity to be directly carried over to the next generation. After two offspring are created using the crossover and mutation operators, they are compared with both of their parents to select the best two among the four parent-offspring solutions. The flow chart of the controlled elitist NSGA-II program is shown in Figure 39. It starts with a random initial generation. First, the parents and offspring are combined, and secondly, the problem variables (controller set points) are encoded into real numbers and concatenated to form a string that represents an individual in the population. Using the VAV model, the energy use and thermal comfort (two-objective functions) are determined. As a result of the constraint functions, a penalty must be imposed on the objective functions. The constraint violation is calculated using the penalty function approach, presented in section A3.5 of Appendix 3. The penalty parameters are set at 100 and 5 for energy use and thermal comfort objective, respectively. When the objective functions of all strings in a generation are calculated, the solutions are classified into various non-dominated fronts. The crowded tournament selection operator (Deb 2001) is used to compare two solutions, and returns the winner of the tournament according to two attributes: (*i*) a non-dominated front in the population, and (*ii*) a local crowding distance. The first condition makes sure that the solution chosen lies on a better non-dominated front, while the second ensures a better spread among the solutions. The number of individuals in the current best non-dominated front is restricted. The simulated binary crossover (SBX) is used here to create two offspring from two-parent solutions. The random simplest mutation operator is applied to randomly create a solution from the entire search space. The control

parameters of NSGA-II must be adjusted to give the best performance. A number of genetic algorithm methods with adjustments made to their control parameters were investigated in Chapter 5. It was found that the NSGA-II with that control parameters produces better convergence and distribution of optimal solutions located along the Pareto optimal solutions. When the program stops searching, the 500 generations are quite enough to find the true optimal solutions. The parameters are: crossover probability p_c=0.9 with distribution index η_c =4, mutation probability p_m=0.04 and population size p_z= 100.

6.5   Evaluation of the Optimization Process on AHU-6 System

The proposed optimization process presented in Figure 38 is applied on the existing AHU-6 system. Evaluations are done for three different weather weeks of July 2002, February 2003, and May 2003. The data acquisition tool provides the averaged monitored data for these periods. The load prediction tool is used in order to determine the loads (using Equation (6.1)). The energy use and thermal comfort are determined by the detailed VAV model, as explained in section 4.6, and presented in Figure 32. The controlled elitist NSGA-II that was evaluated and tested in Chapter 5 is used to solve the optimization problem. Figure 39 also shows how the VAV model links with controlled elitist NSGA-II. Since the goal of these evaluations is to compare the optimal energy use with the actual use, the optimal selection tool is not used; rather, only one solution among the set of feasible solutions is selected. This solution has the same thermal comfort (PPD) as that obtained from the monitored data of the actual system.

The energy use of the actual control (actual energy use) is also simulated using the VAV model presented in Figure 32. In this case, the actual set points are used. It should be noted that when the airflow rates introduced in each zone are calculated in step 2 of section 4.6, the resulting zone airflow rates are the same as the monitored values. The outdoor damper is used to calculate the outdoor airflow rate instead of step 5 of section 4.6.
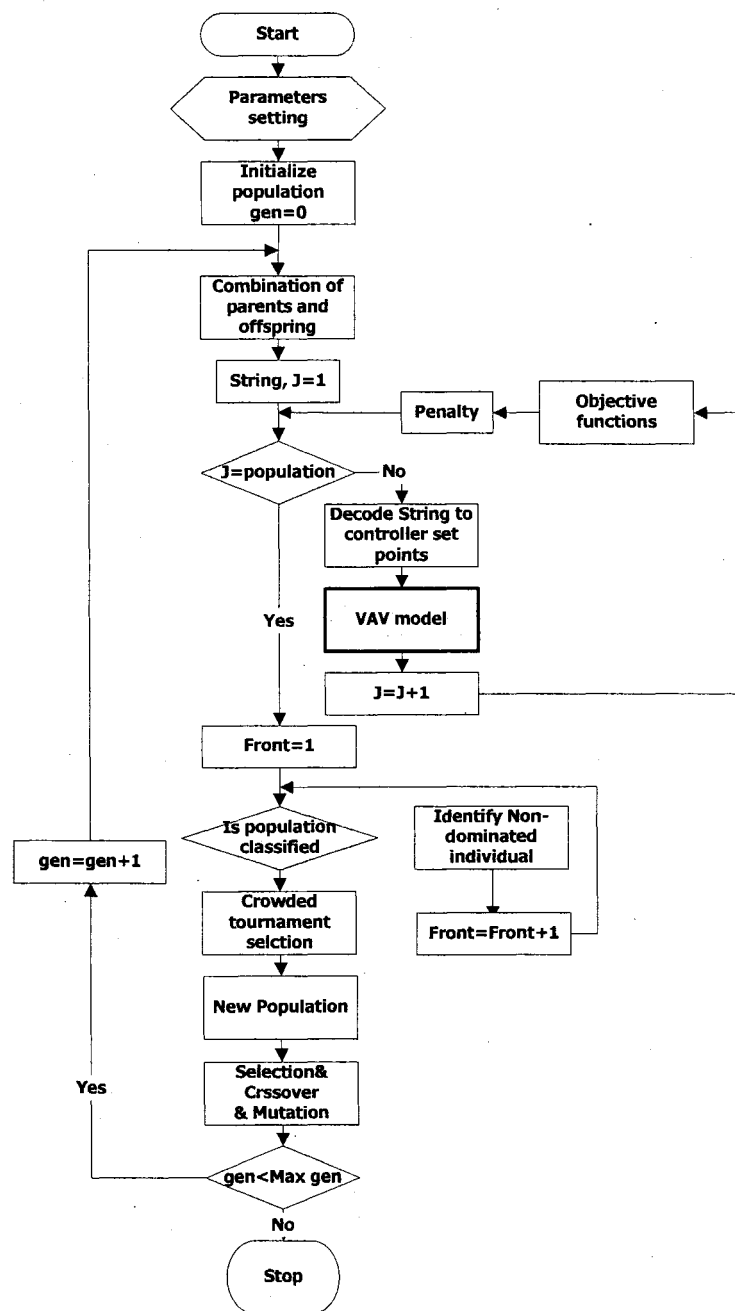
Figure 39   Flow chart of controlled elitist NSGA-II program

6.5.1   Results of AHU-6 Evaluations

The optimization of controller set points was done for three different weeks of July 2002, February 2003, and May 2003. Figure 40 shows the feasible solutions obtained after 500 generations at 4:00PM for July 25. The PPD presented here is the mean value of the PPD determined for each of 70 zones. An increase in thermal comfort (decrease in PPD) requires an increase in energy demand. As mentioned above, to compare the optimal energy use with the actual one, only one solution, with the same PPD value as the actual one is selected (the bold point in Figure 40). Figure 41 shows the actual and optimal energy demand for one week in July. The energy savings by optimization is about 19.5% for this week. Figures 42 through 44 show the optimal supply air and chilled water temperatures, the duct static pressure, and the outdoor airflow rate. The actual supply air temperature, chilled water temperature, and duct static pressure for this investigated week of July are 14°C, 7.2°C, and 250 Pa, respectively.
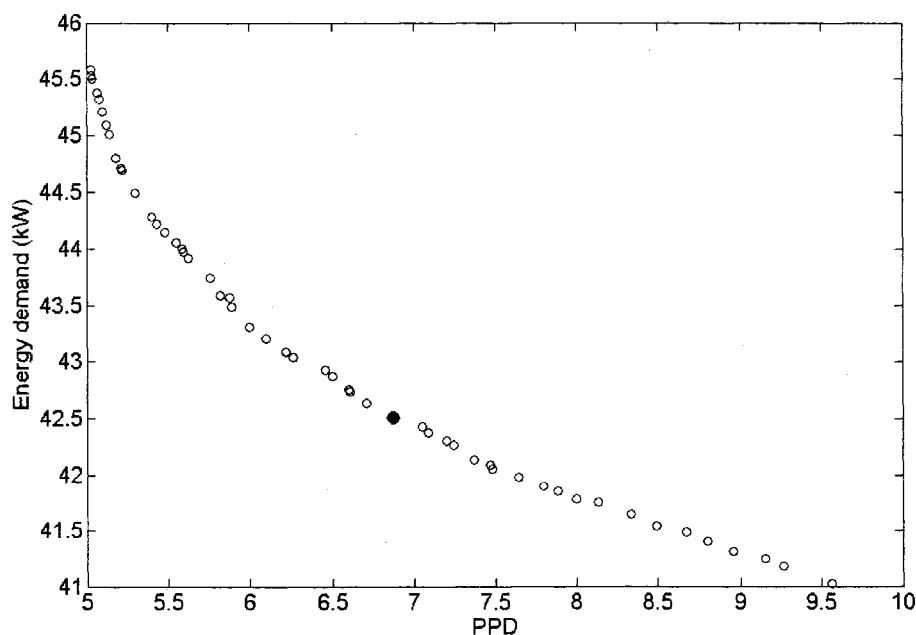
Figure 40   Feasible solutions obtained after 500 generations at 5:00PM for July 25
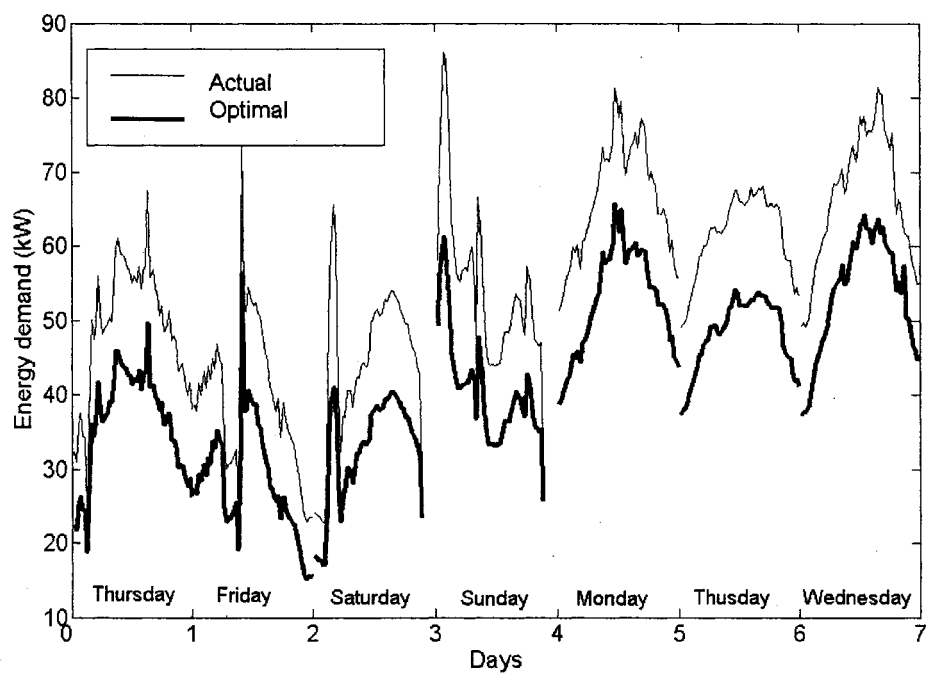
Figure 41   Actual and optimal energy demands for July 25 to 31, 2002
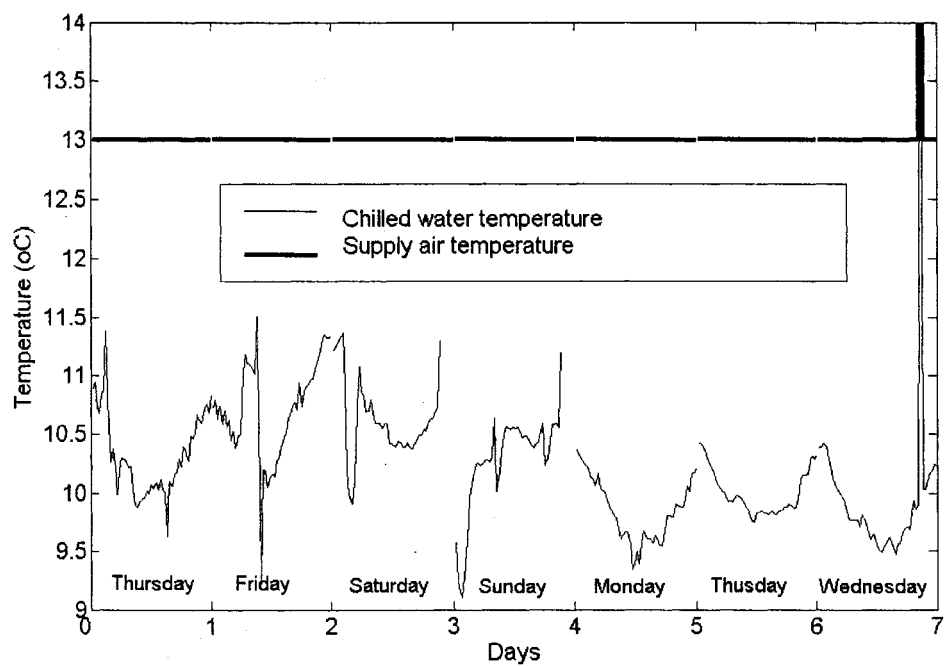
Figure 42   Optimal air supply and chilled water temperature set points for
                 July 25 to 31, 2002
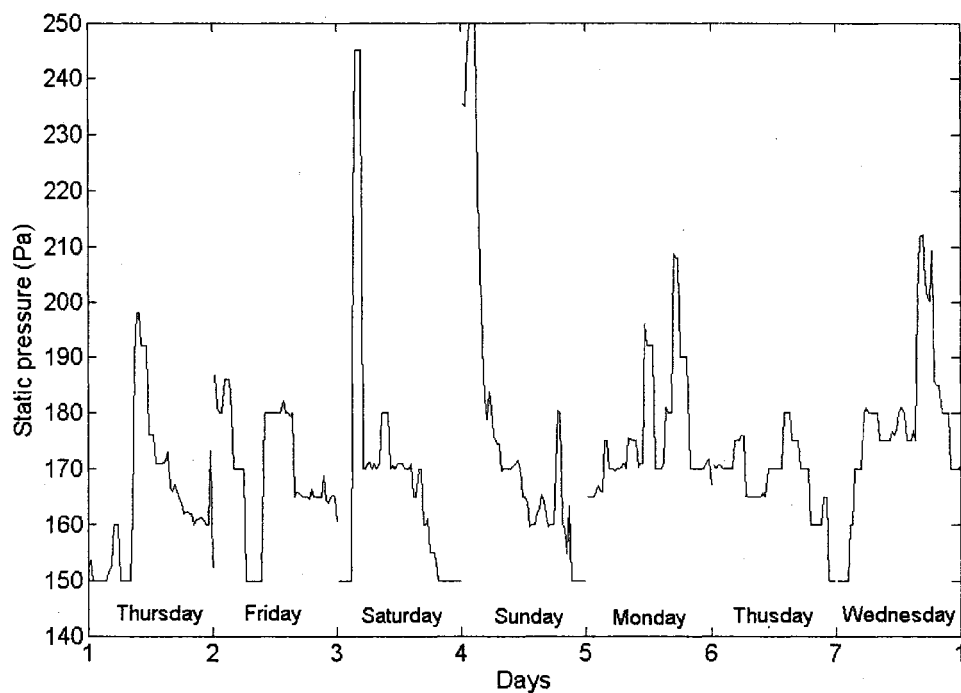
Figure 43   Optimal duct static pressure set point for July 25 to 31, 2002
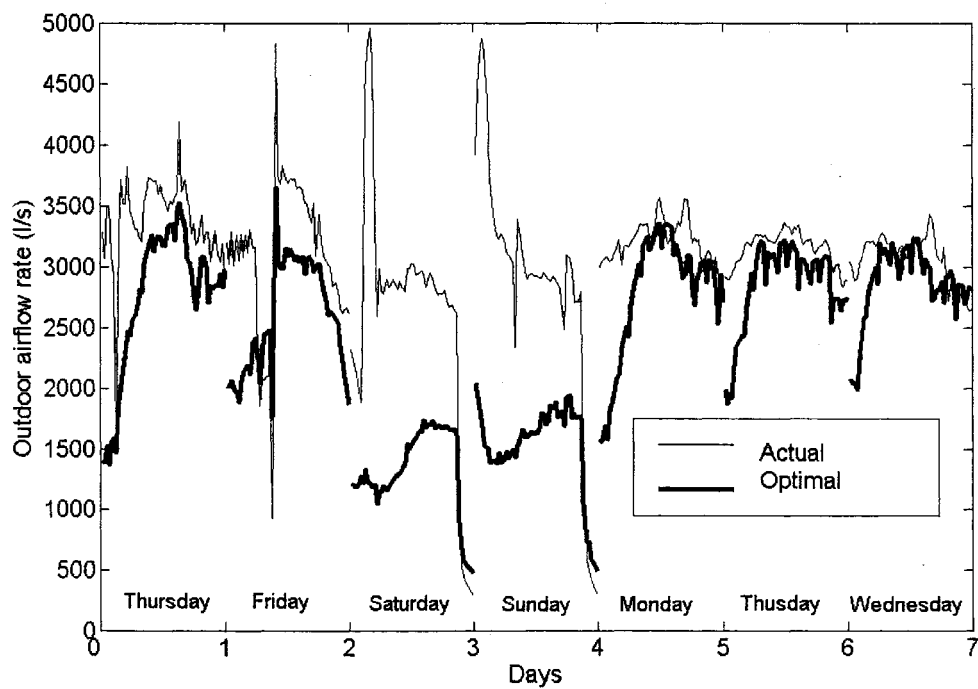
Figure 44   Optimal and actual outdoor airflow rates for July 25 to 31, 2002

The optimization was also done for the cold and midseason weather weeks of February and May, 2003. On these days, since the AHU-6 serves the internal zones without reheat, energy is used only by the fan for May and by the fan and the system heat for February. Figure 45 shows the actual and optimal energy demands for two different days (February 26 and May 4). The saving energy use for each week of February and May are 50% and 40%, respectively.
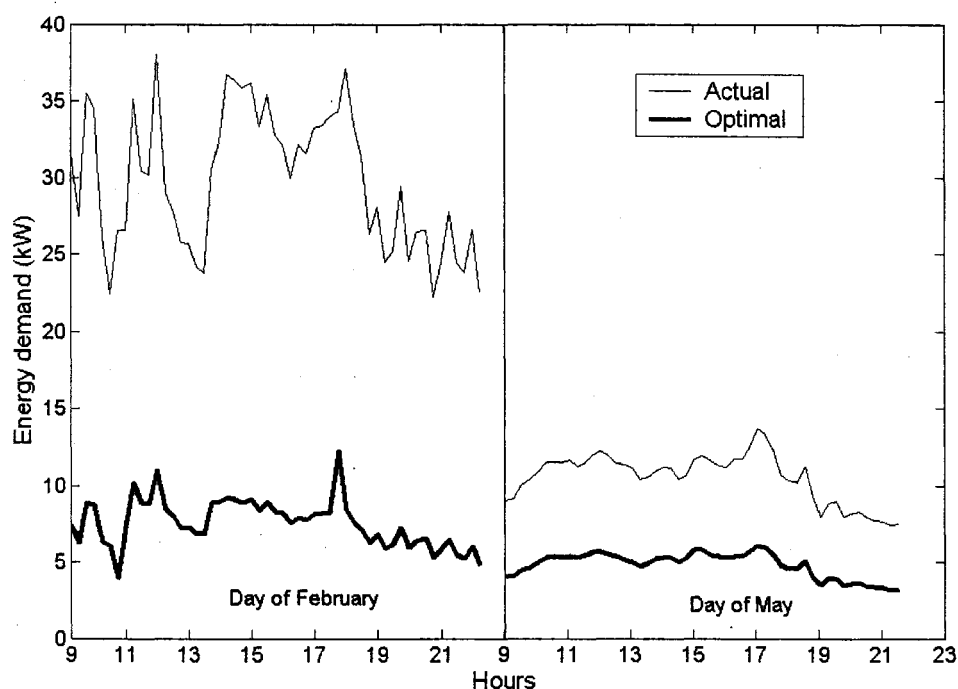
Figure 45   Optimal and actual energy demands for two different days (February 26 and May 4, 2003)

6.5.2   Discussion of the AHU-6 Evaluation Results

The performance of MOGA was evaluated in Chapter 5. The search results indicate that the controlled NSGA-II has the potential of finding Pareto optimal solutions. Figure 46 show the computational effectiveness of the algorithm in finding these solutions. Since defining stopping rules is a difficult task, 500 generations are quite enough to find the true Pareto optimum set, as discussed in Chapter 5. However, it is likely that the number

of generations required to find the Pareto optimum set was much less (100 generations). The search converged to the optimum region within 30 generations. Most solutions in the initial population were infeasible, but within 10 generations, feasible solutions became available.
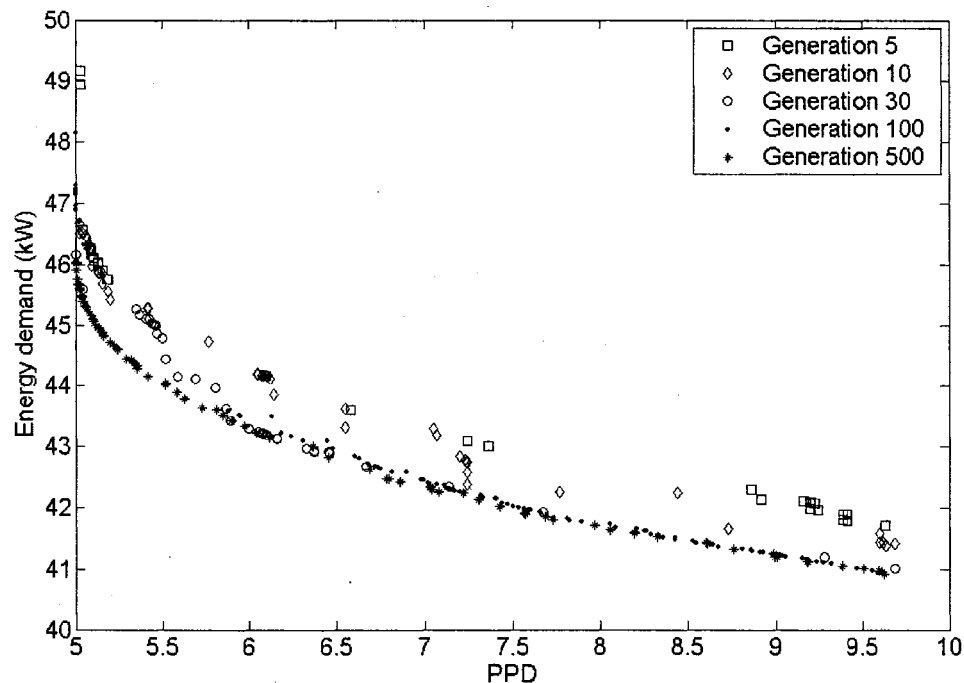
Figure 46   Computational effectiveness of the algorithm in finding optimal solutions

As shown in Figures 41 and 45, significant savings in energy use could be obtained through the optimization of controller set points. On summer days, the optimal chilled water supply temperature (as shown in Figure 42) is higher than the actual one (7.2°C). Thus, chiller energy savings are obtained due to a high coefficient of performance COP. More chiller energy savings are obtained using the ventilation control strategy proposed in Chapter 3 as a result of outdoor airflow rates that are lower than the actual rate (see Figure 44). However, the ventilation control strategy is almost not worked in the periods of May and February because the outdoor air damper is most the time at modulated or

fully position. Figure 47 shows the optimal zone temperature set points for the critical and most non-critical zones for three days of July (26, 27, and 30). The set point for zone 69 should be decreased on the Saturday in order to increase zone airflow rate and consequently decrease the system outdoor airflow rate. However, this set point should be increased on Thursday in order to decrease zone airflow rate and consequently decrease the supply duct static pressure. The non-critical zones (most zones) have set points given the thermal comfort (PPD) as the actual one.
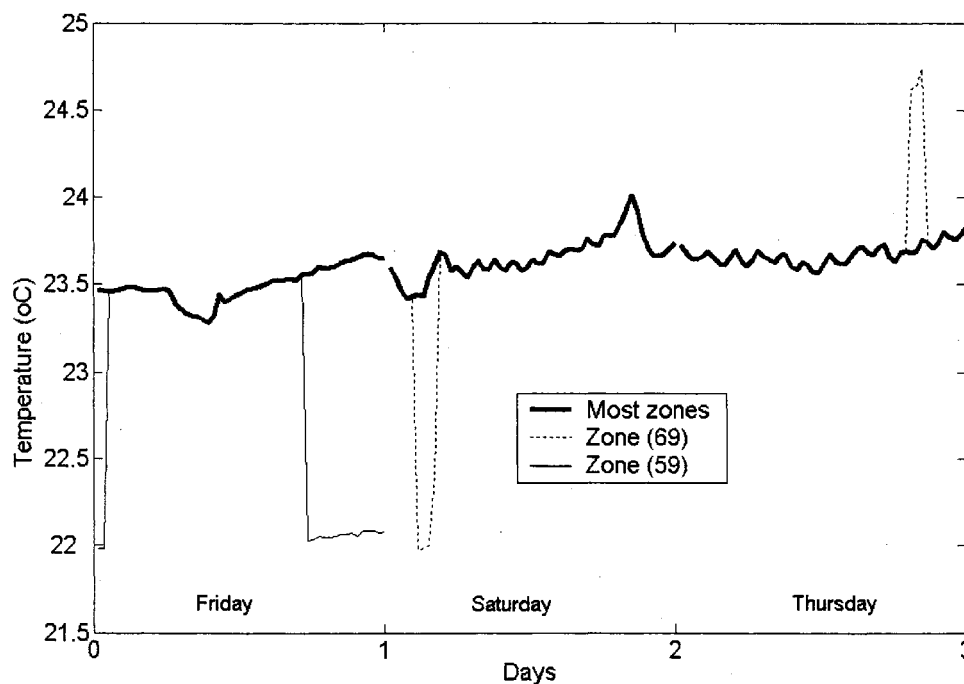
Figure 47   Optimal zone temperature set points for critical and other zones for three days

The actual supply air temperature set points, which are a function of airflow rate and outdoor air temperature, are about 17°C for the investigated winter week (February) due to low outdoor air temperature. However, since no reheat are used in internal zones, the fan energy use only affects the objective function (energy use). The optimal supply air temperature set points are at their lowest values when no zones are overcooled. They are about 15°C. Since the actual supply air temperature set points are higher than the optimal

ones, the actual airflow rate, and consequently, the fan energy use, are also higher. Figure 48 shows the optimal and actual fan airflow rates for February 26. On winter and midseason days, energy use savings reach 50% through the optimal supply air temperature (low temperature), resulting mainly form a decreasing fan airflow rate and duct static pressure. The system heating coil could be opened on very cold days. Figure 49 shows the optimal and actual heating energy demand for February 26.
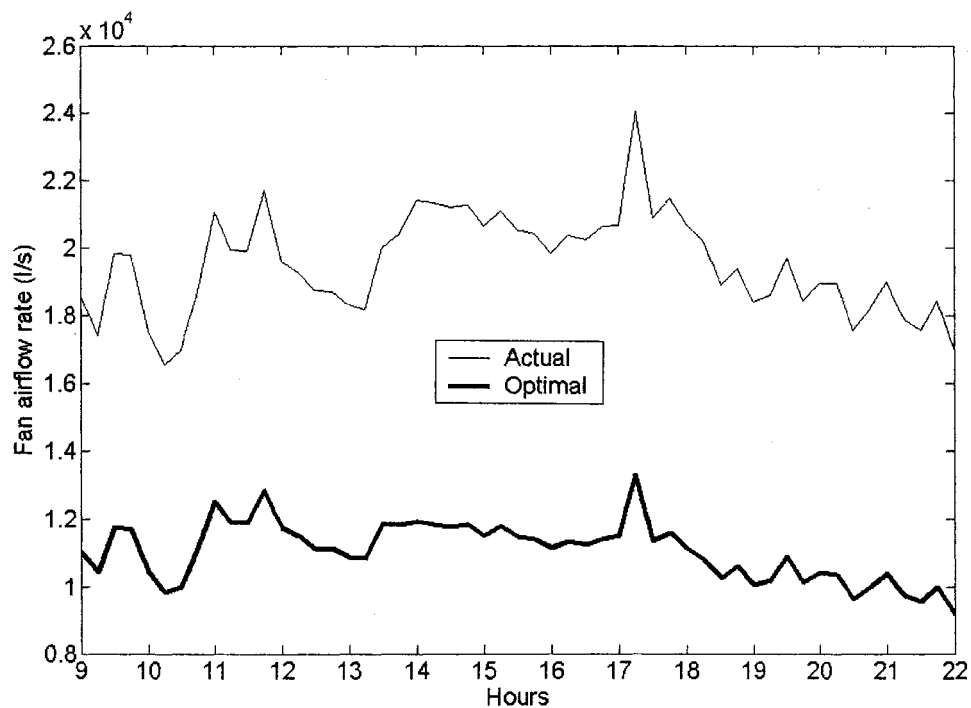
Figure 48   Optimal and actual fan airflow rate for February 26
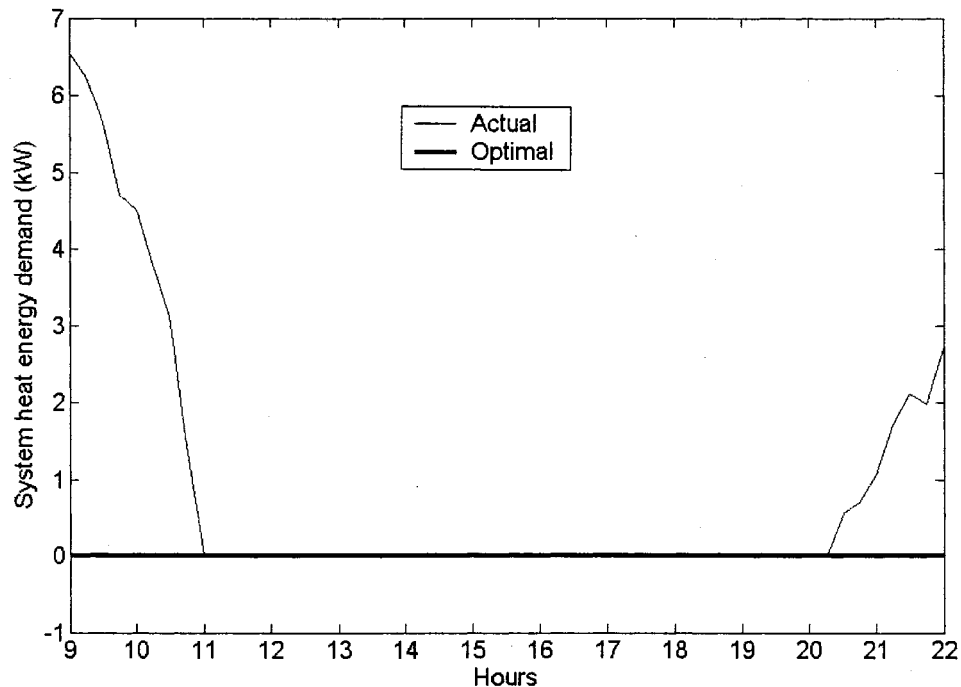
Figure 49   Optimal and actual heating energy demand for February 26

The minimum airflow rate introduced into the zone should be limited in order to provide the required ventilation and a proper mixing of supply and room air. The minimum limit of the zone airflow rates in the existing HVAC system (AHU-6) as reported in the operation manual are within 30-25% of the design airflow rates. Even with the minimum airflow restriction mentioned above, it was observed through monitoring, that the supply air introduced into some zones was less than the minimum zone airflow rate limit or zero. To take into account these operations, three "minimum zone airflow rate constraints" were applied in order to calculate the energy use of the optimized supervisory control strategy of the existing HVAC system.

- *100% constraint*—the minimum zone airflow rates are exactly the same as reported in the operation manual of the existing AHU-6 system.

- *90% constraint*—the minimum zone airflow rates are equal to 90% of the recommended minimum zone airflow rates.

- *Without constraint*—the minimum zone airflow rates could be zero, and thus the zone VAV damper could shut off.
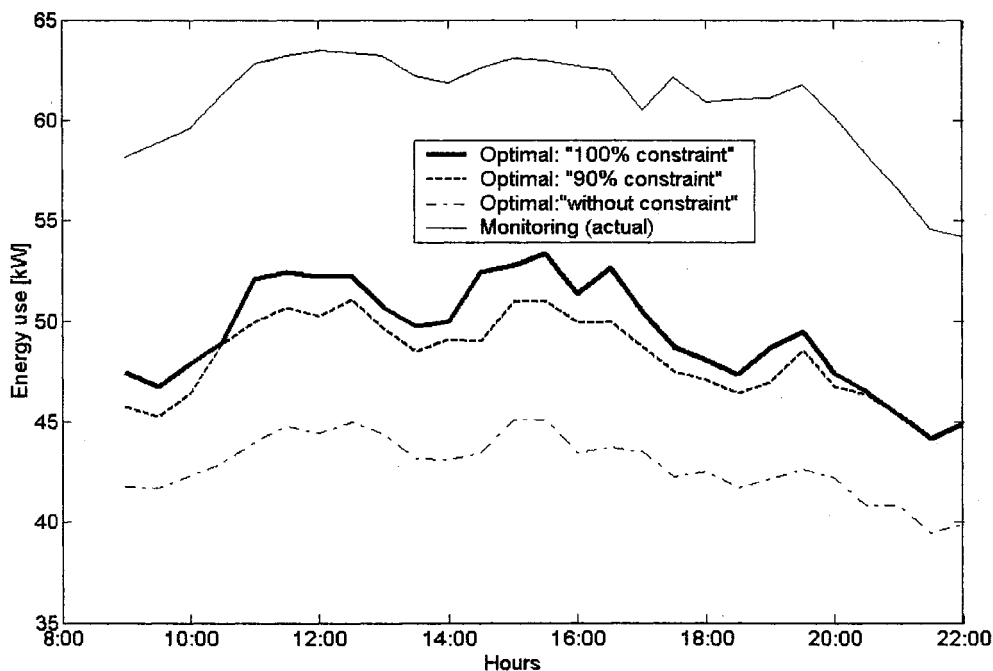
Figure 50   Actual and optimal energy demand at three 'minimum zone airflow rate constraints' and for July 29, 2002

It was found that the energy savings is higher for the case "without constraint," as shown in Figure 50. Concerning the zone variables obtained by monitoring and by optimization, it could be noted that:

- The optimal zone airflow rates are limited by the zone airflow rate constraint described above. The optimization process with "100% constraint" saves energy use while providing ventilation requirements introduced by the limited minimum zone airflow rate. However, since the actual minimum zone airflow rates are not

limited, the "without constraint" option is close to the actual system operation, resulting in this case, in further energy savings.

- Most optimal zone temperatures lie between 23-24.5°C, and the optimal zone PPDs are limited to within the [5-12] range.

- Actual zone temperatures lie between 19-25°C, and most zone PPDs are within the [5-15] range. Some zone PPD values are as high as 30.

These results indicate that the optimization of the control strategy with the required constraints could improve the operating performance of the existing HVAC system. The reader could refer to our reference (Nassif, Kajl, Sabourin 2004c) for more details.

6.6   Evaluation of the Optimization Process on Modified HVAC System

Through monitoring, it was found that the AHU-4 system is oversized. That means the fan airflow rate is most often at the minimum value. In addition, since all zones are located in the same exposure, thermal loads through the zones vary in the same pattern. To investigate the on-line optimization of an HVAC control system serving multiple zones with high-load distributions between them, the multi-zone VAV system was created from the AHU-6 system, on the assumption that this modified system yields significant zone load distributions and that zone reheats are used. The description of this modified system and the optimization results are presented in detail and discussed in our paper (Nassif, Kajl, Sabourin 2005a), which is also summarized in Appendix 2. Three different control strategies applied to that system were evaluated for one typical summer day. The first two strategies (*A* and *B*) use the optimization process described in Figure 38. However, in strategy *B*, the zone reheats are not optimized. The last strategy (C) is the actual strategy applied to the existing system. Comparing the energy demands obtained for the three investigated strategies as shown in Figure 51, the energy use savings are about 2% when the reheat is optimized (compare A with B) and about 12%

by applying the optimization process with zone reheats used (compare A with C). The results are discussed in detail in Appendix 2.
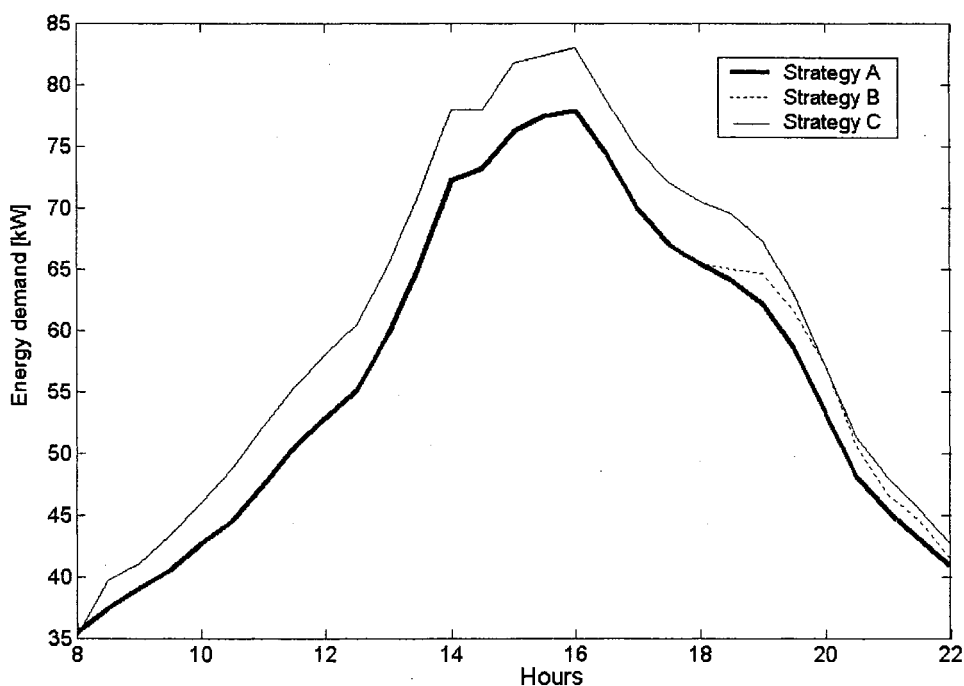
Figure 51   Energy demand obtained for three investigated control strategies

6.7   Two-Objective Optimization and Daily Energy Use Control

Thermal comfort is presented in this study as the objective function, but the optimization problem could be solved by defining the thermal comfort criterion as the constraint. The one single optimal solution would then be obtained, with a high PPD limit. The advantage of using two-objective problems is to minimize daily energy use by fluctuating building PPD during occupied periods, taking into account required energy demands. This is achieved by using the selection tool as follows.

During each period, this tool selects the solution requiring the least energy use (extreme right solution in Figure 40). The additional energy use required for improving thermal

comfort PPD from this selected solution to the next is determined and compared with the permission set point recorded by the operator in the selection tool (E kW/PPD). If this additional energy use requirement is lower than the permission set point, the next solution will be selected; otherwise, the first solution is, and so on, for all the solutions. To evaluate the optimization results of the existing AHU-6 and modified HVAC using the one-objective and the two-objective problems, different permission set point values are settled in the selection tool during occupied periods for the two investigated systems. Daily energy use and daily thermal comfort (*PPD*) are calculated and illustrated as a function of the permission set point in Figure 52 for the modified HVAC, and in Figure 53, for the existing system. When the permission set point is at 1.18 for the modified HVAC (Figure 52), the daily PPD obtained is 6%, and the daily energy use is 403 kWh by using the two-objective optimization problem. However, the daily energy use is 413 kWh for the same daily PPD, using the one-objective optimization problem. In both figures, curves K and J represent optimal solutions using the two-objective and one-objective optimization problems, respectively. While the permission set point is within the [0.1-20] range, the energy savings represented by the area between the two curves can be obtained by using the two-objective problem with the selection tool, as compared to the one-objective problem. If the value of the permission set point is chosen outside this range, the extreme solutions will be selected. In this case, it could be the same as in an objective problem by defining the thermal comfort criterion as the constraint. The optimal daily solution curve varies from day to day according to load and outdoor conditions. If the building load varies significantly during the day, such as with the modified HVAC unit, the energy savings will be greater using the two-objective problem. If the on-line cumulative energy use during the day or current month exceeds the required level (peak energy use), the permission set point could be reset on-line to a lower value. Within the framework of this concept, the month or daily energy use could be controlled to not exceed the required level by varying the permission set point.
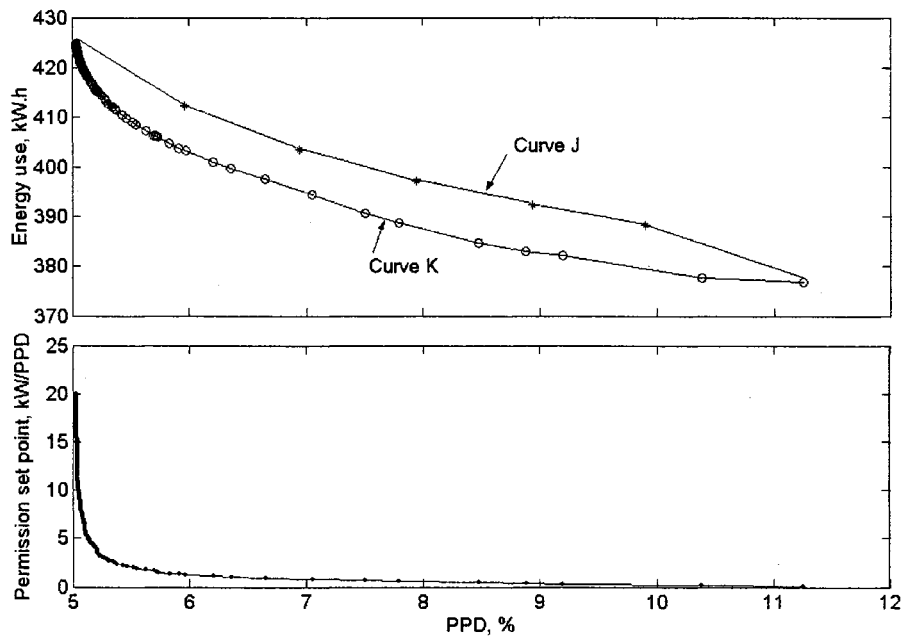
Figure 52   Optimal daily energy use obtained using the two-objective selection tool
(curve k) and one-objective optimization (curve J) for modified HVAC
system
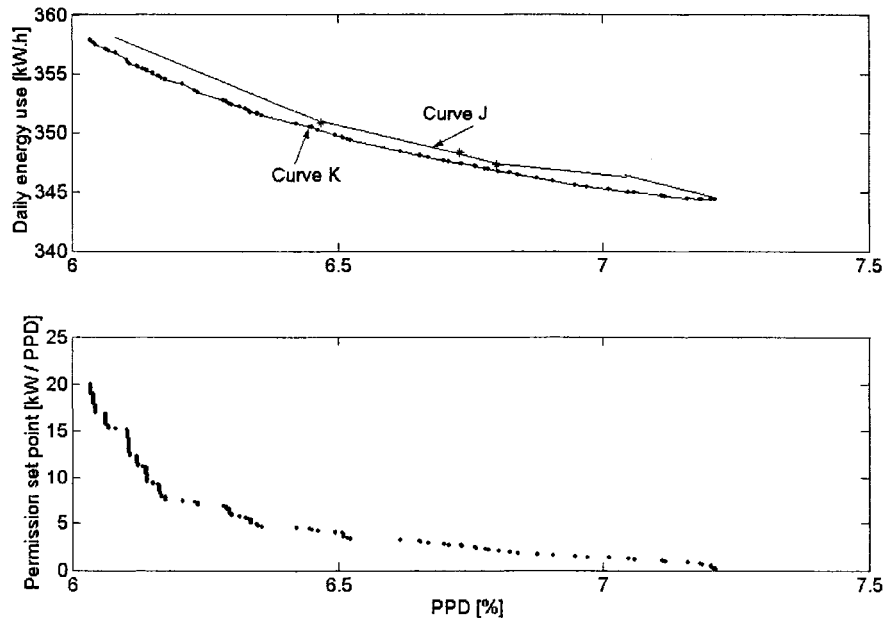
Figure 53   Optimal daily energy use obtained by two-objective selection tool (curve
k) and one-objective optimization (curve J) for existing AHU-6

6.8 Summary and Discussion

The supervisory control strategy set points are optimized using a two-objective genetic algorithm. The set points, such as the zone air temperatures, the supply air temperature, the supply duct static pressure, the required zone supply air temperature or reheat, the minimum outdoor ventilation flow rate, and the chilled water supply temperature, are optimized for the existing and modified HVAC systems. The existing HVAC system results show that by comparing actual and optimal energy use, the optimization of a supervisory control strategy could save energy by 19.5%, 50%, and 40% for one-week periods in July, February, and May, respectively, while satisfying minimum zone airflow rates and zone thermal comfort. These results indicate that the optimization of the control strategy with required constraints could improve the operating performance of the existing HVAC system. Three different control strategies are also evaluated for a typical or modified HVAC system. These results show that the strategy that optimizes all controller set points, including zone temperature and zone reheat, performs better and provides more energy savings. Other results indicate that the application of a two-objective optimization problem could help control daily energy use or daily building thermal comfort while providing further energy use savings as compared to the one-objective optimization problem.

CONCLUSION

In this thesis, we have presented an innovative approach to building operation, called the optimization process. It will permit the automated operation of a building's mechanical systems when installed in parallel with a building central control system. The optimization process utilizing artificial intelligence algorithms can work with most existing building energy management control systems. It can provide an excellent means of reducing utility costs associated with maintaining environmental conditions in buildings through better supervisory control. This supervisor sends the optimal controller set points to local control loops. The set points, such as the supply air temperature, zone temperatures, the zone supply air temperature (zone reheat), the duct static pressure, the chilled water supply temperature, and the supply CO_2 concentration (minimum airflow rate) are then the problem variables, while the thermal comfort and the energy use are the objective functions. To develop the proposed optimization process, the following methodology is employed:

(i)   Monitoring of the investigated existing HVAC system;

(ii)   Development of the new ventilation control strategy;

(iii) Modeling and validation of HVAC components;

(iv)   Development of optimization algorithm;

(v)   Development of proposed optimization process;

(vi)   Validation of the developed optimization process on multi-zone HVAC systems.

The monitoring of the investigated existing HVAC system was done using data over a period of three years. It showed that certain operation problems exist although this HVAC system is considered as the "intelligent buildings". This improper operation leads to energy use waste. However, the optimization process developed in this thesis could improve the performances of this system. By optimizing the supervisory control

strategy, while taking into account the required constraints, the system could overcome the operation problems indicated above as well as decrease energy use while maintaining the required thermal comfort.

Through monitoring, it was seen that the outdoor airflow rate introduced into the system is greater than requirements causing high energy use. Thus, the new ventilation control strategy developed in this thesis could minimize energy use while ensuring proper indoor air quality in all zones, including in critical zone(s). The strategy maintains a supply CO_2 concentration set point that is low enough to dilute CO_2 generated by full occupancy in the critical zone. The supply CO_2 concentration set point could be determined on-line using the monitored zone airflow rates, which has recently become possible with the use of direct digital control terminal boxes. The strategy is a compromise between the multiple-space equation and the CO_2-based demand control ventilation strategies, which take into account: (*i*) the building's actual occupancy and (*ii*) the critical zone ventilation requirement. Thus, the strategy takes into account the on-line over-ventilation occurring in buildings, while considering the critical zone ventilation requirement. The simulation results applied to two existing AHU systems show that the proposed ventilation control strategy needs less outdoor air, and consumes less energy than the multiple-space equation by taking greater advantage of on-line over-ventilated spaces. Although the CO_2-based demand control ventilation strategy uses the lowest outdoor air and energy, there is poor indoor air quality in some zones. The simulation results also showed that energy use could be saved as compared to the case with the actual ventilation control strategy by implementing the proposed ventilation control strategy while ensuring a good indoor air quality in all zones, including the critical one.

The proposed ventilation control strategy was integrated into the on-line optimization process of the supervisory control strategy such that with each simulation, the set points

of the HVAC system, including the supply CO_2 concentration set point (or outdoor airflow rate), could be optimized.

The component models required for the optimization calculations are developed and validated against measured monitored variables or the variables calculated through other validated models. The model validations are achieved in spite of difficulties that are faced due to a lack of required measured data. Since our research is developed the optimization process for the existing system, the component models based on detailed information of this system are developed. For future applications in new or existing HVAC systems, when detailed information is not available, the on-line adaptive component models could be used instead. The validation results show that the component models can be accurately used in the proposed optimization process.

Since many two-objective optimization methods are available, it is natural to ask which of them performs better when compared to other algorithms on the investigated problem. The performances of multi-objective genetic algorithm optimization methods are evaluated through mathematical and HVAC problems. In these evaluations, the following two performance metrics are used: (*i*) metric evaluating the closeness to the Pareto-optimal front, and (*ii*) metric evaluating diversity among non-dominated solutions. To predict the Pareto-optimal front of the HVAC problem, the VAV model is developed and simplified exclusively for this purpose.

The results show that the controlled elitist NSGA-II with over 200 generations has a good potential for finding the set of optimal solutions close to the Pareto-optimal front and for finding solutions that are widely different from each other. The controlled elitist NSGA-II is then used in the optimization process proposed in this research.

The optimization process was applied to the existing HVAC system, which is installed at the École technologie supérieure. The air handling unit, abbreviated AHU-6, and providing conditioned air to internal zones, was investigated. The optimization using a

two-objective genetic algorithm was done for the three different weather weeks taken in July 2002, February 2003, and May 2003. The set points, such as the zone air temperatures, the supply air temperature, the supply duct static pressure, the zone supply air temperature or reheat required, the minimum outdoor ventilation flow rate, and the chilled water supply temperature, are optimized for the existing and modified HVAC systems. The existing HVAC system results showed that by comparing actual and optimal energy use, the optimization of a supervisory control strategy could save energy by 19.5%, 50%, and 40% for one-week periods in July, February, and May, respectively, while satisfying minimum zone airflow rates and zone thermal comfort. These results indicate that the optimization of the control strategy with required constraints could improve the operating performance of the existing HVAC system. However, three different control strategies are also evaluated for a typical or modified HVAC system. The results show that a strategy that optimizes all controller set points, including zone temperature and zone reheat, performs better and provides more energy savings. Other results indicate that the application of a two-objective optimization problem could help control daily energy use or daily building thermal comfort while providing further energy use savings as compared to the one-objective optimization problem.

Future Work

As discussed in this thesis, the performance of an HVAC system could be improved by using a better supervisory control strategy. The findings of our research project are encouraging with respect to further investigations. In order to improve the performance of the optimization process, we believe that the future work can be directed as follows:

- The optimization process can be improved to simultaneously achieve the following two tasks (i) optimization of controller set points and (ii) optimization of controller parameters. At a sampling instant, the optimization OP fetches the necessary data from the sensors and local controllers in order to determine the optimal controller set points and controller parameters.

- To make the optimization process work with most existing building energy management control systems, artificial intelligence algorithms could be used. Adaptive component models using artificial neural networks should be further investigated and used in this optimization process.

- The thermal comfort model used is based on steady-state balance. The tabulated PMV values are used to predict the performance of a VAV system for a combination of variables. More sophisticated thermal comfort models could be used in order to take into considerations the effect of different factors, such as air and radiant temperatures, humidity, and airflow speed.

- Further investigations should be conducted to improve the predictions of the zone sensible loads and ventilation loads.

- Data received from different sensors and used in the optimization process should be examined in order to detect any sensor malfunctions.

APPENDIX 1

MANUFACTURER'S DATA

A1.1   Fan Charaterstics

Table V

Coefficients used in the detailed fan model

Coefficients	Coefficient of Equation (4.5)				
	a_0	a_1	a_2	a_3	a_4
Values	1.8571	-164.35	10125	-249186	0
Coefficients	Coefficient of Equation (4.6)				
	b_0	b_1	b_2	b_3	b_4
Values	-0.0037	1.2093	104.83	3811.1	-52443

A1.2   Damper Charaterstics

Table VI

Coefficients used in damper model

Damper position %	0	10	25	50	75	100
C_{damper}	704.77	501.13	517.19	1052.8	1276.8	2813.3
X	0.1813	0.331	0.3389	0.3521	0.4345	0.4828

Equation 4.11: Q_0 (l/s) and ΔP (Pa)

A1.3 Cooling Coil Characterstics

Table VII

Coil performance specification

General		Air side		Fluid side	
Altitude	0	Tube diameter	5/8"	EWT	45°F
Air flow	48733	Tube wall Thk	0.2"	LWT	53.7°F
Face velocity	485	Fin thickness	0.006"	Flow rate	602 gpm
EAT-DB	82°F	Fin length	133"	Glycol percent	25 %
EAT-WB	68°F	Fin Height	108.75"		
LAT-DB	51.5°F	Tube diameter	5/8"		
LAT-WB	51.3°F				
TMBH	2466.5				
SMBH	1624.0				

A1.4 Chiller Model Coefficients

Table VIII

PLR coefficient presented in Equation 4.19*

Coefficient	Reciprocating	Centrifugal
a_1	0.08144133	0.17149273
b_1	0.41927141	0.58820208
c_1	0.49939604	0.23737257

Table IX

ER_FT coefficient presented in Equation 4.20*

Coefficient	Reciprocating	Centrifugal
a_2	0.46140041	0.51777196
b_2	-0.00882156	-0.00400363
c_2	0.00008223	0.00002028
d_2	0.00926607	0.00698793
e_2	0.00005722	0.00008290
f_2	-0.00011594	-0.00015467

Table X

CAP_FT coefficient presented in Equation 4.21*

Coefficient	Reciprocating	Centrifugal
a_3	0.58531422	-0.29861976
b_3	0.01539593	0.02996076
c_3	0.00007296	-0.00080125
d_3	-0.00212462	0.01736268
e_3	-0.00000715	-0.00032606
f_3	-0.00004597	0.00063139

*Coefficients based on using the temperatures $^\circ$F in Equations 4.19, 4.20 and 4.21.

APPENDIX 2

OPTIMIZATION OF HVAC CONTROL SYSTEM STRATEGY USING TWO-OBJECTIVE GENETIC ALGORITHM

RESUME OF PAPER
PUBLISHED IN HVAC@R RESEARCH 11(3), 2005

A2.1 Abstract

The set points of supervisory control strategy are optimized with respect to energy use and thermal comfort for existing HVAC systems. The multi-objective genetic algorithm is used to solve the optimization problem. HVAC system steady-state models are developed and validated against the monitored data of the existing VAV system. The energy use required for the operation of the existing HVAC system, simulated using the monitoring and validated models, is compared to the energy use required in optimizing the controller set points of this system. A comparison done for one summer week shows that the optimization of supervisory control strategy could save energy by 19.5%, while satisfying the minimum zone airflow rates and thermal comfort. Many control strategies applied in a multi-zone HVAC system are also tested and evaluated for one summer day.

A2.2 System Description

The aim of this study is to realize an on-line optimization of the supervisory control strategy of multi-zone HVAC systems. Two HVAC systems will thus be investigated:

- An existing HVAC system serving interior zones without zone reheats (AHU-6) described in Chapter 2.
- Multi-zone modified HVAC system with zone reheats.

The multi-zone modified HVAC system is created from the existing AHU-6 system by combining the 69 AHU-6 individual zones into four effective zones. The remaining zone considered to be the *critical ventilation* zone remains unchanged. Table XI shows the zone characteristics of the modified HVAC system. Each zone characteristic is derived from the original zone, i.e. the design airflow rate of the effective zone is equal to the sum of the design zone airflow rate of the combined original individual zones. Since the characteristics of the five zones are derived from the original 70 zones, the

validated system components, such as the fan, the cooling coil, and the outdoor damper are thus used for the two systems investigated in this paper (existing and modified HVAC systems). The HVAC system consists of supervisory control and local control loops. The set points of these control loops, including zone air temperatures, the supply air temperature, the supply duct static pressure, the zone supply air temperature or reheat required, the minimum outdoor ventilation flow rate, and the chilled water supply temperature are optimized using the two-objective optimization problem.

Table XI

The zone characteristics of a modified HVAC system

	Z1	Z2	Z3	Z4	Z5
Design zone airflow rate*, m³/s	0.60	7	7	7	7
Minimum zone airflow rate, m³/s	0.18	1.8	1.8	1.8	1.8
Ventilation for zones, m³/s	0.075	0.7	0.7	0.7	0.7
Design zone load, kW	8	88	88	88	88

* Corresponding to design duct static pressure, 250 Pa, named "maximum limit" for other duct static pressure.

A2.3   HVAC System Model

The energy use and thermal comfort are determined by the detailed VAV model as explained in section 4.6 and presented in Figure 32. The minimum outdoor airflow rate is determined by using the corrected fraction of outdoor ventilation air in the supply system (Y), as given in ASHRAE Standard 62-1989:

$$Y = \frac{X}{1 + X - Z} \qquad \text{(A2.1)}$$

The term X is an uncorrected fraction of the outdoor ventilation air in the supply system (the ratio of the sum of the outdoor ventilation airflow rates for all zones to the fan airflow rate). The term Z is the ratio of required outdoor air to primary air in the critical zone.

A2.4   Optimization of Modified HVAC System

The proposed optimization process presented in Figure 38 is applied for existing and modified HVAC system. The data acquisition tool provides the averaged monitored data for these periods. The load prediction tool is used in order to determine the loads (using the Equation (6.1)). The energy use and thermal comfort are determined by the detailed VAV model as explained in section 4.6 and presented in Figure 32. The controlled elitist NSGA-II that was evaluated and tested in chapter 5 is used to solve the optimization problem. The results of optimization of existing HVAC system was presented in Chapter 6 and the reader could also refer to our paper (Nassif, Kajl, Sabourin 2004e). The optimization of modified HVAC system is then only presented and discussed in the next.

A2.4.1   Definition of Investigated Control Strategies

To evaluate the performance of the optimal control strategy of a typical HVAC system using the two-objective genetic algorithm, three different control strategies (A, B, and C) applied to the modified HVAC system are tested:

- *Strategy A*: the set points of zone and supply air temperatures, minimum outdoor airflow rate, chilled water supply temperature, and supply duct static pressure are optimized using zone reheats.
- *Strategy B*: all controller set points described above are optimized without reheat.
- *Strategy C*: it is the same as applying to the existing HVAC system at the ÉTS, such that all controller set points, except the supply air temperature, are constant.

The chilled water supply temperature and supply duct static pressure are 7°C and 250 Pa, respectively. The supply air temperature set point changes linearly within the [13 to 18°C] range when the outdoor temperature varies within the [−20°C to 20°C] range. The supply air temperature calculated above is corrected by adding a value which varies linearly from −2 to +2 °C corresponding respectively to the variation of the fan airflow rate ratio from 50 to 90%. The supply air temperature set point is always limited within [13°C, 18°C].

The zone reheat of strategy C is used differently than in strategy A. The zone reheat of Strategy C is used at a low load when both the zone airflow rate and zone air temperature fall to their minimum limits (i.e. 30% of design zone airflow for zone $Z1$ and 20°C, respectively). However, the zone reheat of strategy A is optimized allowing the reheat to be possibly turned on in order to reduce energy use. Since the zone air temperature set points in strategy C are constant at 23.7°C as in existing ones, the optimization problem is then solved using the one-objective optimization problem respecting only energy use and defining the thermal comfort criterion as the constraint.

A2.4.2   Results of Investigated Control Strategies

The optimization of controller set points is done for one summer day under indoor sensible loads and outdoor conditions, as presented in Figure A2.1 and Figure A2.2, respectively. The outdoor relative humidity varies from 60 to 70%. The two-objective genetic algorithm optimization program was run for 500 generations at each 30 minutes, using the genetic algorithm control parameters described above. To compare the strategies using strategies A and B with those using strategy C, only one solution among strategies A and B, with a building thermal comfort PPD similar to that of strategy C, was selected. The results of the control strategies tested are illustrated in Figures 13-17. Figure A2.3 shows the optimal energy demands simulated for three control strategies (A, B, and C) so that all strategies have the same building PPD. Strategy A, in which the

zone reheats are optimized, needs the least energy as compared to the two other strategies. The energy saving obtained by strategy A as compared to strategy C is about 12%. Since the load acting on zone (Z1) is relatively low, this zone is considered to be the critical ventilation zone. Figure A2.4 shows the ratio of the optimal to design zone airflow rate for the critical ventilation zone (Z1). The 30% value indicates that the airflow rate of zone Z1 falls to its minimum. Figure A2.5 shows the required reheat in the critical ventilation zone (Z1). After 6:00 PM, in both strategies B and C, the airflow rate supplied to zone Z1 is decreased to its minimum limit, whereas, in strategy A, it stays above its minimum limit due to the reheat applied in this zone in order to reduce the outdoor airflow rate. The optimal solution obtained indicates that no reheats are required in other zones. Figure A2.6 shows the optimal supply air temperature set point. The optimal supply duct static pressure set points of strategies A and B obtained for this profile zone loads are 150 Pa. The optimal chilled water supply temperature set points are shown in Figure A2.7.
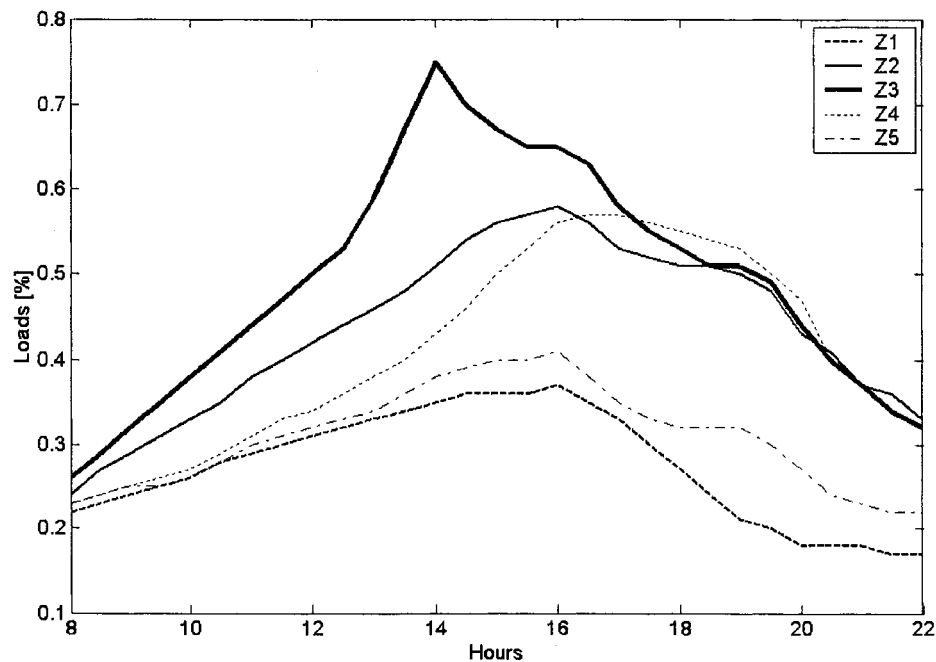
Figure A2.1   Ratio of actual to design sensible loads for zones
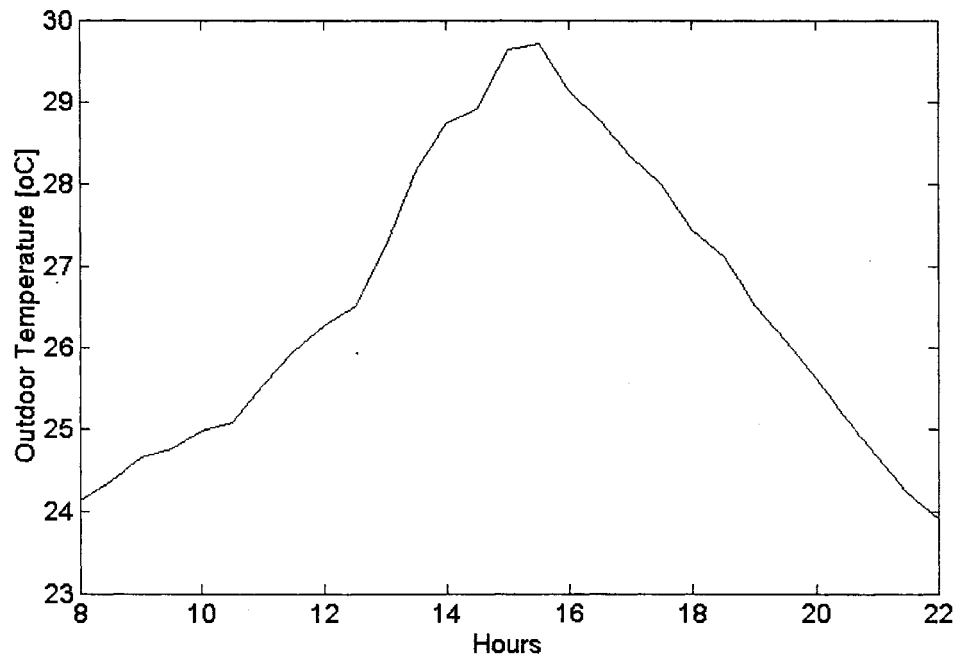
Figure A2.2   Outdoor air temperature profile
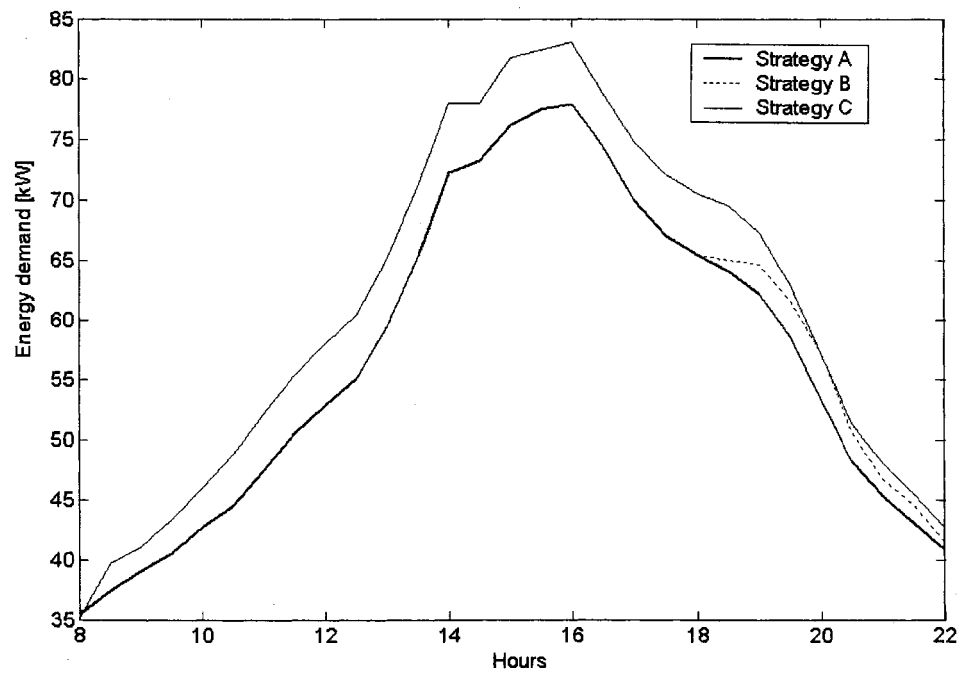
Figure A2.3   Optimal energy demand for A, B, and C control strategies
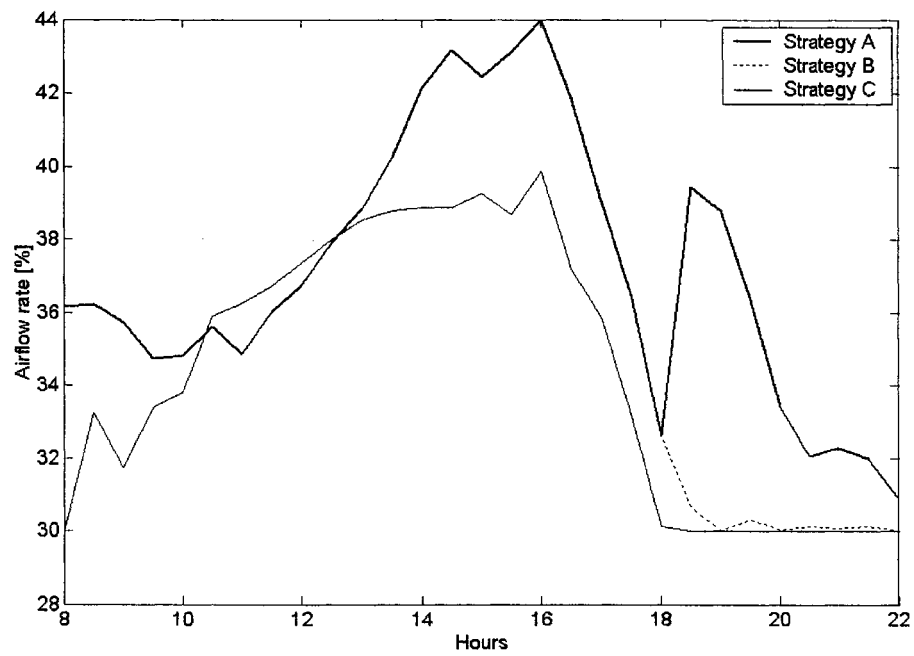
Figure A2.4   Ratio of optimal and design airflow rate of critical ventilation zone (Z1) for A, B, and C control strategies
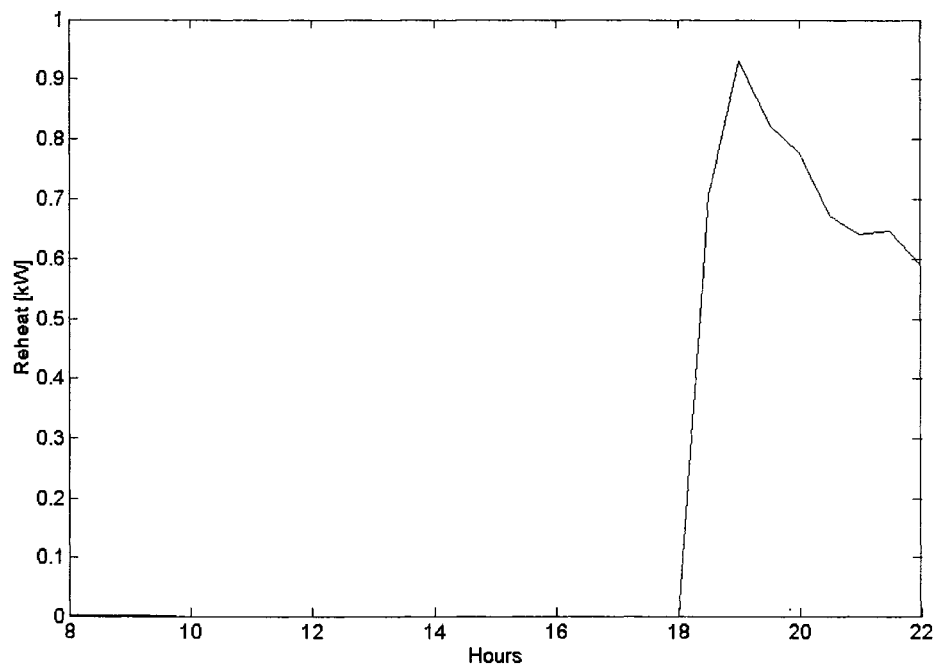
Figure A2.5   Reheat applied to critical zone (Z1) for A control strategy
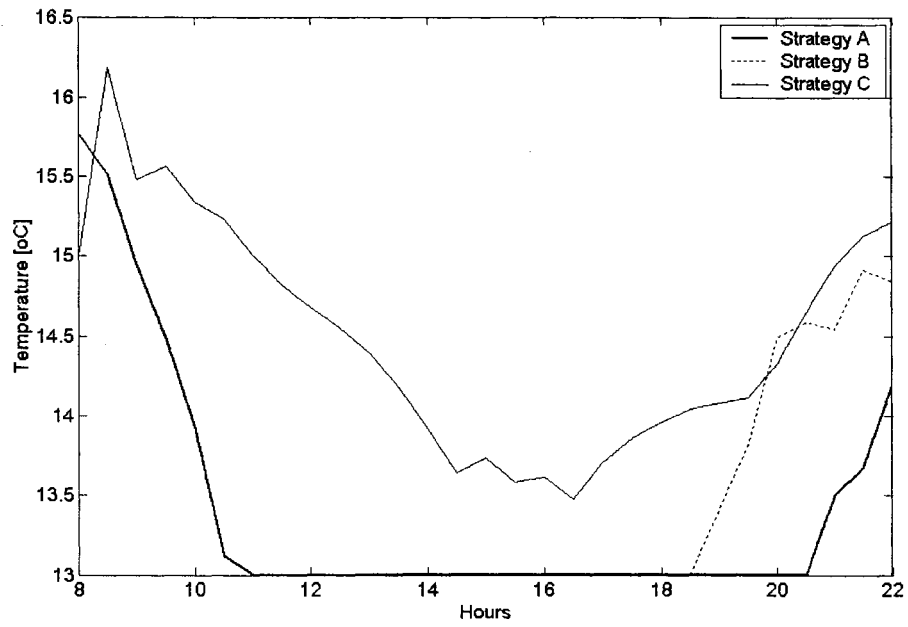
Figure A2.6   Optimal supply air temperature set point for A, B, and C control strategies
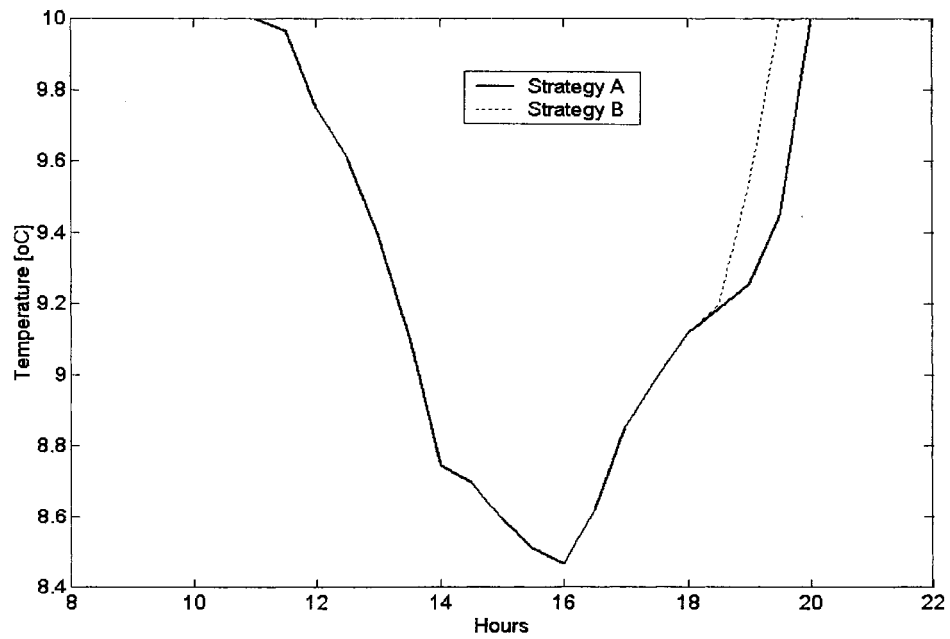
Figure A2.7   Optimal chilled water supply temperature set point for A, and B control strategies
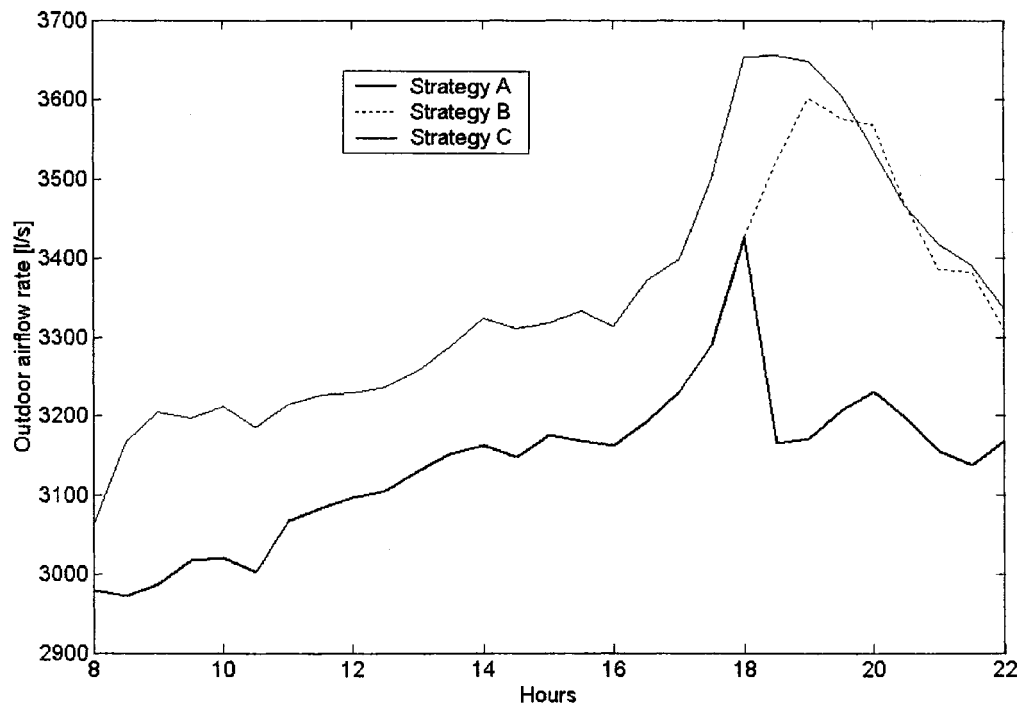
Figure A2.8   Outdoor airflow rate for A, B, and C control strategies

A2.5   Discussion of Results

A2.5.1   Reheat Versus Minimum Outdoor Airflow Rate

To optimize the minimum outdoor airflow rate set point, the reheat applied in the zones must be considered. This concept was investigated by Mumma and Bolin (1994) using the corrected fraction of outdoor ventilation air in the supply system (Y), as presented in Equation (A2.1). The reheat applied to the critical zone could reduce the fraction of outdoor ventilation air in the supply zone (Z), and consequently, reduces the fraction of outdoor ventilation air in the supply system (Y). Depending on the outdoor conditions, this could represent a very significant reduction in the chiller load. At 6:30 PM, since the load in zone ($Z1$) is relatively small, the airflow rate introduced into this zone must be decreased to its minimum limit (180 l/s) when no reheat is applied (strategy B); in this

case, the corrected outdoor ventilation fraction in the supply system (Y) is 27.454%, and the outdoor airflow rate is then 3521.6 l/s. Applying a 0.7 kW reheat in this zone (strategy A) brings this fraction (Y) to 24.8% and the outdoor airflow to 3165.1 l/s due to the increasing critical zone airflow rate. Figure A2.8 shows the outdoor airflow rate for three strategies. Since the reheat is applied in the critical zone (Z1) for strategy A after 6:00 PM, the outdoor airflow rate is significantly decreased.

A2.5.2 System Supply Air Temperature

The optimal supply air temperature set point is determined to give a minimum sum of reheat, fan, and chiller powers while respecting thermal comfort. Before 6:00 PM, since there are no zone reheats, the optimal supply air temperature is determined taking into account the fan and chiller power. As the fan power saving is greater than the chiller power penalty due to decreasing chilled water supply temperature (from 10 to about 8°C) as shown in Figure A2.7, the optimal supply air temperature is at its minimum level (13°C) while the fan and zone airflow rates within their respective limits can meet zone loads. After 6:00 PM, since the load acting on zone Z1 is relatively low, the zone airflow rate at its minimum limit is high enough to satisfy this low load with a relatively low air supply temperature set point (13°C), thus leading to the zone temperature falling below the minimum limit (i.e. 20°C). To increase this zone temperature, there are two possibilities: (i) increasing the supply air temperature, leading to a higher fan power and higher chiller coefficient of performance COP, and (ii) using some reheat in this zone. If the fan energy saving is greater than the reheat penalty, the second method will be applied, as in our case after 6:30 PM (Strategy A). Figure A2.9 shows the reheat, fan, and chiller energy demand for a period after 6:00 PM (when the reheat is used). The chiller energy demand for strategy A (using reheat) is smaller than that for strategy B due to the decreasing outdoor airflow rate, although the COP is greater for strategy B. The fan energy demand for strategy B is greater than that for strategy A after 6:30 PM due to the increasing supply air temperature set point for strategy B – from 13 to 14.5°C.

It was concluded that, as in our case, using reheats in relative low zone loads could save fan energy use as a result of working at low supply temperature set points; as well there could savings in chiller energy use due to a decrease in the outdoor airflow rate. In both cases, the saving must be lower than the energy penalty resulting from reheat and the decrease in COP at low air supply temperatures.
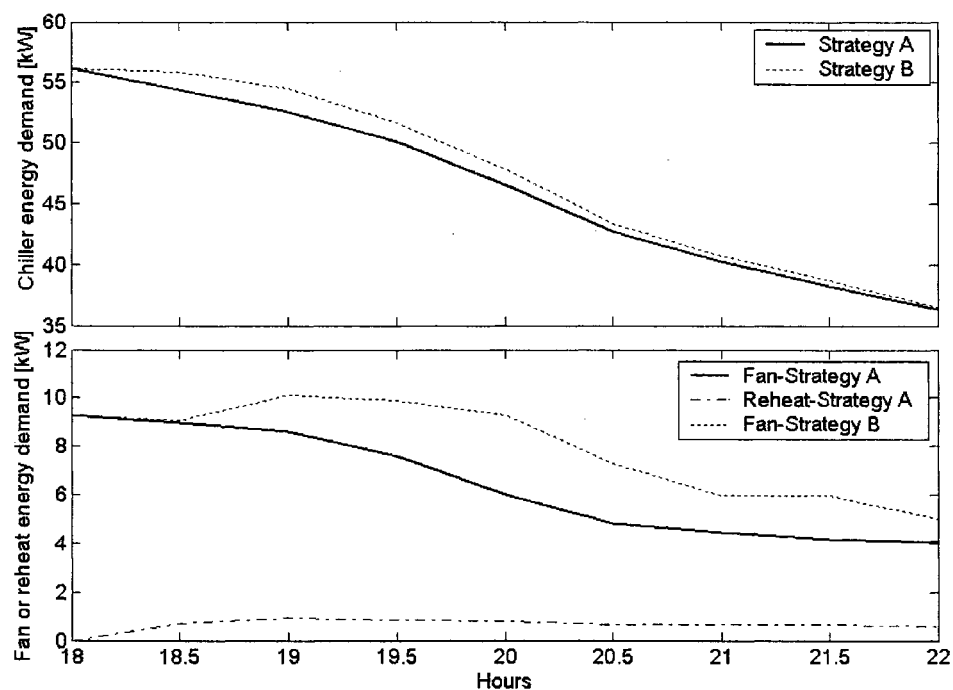
Figure A2.9   Reheat, fan, and chiller energy use for a period after 6:00 PM when the reheat is used

A2.5.3   Optimization of Zone Temperature Set Points

Typically, zone air temperatures are maintained at constant set points in the comfort zone during occupied periods. However, during unoccupied times, the set points are set up for cooling and set back for heating in order to reduce energy use. A strategy using the optimization of the individual zone temperature set points combined with other controller set points during occupied periods could further reduce system energy use.
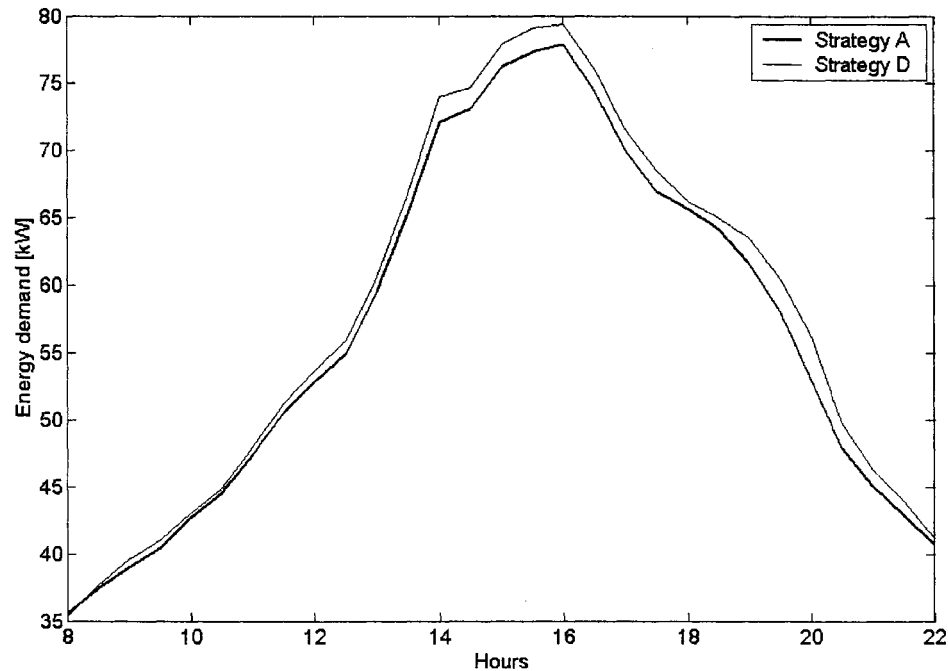
Figure A2.10 Energy demand for similar and different individual zone temperature set
points (strategy D and A, respectively)

The variation of individual zone air temperature set points has an effect on the system controller set points such as outdoor airflow rate, supply air temperature, and supply duct static pressure. To evaluate the effect of individual zone air temperature on supply duct static pressure, the individual zone with a relative high load must be examined because this pressure is determined according to this zone airflow rate. At 2:00 PM, since the load acting on Z3 (see Figure A2.1) is relatively high, with the resulting high airflow supplied to this zone $(R_a)_{cr}$, the duct static pressure set point is accordingly determined by Equation 4.25. When the temperature set point of this zone is set to 22.8°C, the duct static pressure set point is 170 Pa. If this individual zone temperature set point is increased from 22.8 to 23.5°C, the airflow rate of zone Z3 to satisfy the load is decreased, and consequently, the duct static pressure set point could be 150 Pa; this results in an amount of fan energy saving which depends also on the required fan airflow rate. In order to evaluate the effect of individual zone temperature on the outdoor airflow

rate and the air supply temperature set points, the individual zone with a relative low load (Z1) must be examined. The temperature set point of zone (Z1) could be decreased in order to increase the zone airflow required to satisfy this zone load, and consequently, to decrease the outdoor airflow rate (Y from Equation A2.1).

Another advantage of optimum zone temperature set points is their reduction of energy use while maintaining building thermal comfort. When the load distributions between zones change significantly, the individual determination of optimal zone temperature set points according to proper loads could decrease energy use significantly. If a certain average building thermal comfort is required, two methods could be applied: (*i*) the set points of zone air temperatures are optimized to give the required building thermal comfort (building PPD), (*ii*) the set points of zone air temperatures are set to the same value to give the required building PPD. It should be noted that the building PPD is equal to the mean zone PPD respecting the zone PPD constraint. As discussed above, the variation of individual zone temperature set points has an effect on system controller set points, such as outdoor airflow rate, supply air temperature, and supply duct static pressure, and consequently, an effect on energy use. The following two strategies have been tested and evaluated:

- *Strategy A*: as strategy described above, so that the zone air temperature set points are optimized.
- *Strategy D*: as strategy *A*, except that the zone air temperature set points are kept constant at $23.7^{\circ}C$.

Figure A2.10 shows the energy demand for strategies *A* and *D*. It is clear that, for the required building thermal comfort, the energy demand using optimal zone temperature set points (strategy *A*) is less than for strategy *D* using identical set points for all zones without considering load distributions between zones. Optimal solutions for strategy *D* are obtained by running the one-objective optimization program with constant zone

temperature set points equal to 23.7°C. Optimal solutions for strategy *A* are obtained by running the two-objective optimization program with the optimization of individual zone temperature set points. To compare strategy A with strategy D, only one solution having the same PPD of strategy D is selected at each period.

A2.6   Conclusion

The supervisory control strategy set points are optimized using a two-objective genetic algorithm. The set points, such as zone air temperatures, supply air temperature, supply duct static pressure, zone supply air temperature or reheat required, minimum outdoor ventilation flow rate, and chilled water supply temperature, are optimized for the existing and modified HVAC systems. To establish the optimization process, the VAV system and component models were developed and validated against the monitored data of the existing HVAC system. Energy use was simulated during the optimization process using these models, while the actual operation energy use was determined through monitoring data and appropriate validated models. The existing HVAC system results show that by comparing actual and optimal energy use, the optimization of a supervisory control strategy could save energy by 19.5%, while satisfying minimum zone airflow rates and zone thermal comfort. These results are obtained for one summer week. However, three different control strategies are also evaluated for a typical or modified HVAC system. These results show that the strategy that optimizes all controller set points, including zone temperature and zone reheat, performs better and provides more energy savings.

APPENDIX 3

EVALUATION OF MULTI-OBJECTIVE GENETIC ALGORITHM OPTIMIZATION

A3.1 Introduction

Different multi-objective genetic algorithms (MOGA) are investigated in this Appendix. The MOGAs are evaluated and tested on mathematical problem. The potential of MOGAs to find the set of optimal solutions closed to Pareto-optimal front is investigated and presented. In these evaluations, the following two performance metrics are used: (*i*) metric evaluating the closeness to the Pareto-optimal front, and (*ii*) metric evaluating diversity among non-dominated solutions.

A3.2 Multi-Objective Genetic Algorithm Optimization

The principles of multi-objective genetic algorithm optimization are different from that in a single-objective genetic algorithm optimization. The main goal in a single-objective optimization is to find the global optimal solution, resulting in the optimal value for the single objective function. However, in a multi-objective optimization, there is more than one objective function, each of which may have a different individual optimal solution. If there is sufficient difference in the optimal solutions corresponding to different objectives, the objective functions are often known as conflicting to each other. Multi-objective genetic algorithm with such conflicting objective functions gives rise to a set of optimal solutions, instead of one optimal solution. The reason for the optimality of many solutions is that no one can be considered to be better than any other with respect to all objective functions. These optimal solutions have special name-Pareto-optimal solutions.

A3.3 Non-Dominated Sorting Genetic Algorithms (NSGA)

The NSGA varies from simple genetic algorithm only in the way the selection operator works. The crossover and mutation operators remain as usual. NSGA use two strategy before the reproduction operator non-dominated sorting strategy and the sharing strategy

(niche method) presented below. The idea behind the non-dominated sorting procedure is that a ranking selection method is used to emphasize good points and a niche method is used to maintain stable subpopulations of good points.

A3.3.1   Reproduction or Selection Operator

The primary objective of the reproduction operator is to make duplicates of good solutions and eliminate bad solutions in a population, while keeping the population size constant. There exists a number of ways to achieve the above tasks. Some common methods are tournament selection, proportionate selection and ranking selection.

In this study, the stochastic universal sampling-SUS version of proportionate selection is used here (Deb 2001). In this version, only one random number r is chosen for the whole selection process. Since N different solutions have to be chosen, a set of N equi-spaced numbers is created: $R = \left\{ r, r + \dfrac{1}{N}, r + \dfrac{2}{N}, ..., \dfrac{N-1}{N} \right\}$. Thereafter, a solution corresponding to each member of R is chosen from the cumulative probability values. The cumulative probability can be easily simulated on a computer. Using the fitness value f_i of all solutions, the probability of selecting the i-th solution is $P_i = f_i / \sum\limits_{j=1}^{N} f_j$.

Thereafter, the cumulative probability $P_i = \sum\limits_{j=1}^{i} P_j$ of each solution can be calculated by adding the individual probabilities from the top of the list. Thus, the bottom-most solution in the population has a cumulative probability (P_n) equal to 1. This operator is implemented for two real and binary algorithms.

A3.3.2   Crossover Operator

A crossover operator is applied next to the solutions of the mating pool. Like the reproduction operator, there exists a number of crossover operators in GA literature, but

in almost all crossover operators, two strings are picked from the mating pool at random and some portion of the strings are exchanged between the strings to create two new strings. In this study, a single-point crossover operator is implemented in binary-coded algorithm and simulated binary crossover is used for real- coded algorithm. The single-point crossover operator is performed by randomly choosing a crossing site along the string and by exchanging all bits on the right side of the crossing site. The simulated binary crossover SBX operator simulates the working principle of the single-point crossover operator on binary strings. The procedure of computing the offspring $x_i^{(1,t+1)}$ and $x_i^{(2,t+1)}$ from parent is described as follows. First, a random number u_i between 0 and 1 is created. Thereafter, from a specified probability distribution function, the ordinate β_{qi} is found:

$$\beta_{qi} = \begin{cases} (2u_i)^{\frac{1}{\eta_c+1}} & if \quad u_i \leq 0.5; \\ (\dfrac{1}{2(1-u_i)})^{\frac{1}{\eta_c+1}} & if \quad otherwise. \end{cases} \qquad (A3.1)$$

In the above expressions, the distribution index η_c gives a higher probability for creating 'near-parent' solutions and a small value of η_c allows distant solutions to be selected as offspring. After obtaining β_{qi} from the above probability distribution, the offspring are calculated as follows:

$$x_i^{(1,\ t+1)} = 0.5\left[(1+\beta_{qi})x_i^{(1,t)} + (1-\beta_{qi})x_i^{(2,t)}\right]$$
$$x_i^{(2,\ t+1)} = 0.5\left[(1-\beta_{qi})x_i^{(1,t)} + (1+\beta_{qi})x_i^{(2,t)}\right] \qquad (A3.2)$$

A3.3.3 Mutation Operator

The crossover operator is mainly responsible for the search aspect of genetic algorithms, even though the mutation operator is also used for this purpose. The bit-wise mutation operator changing a 1 to a 0, and vice versa, is used for the binary-coded algorithm with the mutation probability of 1/50 (binary strings of lengths 50). However, the following equation is used for the real-coded algorithm:

$$y_i^{(1,\ t+1)} = x_i^{(1,t)} + (r_i - 0.5)\Delta_i \qquad\qquad (A3.3)$$

Where Δ_i is the user-defined maximum perturbation allowed in i-th decision variable. This method is used in this study with taking care to check if the above calculation takes $y_i^{(1,\ t+1)}$ outside of the specified lower and upper limits.

A3.3.4 Non-Dominated Sorting of a Population

The first step of NSGA is to sort the population P according to non-domination. There are different algorithms suitable for this task, these algorithms classify the population into various non-domination level. The best non-dominated solutions are called non-dominated solutions of level 1. In order to find solutions for the next level of non-domination, there is a simple procedure which is usually followed. Once the best non-dominated set is identified, they are temporarily disregarded from the population. The non-dominated solutions of the remaining population are then found and are called non-dominated solutions of level 2. In order to find the non-dominated solutions of level 3, all non-dominated solutions of levels 1 and 2 are disregarded and new non-dominated solutions are found. This procedure is continued until all population members are classified into a non-dominated level. In this study, Naive and Slow approach (Deb 2001) is used to find a non-dominated set so that each solution i is compared with every

other solution in the population to check if it is dominated by any solution in the population. Therefore, the solution $x^{(1)}$ is said to dominate the other solution $x^{(2)}$ if both following conditions are true:

- The solution $x^{(1)}$ is no worse than $x^{(2)}$ in all objectives.
- The solution $x^{(1)}$ is strictly better than $x^{(2)}$ in at least one objective

A3.3.5   Sharing Function Method

Sharing is achieved by performance selection operation using degraded fitness values which are obtained by dividing the original fitness value of an individual by a quantity proportional to the number of individuals around it. The sharing in each front is achieved by calculating a sharing function value between two individuals in the same front as follows:

$$Sh(d_{ij}) = \begin{cases} 1 - \left(\dfrac{d_{ij}}{\sigma_{share}} \right)^2 & \text{if } d_{ij} \le \sigma_{share} \\ 0 & \text{otherwise} \end{cases} \qquad (A3.4)$$

The parameter d_{ij} is the phenotypic distance between two individuals i and j in the current and σ_{share} is the maximum phenotypic distance allowed between any two individuals to become members of a niche (Deb 2001). Several values of sharing parameter σ_{share} are used to solve the mathematic problem described next. The *Dynamic update of the sharing parameter* σ_{share} is also used as suggested by (Fonseca and Fleming1993) for two-objective function:

$$\sigma_{share} = \frac{u_2 - l_2 + u_1 - l_1}{N - 1} \qquad (A3.5)$$

where u_1, u_2, l_1, l_2 the maximum (u_1, u_2) and minimum (l_1, l_2) bounds of each of the objective function values in the current population.

A3.4 Elitist Non-Dominated Sorting Genetic Algorithms (NSGA-II)

NSGA-II is multi-objective evolutionary algorithms which use elite-preserving and crowded tournament selection operators. The crossover and mutation operators remain as NSGA, but NSGA-II uses crowded tournament selection operator instead of selection operator (Stochastic universal sampling-SUS).

This algorithm is explained in Deb's book (Deb 2001). The offspring population Q_t is first created by using the parent population P_t. However, instead of finding the non-dominated front of Q_t only, first the two populations are combined together to form R_t of size 2N. Then, a non-dominated sorting is used to classify the entire population R_t. Since the overall population size of R_t is 2N, not all fronts may be accommodated in N slots available in the new population. All fronts which could not be accommodated are simply deleted. When the last allowed front is being considered, there may exist more solutions in the last front than the remaining slots in the new population. Instead of arbitrarily discarding some members from the last front, a nishing strategy is used to choose the members of the last front, which reside in the least crowded region in that front. NSGA-II uses the binary tournament selection as the following.

A3.4.1 Crowded Tournament Selection Operator

The crowded comparison operator used by NSGA-II compares two solutions and returns the winner of the tournament. It assumes that every solution i has two attributes:

- A non domination rank r_i in the population.
- A local crowding distance d_i in the population.

The crowding distance d_i of a solution i is a measure of the search space around i which is not occupied by any other solution in the population (Deb 2003). Based on these two attributes, the crowded tournament selection operator is defined as follows. A solution i wins a tournament with another solution j if any of the following condition are true:

- If the solution i has a better rank, that is, $r_i < r_j$
- If they have the same rank but the solution i has a better crowding distance than solution j, that is, $r_i = r_j$ and $d_i > d_j$.

The first condition makes sure that chosen solution lies on a better non-dominated front. The second condition resolves the tie of both solutions being on the same non-dominated front by deciding on their crowded distance. The one residing in a less crowded area (with a larger crowding distance d_i) wins.

A3.5 Penalty Function Approach

This is a popular constraint handling strategy. All constraints are normalized before the constraint violation is calculated. Thus, the resulting functions are $\overline{g}_j(x^{(i)}) \geq 0$ for $j=1,2,\ldots,J$. For each solution $x^{(i)}$, the constraint violation for each constraint is calculated as follows:

$$\omega_j\left(x^{(i)}\right) = \begin{cases} \left|\overline{g}_j\left(x^{(i)}\right)\right|, & \text{if } \overline{g}_j\left(x^{(i)}\right) < 0 \\ 0, & \text{otherwise} \end{cases} \tag{A3-6}$$

Thereafter, all constraint violations are added together to get the overall constraint violation;

$$\Omega\!\left(x^{(i)}\right)=\sum \omega_j\!\left(x^{(i)}\right)$$

(A3-7)

This constraint violation is then multiplied with a penalty parameter R_m and the product is added to each of the objective values:

$$F_m\!\left(x^{(i)}\right)=f_m\!\left(x^{(i)}\right)+R_m\Omega\!\left(x^{(i)}\right)$$

(A3-8)

A3.6 Performance Metrics

The performance of investigated optimization methods is evaluated using the following performance metrics: (*i*) metric evaluating the closeness to the Pareto-optimal front, and (*ii*) metric evaluating diversity among non-dominated solutions.

A3.6.1 Metrics Evaluating Closeness to the Pareto-Optimal Front

This metric explicitly computes a measure of the closeness of a set Q of N solutions from a known set of the Pareto-optimal set. In this study, the *Generation distance* method is used (Vedhuizen, 1999):

$$GD = \frac{\left(\sum_{i=1}^{|Q|} d_i^{\,p}\right)^{1/p}}{|Q|}$$

(A3-9)

For *p=2*, the parameter d_i is the Euclidean distance (in the objective space) between the solution $i \in Q$ and the nearest member of the Pareto-optimal set $\overset{\bullet}{P}$:

$$d_{ij} = \min_{k=1}^{p^*} \sqrt{\sum_{m=1}^{M} \left(f_m^{(i)} - f_m^{*(k)}\right)^2} \qquad \text{(A3-10)}$$

where $f_m^{*(k)}$ is the $m-th$ objective function value of $k-th$ member of p^*.

A3.6.2   Metrics Evaluating Diversity Among Non-Dominated Solutions

There exists a number of metrics to find the diversity among obtained non-dominated solutions. In this study, the spread metric is used as suggested by Deb (2000):

$$\Delta = \frac{\sum_{m=1}^{M} d_m^e + \sum_{i=1}^{|Q|} \left| d_i - \overline{d} \right|}{\sum_{m=1}^{M} d_m^e + |Q| \overline{d}} \qquad \text{(A3-11)}$$

Where d_i can be any distance measure between neighboring solutions and $\overline{d}$ is the mean value of these distance measures. The Euclidean distance, the sum of the absolute differences in objective values or the crowding distance can be used to calculate d_i In this study, the sum of the absolute differences in objective values is used. The parameter d_m^e is the distance between the extreme solution of p^* and Q corresponding to $m-th$ objective function.

A3.7   Definition Min-Ex Problem

Min-Ex is two objectives example problem written as following:

$$(Minimize) \quad f_1(x) = x1$$

$$(Minimize) \quad f_2(x) = \frac{1+x_2}{x_1}$$

$$Subject \ to \quad 0.1 \le x_1 \le 1$$

$$0 \le x_2 \le 5.$$

(A3-12)

Although this problem looks simple, it produces conflicting scenarios between both objectives, resulting in a set of Pareto-optimal solutions. The optimal solutions are $0.1 \le x_1 \le 1$ and $x_2=0$. It is important to highlight that the resulting Pareto-optimal region is convex.

A3.8 Min-Ex problem Test

Our objective is to determine the best performance among of four algorithms real-coded NSGA, binary-coded NSGA, real-coded NSGA-II, and binary-coded NSGA-II. The algorithms run using the following conditions.

- Size of population = 50 and generations = 50
- Length binary coded = 50 ;
- Different crossover probability index for real coded (η_c, in Equation A3.1);
- Different crossover probability for binary and real coded;
- Different values of sharing (σ_{share}, in Equation A3.4)
- Dynamic update of sharing value over generations described in section 5-5.
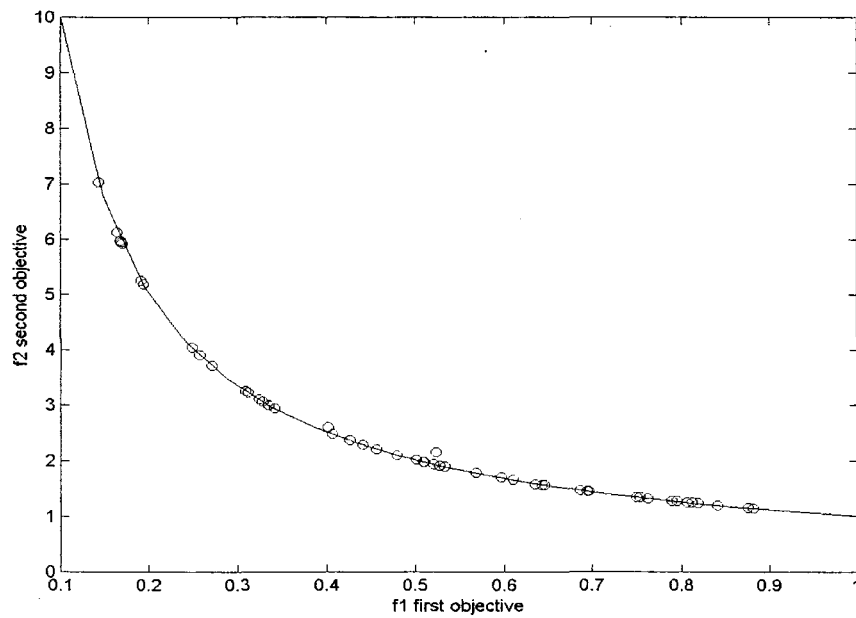
Figure A3.1   Real coded NSGA with crossover probability p_c=0.9, distribution index η_c =4, mutation probability p_m=0.04, and 50 generations
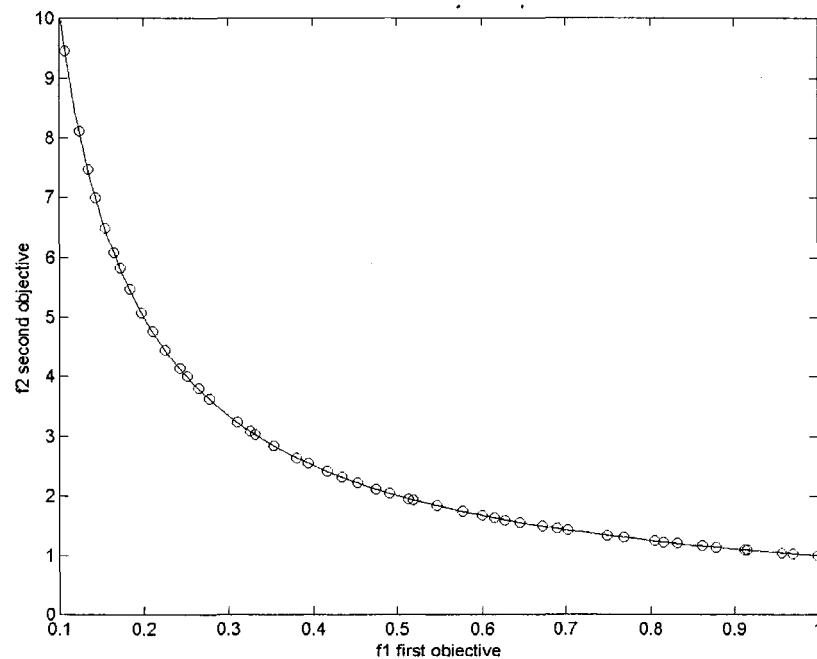

Figure A3.2   real coded NSGA-II with crossover probability p_c=0.9, distribution index η_c =4, mutation probability, and 50 generations

Table XII summarizes the results for investigated algorithms. The best results are only presented. With crossover probability p_c=0.9, distribution index η_c =4, and mutation probability p_m=0.04, real coded NSGA with update of the sharing performs best among other investigated NSGA algorithms. Figure A3-1 shows real coded NSGA with crossover probability p_c=0.9 and distribution index η_c =4, mutation probability p_m=0.04. Real coded NSGA-II with the same parameters performs best among all investigated algorithms. Figure A3-2 shows real coded NSGA-II with crossover probability p_c=0.9 and distribution index η_c =4, mutation probability p_m=0.04. ..

Table XII

Spread and distance metrics for the investigated algorithms

	Spread	Distance	Parameters
			Crossover probability 0.90, distribution index η_c =4, mutation probability p_m=0.04 (if used).
Real coded NSGA	1.11	0.0018	No mutation, sharing value=0.158
	1.2	0.012	Mutation, sharing value=0.158
	1.0126	0.0017	No mutation, update of sharing value
	1	0.006	Mutation, update of sharing value
Binary coded NSGA	1.23	0.000062	No mutation, sharing value=0.158
	1.344	0.000062	Mutation, sharing value=0.158
	1.2	0	No mutation, update of sharing value
	1.6	0.00002	Mutation, update of sharing value
Real coded NSGA-II	0.859	0	No mutation
	0.824	**0**	**With mutation**
Binary code NSGA-II	1.1	0	No mutation
	1	0	With mutation

A3.9   Summary and discussion

Different multi-objective genetic algorithms (MOGA) are investigated in this Appendix. The MOGAs are evaluated on mathematical problem (Min-Ex). The potential of MOGAs to find the set of optimal solutions closed to Pareto-optimal front is investigated and presented. In these evaluations, the following two performance metrics are used: (i) metric evaluating the closeness to the Pareto-optimal front, and (ii) metric evaluating diversity among non-dominated solutions. Real and binary coded Non-dominated sorting genetic algorithm (NSGA) and elitist non-dominated sorting genetic algorithm (NSGA-II are tested to solve Min-Ex problem. The results showed that the real coded NSGA-II has the best performance with spread of 0.824 and the distance of 0. These algorithms are also evaluated on HVAC system problem using simplified models as presented in Chapter 5. The evaluation results based on Min-Ex are consistent with the conclusion reach by the evaluation based on investigated HVAC system problem (Chapter 5). The Min-Ex was first investigated for the following reasons:

- Inspection the results obtained from (Wright, Loosemore, and Farmani 2002) indicates that the optimum pay-off characteristic curve between the daily energy cost and occupant thermal discomfort for summer design day has the same configuration of Min Ex Pareto-optimal solution front.

- Some variables of HVAC optimization are operating near the upper or lower limits as optimal value of x_2 in Min-Ex problem.

- The second objective (consumption energy) in HVAC system problem depends on all problem variables the same thing for Min-Ex problem. The first objective in Min-Ex depends only on x_1 variable, and it depends only on certain variables such as zone air and radiant star temperatures in HVAC optimization problem.

BIBLIOGRAPHY

Alalawi, M. and M. Krarti. 2002. Experimental evaluation of CO_2 –based demand-controlled ventilation strategies. *ASHRAE Transactions* 108(2): 307-317.

Ahmed, O., J.W. Mitchell, and S. Klein. 1996. Application of general regression neural network (GRNN) in HVAC process identification and control. *ASHRAE Transactions* 102 (1): 625-634.

American Society of Heating Refrigerating Air-Conditioning Engineers. 2003. ASHRAE handbook. Heating, ventilating, and air-conditioning applications (Vol. 1). Atlanta, Ga.: American Society of Heating Refrigerating and Air-conditioning Engineers.

American Society of Heating Refrigerating Air-Conditioning Engineers. 1996. ASHRAE handbook. Heating, ventilating, and air-conditioning systems and equipment (SI ed.) (Vol. 1). Atlanta, Ga.: American Society of Heating Refrigerating and Air-Conditioning Engineers.

ASHRAE. 2001. ASHRAE Standard 62-2001, Ventilation for acceptable indoor air quality. Atlanta: American Society of Heating, Refrigerating and Air-Conditioning Engineers, Inc.

Asiedu, Y., R.W. Besant, and P. Gu. 2000. HVAC duct system design using genetic algorithms. *HVAC @ R Research* 6(2): 149-173.

Brandemuel, M.J., S. Gabel, and I. Andersen. 1993. A Toolkit for secondary HVAC system energy calculation. *Published for ASHRAE by Joint Center for Energy Management, University of Colorado at Boulder.*

Braun, J.E., S.A. Klein, J.W. Mitchell, and W.A. Beckman. 1989a. Application of optimal control to chilled water systems without storage. *ASHRAE Transactions* 95(1).

Braun, J.E., S.A. Klein, J.W. Mitchell, and W.A. Beckman. 1989b. Methodologies for optimal control to chilled water systems without storage. *ASHRAE Transactions* 95(1).

Cappellin, T.E. 1997. VAV systems - what makes them succeed? What makes them fail? *ASHRAE Transactions* 103(pt 2): 814-822.

Carpenter, S.C. 1996. Energy and impacts of CO2 –based demand-controlled ventilation. *ASHRAE Transactions* 102(2):80-88.

Chen, S. and S. Demster. 1995. Variable air volume system for environment quality. New York: McGraw-Hill.

Clark, D. R. 1985. Building Systems and Equipment Simulation Program HVACSIM+ - User's Manual, National Bureau of Standards and Technology, Washington, DC.

Cumali, Z. 1988. Global optimization of HVAC system operations in real time. *ASHRAE Transactions* 94(1): 1729-1743.

Cumali, Z. 1994. Application of real-time optimization to building systems. *ASHRAE Transactions* 100(1).

Curtiss, P.S., M.J. Brandemuehl, and J.F. Kreider. 1994. Energy management in central HVAC plants using neural networks. *ASHRAE Transactions* 100(1): 476-493.

Deb, K. 2001. Multi-objective optimization using evolutionary algorithms (1st ed.). New York: John Wiley & Sons.

Deb,K., S. Agrawal, S. Pratap, and T Meyarivan. 2000. Fast elitist non-dominated sorting genetic algorithm for multi-objective optimization: NSGA-II. *LNCS* 1917: 849-859.

Deb, K. and T. Goel. 2001. Controlled elitist non-dominated sorting genetic algorithms for better convergence. *LNCS* 1993: 67-81.

Degelman, L.O. 1984. Development of bin weather data. *ASHRAE RP-385.* Atlanta: American Society of Heating, Refrigerating and Air-Conditioning Engineers, Inc.

Elovitz, D. M. 1995. Minimum outside air control methods for VAV systems. *ASHRAE Transactions* 101(Pt 2): 613-618.

Englander, S.L. and L.K. Norford, L.K. 1992. Saving fan energy in VAV systems parts 2: Supply fan control for static pressure minimization using DDC zone feedback. *ASHRAE Transactions* 98 (1): 19-32.

Fonseca, C. M. 1995. An overview of evolutionary algorithms in multi-objective optimization. *Evolutionary Computation* 9(1): 1-16.

Gen, M. and R. Cheng. 2000. Genetic algorithms and engineering design. New York; Chichester: Wiley.

Goldberg, D.E. 1989. Genetic algorithms in search, optimization, and machine learning. Addison-Wesley Pub. Co.

Haines, R.W. and C.L. Wilson 1994. HVAC systems design handbook (2nd ed.). New York, N.Y.: McGraw-Hill.

Hartman, T. 1993. Terminal regulated air volume (TRAV) systems. *ASHRAE Transactions* 99(1): 791-800.

Holland, J. H. 1992. Adaptation in natural and artificial systems: an introductory analysis with applications to biology, control, and artificial intelligence (1st MIT Press ed.). Cambridge, Mass.: MIT Press.

House, J.M. and T.F. Smith. 1995. A system approach to optimal control for HVAC and building systems. *ASHRAE Transactions* 101(2): 647-660.

House, J.M., T.F. Smith, and J.S. Arora. 1991. Optimal control of a thermal system. *ASHRAE Transactions* 97(2): 991-1001.

Huang, W. and H.L. Lame. 1997. Using genetic algorithms to optimize controller parameters for HVAC systems. *Energy and Building* 26, 277-282.

Janu, G. J., J.D. Wenger, and C.G. Nesler. 1995. Strategies for outdoor airflow control from a systems perspective. *ASHRAE Transactions* 101(2): 631-643.

Kajl, S., J.P. Kenné, L. Paquin, and M. Daigle. 2003. Amélioration des performances des systèmes CVCA : approche basée sur le monitoring. 6e Colloque interuniversitaire franco-québécois, Québec, Canada.

Kajl, S. and N. Nassif. 2003. Monitoring: un outil d'optimization de l'operation des systemes CVCA. 1st International Conference on Susstainale Energy and Green Architecture, Bangkok, Octobre 2003, pp.:GA 65-72.

Katz, A.J. and P.R. Thrift. 1994. Generating image filters for target recognition by genetic learning. *IEEE Transactions on Pattern Analysis and Machine Intelligence* 16(9): 906-910.

Ke, Y.P. and S.A. Mumma. 1997. Using carbon dioxide measurements to determine occupancy for ventilation controls. *ASHRAE Transactions* 103(2):364-374.

Ke, Y.P. and S.A. Mumma. 1999. Variable air volume ventilation control strategies analyzed in six climate zones. *International Journal of Energy Research* 23(5): 371-387.

Ke, Y.P. and S.A. Mumma. 1997. Optimized supply -air temperature (SAT) in variable air volume (VAV) systems. *Energy* 22(6), 601-614.

181

Kettler, J. 2003. Standart 62's Multiple spaces equation: for design, not control. *ASHRAE Journal* 45(8): 20-22.

Krakow, K.I., F. Zhao, and A.E. Muhsin. 2000. Economizer control. *ASHRAE Transactions* 106: 13-25.

Kreider, J.F. and A. Rabl. 1994. Heating and cooling of buildings: design for efficiency. New York, N.Y.: McGraw-Hill.

Lam, H. N. 1995. Intelligent computer control of air conditioning systems based on genetic algorithm and classifier system. Proceedings of 4th Building Simulation 95. Building Performance Simulation Association, Madison.

Lee, K.W. and H.N. Lam. 1995. Optimizing neural network weights using genetic algorithms: A case study. Proceedings of the 1995 IEEE International Conference on Neural Networks. Part 3 (of 6), Perth, Aust.

Linder, R. and C.B. Dorgan. 1997. VAV systems work despite some design and application problems. *ASHRAE Transactions* 103(2): 807-813.

MacArthur J.W. and M.A. Woessner. 1993. Receding horizon control: A model-based policy for HVAC applications. *ASHRAE Transactions* 99(1).

McQuiston, F.C., J.D. Parker, and J.D. Spitler. 2000. Heating, ventilating, and air conditioning: analysis and design (5th ed.). New York, N.Y.: J. Wiley and Sons.

Mitchell, M. and NetLibrary Inc. 1996. An introduction to genetic algorithms. Cambridge, Mass.: MIT Press.

Michalewicz, Z. 1994. Genetic algorithms + data structures = evolution programs (2nd, extended ed.). New York: Springer-Verlag.

Morisot, O., D. Marchio, and P. Stabat. 2002. Simplified model for the operation of chilled water cooling coils under non-nominal conditions. *HVAC&R Research Journal* 8 (1): 135-155.

Mumma, S. A. and R.J. Bolin. 1994. Real-time, on-line optimization of VAV system control to minimize the energy consumption rate and to satisfy ASHRAE standard 62-1989 for all occupied zones. *ASHRAE Transactions* 100(1): 168-177.

Nassif, N., S. Kajl, R. Sabourin. 2005a. Optimzation of HVAC system strategy using two-objective genetic algorithm. *HVAC&R Research Journal* 11(3), in press.

Nassif, N., S. Kajl, R. Sabourin. 2005b. Ventilation control strategy using supply CO_2 concentration. *HVAC&R Research Journal* 11(2): 239-262.

Nassif, N., S. Kajl, R. Sabourin. 2004a. Modeling and validation of existing VAV system components. *Proceeding of Esim, Canadian Conference on Building Simulation,* Vancouver, Canada, 135-141.

Nassif, N., S. Kajl, R. Sabourin. 2004b. Evolutionary algorithms for multi-objective optimization in HVAC system control strategy. *Proceeding of NAFIPS, North American Fuzzy Information Processing Society,* Alberta, Canada.

Nassif, N., S. Kajl, R. Sabourin. 2004c. Two-objective on-line optimization of supervisory control strategy. *Building Serv. Eng. Res. Technol.* 25(3): 241-251.

Nassif, N., S. Kajl, R. Sabourin. 2003a. Modélisation des composants d'un système CVCA existant. VI Colloque interuniversitaire franco-québécois, Québec.

Nassif, N., S. Kajl, R. Sabourin. 2003b. Two-objective on-line optimization of supervisory control strategy. *Proceedings of eight IBPSA conference,* Eindhoven. 927-934.

Nassif, N. 2002. The performance of elitist non-dominated sorting genetic algorithm. Montreal. Raport, Cours SYS-843.

Nordvik, J.P. and J.M. Renders. 1991. Genetic algorithms and their potential for use in process control: a case study. Paper presented at the Proc. 4th Int. Conf. On Genetic Algorithms, SanDiego, CA.

NRCC. 1999. Performance compliance for building. Canadian Commission on Building and Fire Codes. National Research Council Canada (NRCC).

Persily, A.K. 1993. Ventilation, carbon dioxide and ASHRAE Standard 62-1989. *ASHRAE Journal* 35 (7): 40-44.

Reddy, T.A., M. Liu, and D.E. Claridge. 1998. A study of energy use and satisfactory zone ventilation of different outdoor air ventilation strategies for terminal reheat variable air volume systems. *Energy and Buildings* 29: 65-75.

Schell, M. 1998. Saving energy and optimizing air quality using carbon dioxide (CO2). Energy Engineering 95(2): 19-33.

Schroeder, C., M. Krarti, and M. Brandemuel. 2000. Error analysis of measurement and control techniques of outside air intake rates in VAV systems. *ASHRAE Transactions* 106 (2): 26-38.

Seem, J.E., C. Park, and J.M House. 1999. New sequencing control strategy for air-handling units. *HVAC&R Research* 5(1): 35-58.

Seem, J. E., J.M. House, and C.J. Klaassen. 1998. Volume matching control: Leave the outdoor air damper wide open, *ASHRAE Journal* 40: 58-60.

Srinivas, N. and K. Deb. 1994. Multi-objective function optimization using non-dominated sorting genetic algorithms. *Evolutionary Computation* 2(3): 221-248, 1994

Valve and Actuator Manual 977. 1994. Engineering data Book Vb1, Johnson Control, Inc. Code No LIT-347Vb.

Veldhuizen, D.V. and G.B. Lamont. 1998. Multiobjective evolutionary algorithm research: a history and analysis. *Evolutionary Computation* 8(2): 125-148.

Veldhuizen, D.V. 1999. Multiobjective evolutionary algorithms: classifications, analyses, and new innovations. Dissertation (AFIT/DS/ENG/99-01). Dayton: Air Force Institute of Technology.

Vose, M.D. 1999. Simple genetic algorithm: foundations and theory. Cambridge, Mass.: MIT Press.

Wang, S. 2000. Handbook of Air Conditioning and Refrigeration: McGraw-Hill.

Wang, S. and X. Jin. 2000. Model-based optimal control of VAV air-conditioning system using genetic algorithm. *Building and Environment* 35: 471-487.

Wang, S. and X. Jin. 1998. CO_2 –based occupancy detection for on-line outdoor air flow control. *Indoor Built Environment* 7: 165-181.

Wang, S. and X. Xu. 2002. A robust control strategy for combining DCV control with economizer control. *Energy Conversion and Management* 43: 2569-2588.

Warren, M. and L.K. Norford. 1993. Integrating VAV zone requirements with supply fan operation. *ASHRAE Journal* 35(4): 43-46.

Wendes, H. 1991. Variable air volume manual. Lilburn, Ga.: Fairmont Press.

Wright, J.A. 1996. HVAC optimization studies: Sizing by genetic algorithm. *Building Services Engineering Research & Technology* 17 (1): 7-14.

Wright J.A. and R. Farmani. 2001. The simultaneous optimization of building fabric construction, HVAC system size, and the plant control strategy. Seventh International IBPSA Conference, Rio de Janeiro, 863-872.

Wright, J., H. Loosemore, and R. Farmani. 2002. Optimization of building thermal design and control by multi-criterion genetic algorithm. *Energy and buildings* 34: 959-972.

Wright, J.A. and H. Loosemore. 2001. The multi-criterion optimization of building thermal design and control. Seventh International IBPSA Conference, Rio de Janeiro, 873-880.

Zaheer-Uddin, M. and R. Patel. 1993. The Design and simulation of a sub-optimal controller for space heating. *ASHRAE Transactions* 98(1).

Zhao, F. 1998. Operation strategies for economizer control in an air conditioning system. Concordia University, Montreal.

Zheng, G.R. and M. Zaheer-Uddin. 1996. Optimization of thermal processes in a variable air volume HVAC system. *Energy* 21(5): 407-420.